CHEMICAL REVIEWS

REVIEW

pubs.acs.org/CR

Structural and Immunological Principles Leading to Chemically Synthesized, Multiantigenic, Multistage, Minimal Subunit-Based Vaccine Development

Manuel Elkin Patarroyo,[*,‡,§,†] Adriana Bermúdez,[‡,∥] and Manuel Alfonso Patarroyo[‡,∥,†]

[‡]Fundación Instituto de Inmunología de Colombia (FIDIC), Carrera 50, No. 26-00, Bogotá, Colombia

[§]Universidad Nacional de Colombia

[∥]Universidad del Rosario

CONTENTS

Received: July 15, 2010
Published: March 25, 2011

dx.doi.org/10.1021/cr100223m | *Chem. Rev.* 2011, 111, 3459–3507

1. INTRODUCTION

The worldwide increase in infectious and transmissible diseases exerts a tremendous toll on humankind, as more than 17 million people are killed annually, afflicting two-thirds of the world's population. Intrinsic and extrinsic factors, such as drug and insecticide resistance, the susceptible host's immune compromise, human migration into previously nonaccessible areas, global warming, poor sanitary conditions, overcrowding, *etc.*, are among the main causes favoring not only the increase of these threats to humankind but also the re-emergence of diseases once considered under control as well as the emergence of new and more aggressive ones. Consequently, mortality and morbidity indicators regarding diseases affecting humans worldwide, such as malaria, tuberculosis, AIDS, hepatitis, respiratory infections, diarrhea, Ebola, SARS, avian flu, and influenza A (H1N1), become daily headline news. The speed at which these diseases spread stresses the need for implementing a logical, rational methodology aimed at developing new drugs and vaccines.

One of the four etiological agents for perhaps the most devastating of these diseases (malaria) is the *Plasmodium falciparum* parasite causing the most lethal form of human malaria; it afflicts around 500 million people and kills over 2 million of them each year, most of whom are sub-Saharan children under the age of 5.[1] Such a great impact on global public health has made it imperative to develop a vaccine against this parasite.[2]

In an attempt to contribute to resolving these problems (taking malaria as our prototype disease and being aware of the tremendous complexity of the *P. falciparum* parasite's life-cycle), our efforts have been orientated toward identifying the shortest amino acid sequences (or minimal subunits) from the most relevant proteins (multiantigenic) from the different stages (multistage) involved in parasite invasion of host cells to render them highly immunogenic and use them in developing a chemically synthesized fully effective antimalarial vaccine. Our endeavors have thus been focused on identifying the principles and rules for developing a logical, rational vaccine methodology against these diseases, the *raison d'être* for our institute and this manuscript.

SPf66, the first multiantigenic, multistage, minimal subunit-based, chemically synthesized anti-*P. falciparum* malaria vaccine, developed 24 years ago, provided complete protection for ∼40% of *Aotus* monkeys immunized with this molecule[3] and 2/5 of human volunteers following experimental challenge.[4] This chemically synthesized vaccine proved safe and immunogenic when administered with only aluminum hydroxide (without any other adjuvant system or immunopotentiator)[5,6] in large phase II trials and induced protection (the percentage of people being fully protected, as shown by the *complete absence of any parasites in their blood*) in large-scale human phase III field trials performed (some of them 20 years ago) by different groups of scientists on thousands of people aged >1 year from different ethnic groups and in different parts of the world, such as in Colombia (38%),[7] Venezuela (55%),[8] Ecuador (60%),[9] and Tanzania (31%).[10] Protection induced by **SPf66** was shown to last for at least 2 years in a field-trial carried out in Colombia (35%)[11] and for at least 18 months in another trial performed in Tanzania (26%).[12] However, a batch produced elsewhere having a different degree of polymerization tested in Thailand on children from the Karen tribe aged 6−12,[13] as well as a batch of SPf66 tested in newborn babies in Mozambique, did not provide any protective efficacy,[14] dropping their overall protective efficacy in a recent meta-analysis.[15] This data clearly suggested that although SPf66 was protective for some people aged >1 in different parts of the world, it was not effective for newborn children in the developing world where the expanded program on immunization (EPI) is a WHO goal for making vaccines available to all children worldwide. Due to this, and being very much aware of the *P. falciparum* parasite's complexity, we decided to stop vaccinating 16 years ago to concentrate our efforts on the search for the other components required to develop a fully protective antimalarial vaccine, this manuscript's *raison d'être*.

SPf66 is a chemically synthesized, 45-amino acid-long, multistage, multiepitopic, minimal subunit-based, polymerized chimeric molecule containing the circumsporozoite protein (CSP) NANP amino acid sequence, which is expressed on the surface of the sporozoite (the parasite's first stage, invading liver cells). The Asn-Ala-Asn-Pro (NANP) sequence is intercalated twice within three short amino acid sequences derived from merozoite proteins (the second stage of parasite development, invading

the red blood cell or RBC),[4] where two sequences bind with high affinity to RBCs,[16] one being semiconserved (i.e., having limited amino acid sequence variability).

Based on (a) the results provided by **SPf66** almost 20 years ago showing that chemically synthesized, minimal subunit-based, multiantigenic, multistage vaccines were feasible, although not fully effective by then, (b) the fact that 2 out of the 3 SPf66 merozoite-derived amino acid sequences had high RBC binding capacity, and (c) the broad genetic variability of *P. falciparum*, our efforts since then have been concentrated on the search for *conserved* malarial synthetic peptides having high specific RBC binding activity, named high activity binding peptides (HABP).[16−20] These peptides have thus become the basis for developing the basic components of a new chemically synthesized, multiantigenic, multistage, minimal subunit-based, antimalarial vaccine.

We were more attracted to the use of chemically synthesized peptides as a tool for producing vaccines (like SPf66)[21] to tackle the vaccine development problem, due to the multiple advantages provided by this chemical methodology, whose rules were defined by Bruce Merrifield's outstanding work almost 50 years ago.[22] The following advantages should be highlighted:

(a) Synthetic vaccines are chemically and physically very well-defined, at a single atom level, by numerous physical techniques such as high performance liquid chromatography (HPLC), mass spectroscopy (MS), circular dichroism (CD), infrared spectroscopy (IR), nuclear magnetic resonance (^{1}H NMR), X-ray crystallography, and currently available chemical methods (as will be shown later on), guaranteeing their purity and the reproducibility of their results.
(b) They are free of contaminants such as endotoxins, peptide analogues, byproducts, reagents, *etc.*, which can be easily detected by HPLC, MS, or biological tests, *etc.*, which can jeopardize their use in humans, leading to weird or even deleterious secondary adverse reactions.
(c) They can be easily synthesized, in unlimited amounts, in a reproducible and automated manner, using very simple, cheap, and affordable technologies.
(d) Their lyophilized products remain stable at room temperature for several years and do not require refrigeration or maintenance in a cold chain, thereby facilitating their delivery and storage in the world's most underdeveloped areas.
(e) They can be modified *ad libitum* by following the principles herein described for inducing or improving their immunogenicity and protective efficacy.

Besides the undeniable public health impact an antimalarial vaccine would have, some of the reasons for choosing *P. falciparum* malaria as a disease model for vaccine development were as follows:

(a) Infection caused by this parasite induces an acute disease that can be easily and rapidly diagnosed via simple microscope examination of a drop of blood using Giemsa or highly specific and sensitive Acridine Orange staining methods 4−5 days after natural infection occurs or experimental intravenous inoculation. It can also be detected by very sensitive molecular biology methods 2 days before the onset of clinical symptoms.
(b) It can be easily treated and cured with quinine, its derivatives, or new pharmacological products, when proper and timely diagnosis has been made.
(c) There is an appropriate animal model available in large numbers (the *Aotus* monkey in our case: ∼40−200 per km^2 in the Amazon basin). These monkeys' high susceptibility to different forms of human malaria allows them to be easily infected by intravenous inoculation without any further manipulation.[23,24]

Based on the reasons mentioned above and being aware of the multiple developmental stages during which the parasite's action can be blocked (either when the sporozoite infects the hepatic cells or the merozoite invades the RBC), we developed a robust, sensitive, and specific methodology for defining the intimate molecular interactions mediating merozoite invasion of RBC by synthesizing short (15−20-amino acid-long) merozoite-derived protein peptides binding specifically and with high affinity (HABPs) to RBCs.

This was followed by profound analysis of the HABP−RBC binding interaction at a single amino acid level to identify their critical binding residues, kinetics, physicochemical constants, and biological characteristics.[16−20,25] Likewise, the secondary structure of each of them was determined by CD spectroscopy[26] and the three-dimensional (3D) structure of a large number of them (∼90) has also been determined by ^{1}H NMR (most of them shown in this manuscript), such parameters once more reinforcing the advantage of working with chemically synthesized molecules for obtaining *accurate and reproducible results in vaccine development.*

Regarding the parasite stage, we chose the thoroughly studied *P. falciparum* merozoite because this asexual stage of the parasite is responsible for RBC invasion, malarial symptoms (fever, chills, headache, nausea, vomiting, malaise, *etc.*), pathophysiology (anemia, vasculitis, cerebral, placental malaria, *etc.*), and even the death of an infected person.

Specifically handling the merozoite provided the following advantages:

(a) This parasitic stage can be easily isolated in large amounts from either infected blood or RBC cultures, a methodology developed more than 35 year ago, thanks to the seminal work by William Trager et al.[27]
(b) This parasitic stage has been characterized in detail from biological, biochemical, functional, genomic (with a genome encoding ∼5,400 proteins),[28,29] proteomic,[30−32] and transcriptome perspectives,[33,34] which has led to the conclusion that 58−90 proteins are involved in RBC invasion.[35]
(c) An infective dose can be accurately quantified (by microscopy, cell sorting, PCR, *etc.*) and immediately transferred from one infected monkey to an uninfected one via *intravenous inoculation* (or challenge), without further manipulation,[24] this being the most stringent test for determining protective immunity.
(d) The degree of infection can be accurately quantified and the impact of the immune response and its progression can be clearly monitored.[24]
(e) Hundreds of strains have been obtained from different parts of the world, and their genomic characteristics have been completed for some of them, thereby providing critical information about the characteristics of this parasite stage.
(f) A large number of *P. falciparum* strains have been adapted for growing *in vitro*, and some others have been specifically adapted for infecting *Aotus* monkeys *in vivo*, thus providing esential information regarding the host's genetic and immune factors during the course of infection.

The role played by the parasite's genetic variability, as well as that of the genetic characteristics of the host in the immune

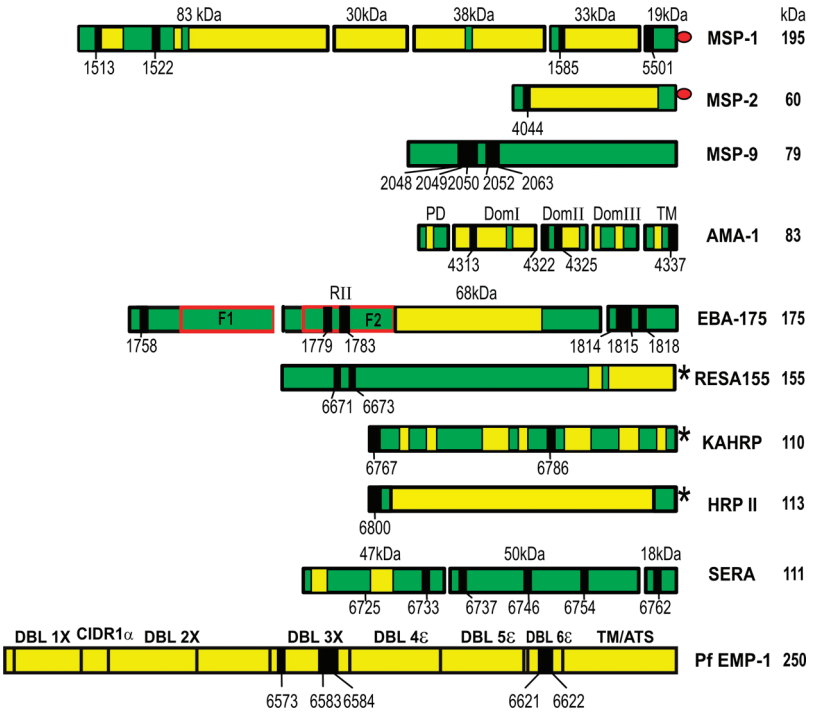

Figure 1. Diagrammatic representation of the 10 most relevant *P. falciparum* merozoite proteins involved in RBC invasion and endothelial cell attachment. The length of the bars corresponds to approximate molecular weights and putative cleavage places and fragments. Green regions correspond to conserved amino acid sequences while yellow regions correspond to variable amino acid sequences. Each HABP identified in each protein or protein fragment is indicated by our Institute's corresponding serial number.[36] GPI-anchoring tails are represented as large red balls at the proteins' C-terminus while transmembrane domains are labeled by an asterisk.

response and their interplay, can thus be analyzed at the single amino acid level (and even at the single atom level), providing the unique possibility of studying both at the deepest level for vaccine development, as will be shown later on.

Characterizing the proteins and their amino acid sequences implicated or playing a crucial role in parasite invasion has therefore been an obligatory step in our endeavors to obtain a logical and rational methodology for developing a chemically synthesized, multiantigenic, multistage minimal subunit-based vaccine.[16−20,25]

Fifty (50) out of the 58 different proteins suggested as being involved in merozoite invasion of RBCs have been molecularly defined, characterized, and thoroughly analyzed at the single amino acid level, as has been summarized in later publications and a recent review.[36−44] Furthermore, 20 additional proteins implicated in sporozoite invasion of the hepatic cell or hepatocytes[45−48] have been analyzed to identify their HABPs to develop a fully protective antimalarial vaccine effective against both sporozoite and merozoite parasite stages.

The 10 most studied proteins involved in mediating binding to and invasion of RBCs or attachment to endothelial cells are analyzed in depth in this manuscript (Figure 1). These molecules include the following: **m**erozoite **s**urface **p**rotein 1 (MSP-1),[49,50] **m**erozoite **s**urface **p**rotein 2 (MSP-2),[51,52] **m**erozoite **s**urface **p**rotein 9 (MSP-9)[53] or **a**cid **b**asic **r**epeat **a**ntigen (ABRA), **a**pical **m**erozoite **a**ntigen 1 (AMA-1),[54,55] **e**rythrocyte **b**inding **a**ntigen 175 (EBA-175),[56,57] **r**ing **e**rythrocyte **s**urface **a**ntigen 155 (RESA-155),[58−60] **h**istidine **r**ich **p**roteins I and II (HRPI, II),[61] **s**erine **r**ich **a**ntigen 5 (SERA-5),[62,63] and *P. falciparum* **e**rythrocyte **m**embrane **p**rotein 1 (PfEMP-1).[64−67] All of them have been thoroughly examined as probable vaccine candidates and systematically analyzed by us at the single amino acid level, as described in a recently published review article,[36] and shown here at the single atom level.

Further characterization of the 3D structure of native and modified HABPs identified in these merozoite proteins has led to correlating these minimal subunits' ability to form stable immunogenic complexes with **m**ajor **h**istocompatibility **c**omplex (MHC) class II (MHCII) molecules in *Aotus* monkeys and humans (named **h**uman **l**eukocyte **a**ntigen **D** region **r**elated (HLA-DR) to be presented to the T-cell receptor (TCR) and form an appropriate MHCII−peptide−TCR (MHCII/pTCR) macromolecular complex capable of inducing a proper immune system response.[68] Furthermore, deeper knowledge of the amino acid residues and electrostatic forces involved in MHCII/pTCR complex formation has led us to elucidate some of the principles behind eliciting fully protective *sterile immunity* against infectious agents.

This approach has thus led us to discover several completely new physicochemical, functional, immunological, and structural principles emerging during our search for a logical and rational methodology for vaccine development, representing this work's *raison d'être*.

2. PRINCIPLES FOR DEVELOPING MINIMAL SUBUNIT-BASED, CHEMICALLY SYNTHESIZED SYNTHETIC VACCINES

2.1. Support for the Minimal Subunit-Based, Synthetic Vaccine Concept

2.1.1. Atomic Fidelity between Conserved HABPs' 3D Structures and Their Corresponding Amino Acid Sequences in Recombinant Proteins. Frequent suggestions regarding short peptides' (15−20 mer-long) inability to mimic

dx.doi.org/10.1021/cr100223m |*Chem. Rev.* 2011, 111, 3459–3507

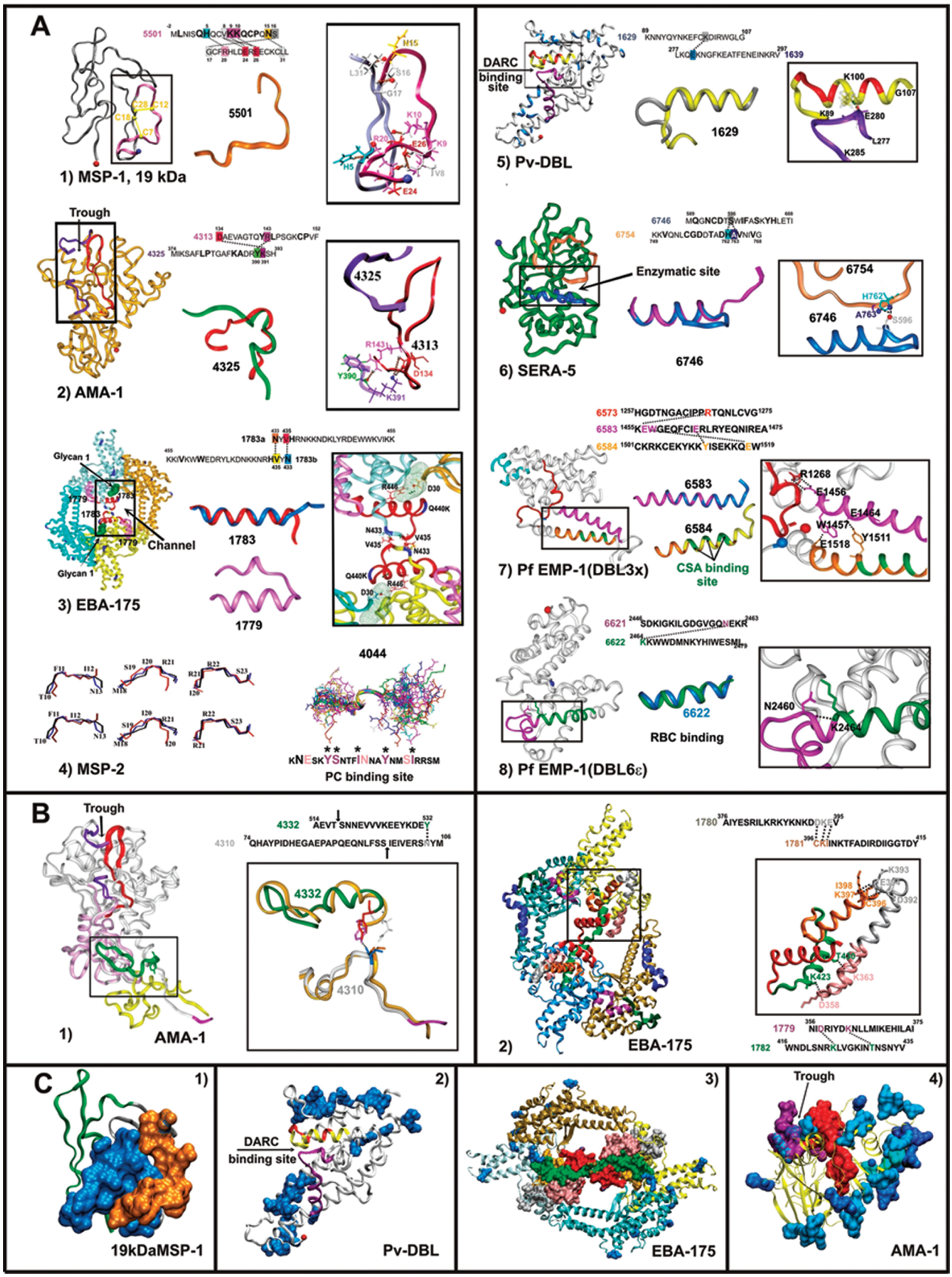

Figure 2. Conserved HABPs' three-dimensional analysis. (A) Conserved HABPs' atomic fidelity in their corresponding recombinant proteins: On the left, the 3D structure of the complete protein or its recombinants fragment, as determined by X-ray crystallography. The region including the HABPs is

dx.doi.org/10.1021/cr100223m |*Chem. Rev.* 2011, 111, 3459–3507

shown in the box. In the middle, the 3D structure of the corresponding HABP as assessed by ^{1}H NMR superimposed on the corresponding molecule sequence. On the right, the H-bonds established with other HABPs, inside the same HABP or with other regions of the protein are shown in the box and have been enlarged. At the top, the HABPs' amino acid sequence is shown in one single letter code and the H-bonds established between the different critical binding residues are shown in bold. (1) 19 kDa MSP-1 is shown as a gray ribbon (PDB code 1cei), and the HABP 5501 location is shown in orange.[71] (2) *P. falciparum* AMA-1 (PDB code 1Z40) is shown by the golden ribbon, the location of 4313 HABP in purple, and 4325 HABP in red, forming a trough. In the middle, the 4325 HABP structure[74] is shown in green superimposed on the AMA-1 protein, displaying the same β-turn. (3) The EBA-175 R II recombinant fragment displays the "hand-shake" dimer formation[76] (PDB code 1ZRO), localizing HABPs 1779 (pink) and 1783 (red), in the box and the channel formed by such dimerization. In the middle, 1783 HABP (dark blue)[77] superimposed on the corresponding EBA-175 R II sequence.[76] The EBA-175 RII region is boxed and enlarged; it mediates dimerization via antiparallel 1783 H-bond formation as well as H-bonds established with glycophorine A glycan 5 (green dotted structure). (4) Stereoview of the MSP-2 β-turn structure corresponding to the segment where HABP 4044 is located. The different colors used in the amino acid sequence (the darker, the more relevant) show the critical binding residues; those marked by an asterisk show binding to PC. (5) The *Plasmodium vivax* DBL 3D structure (PDB code 2C6J) is shown in pale gray, the location of HABP 1629 is boxed (in yellow, DARC binding residues highlighted in red), and the fragment corresponding to HABP 1639 is shown in purple. In the middle, the superimposition of HABP 1629 3D is shown in white on top of the Pv DBL structure. The H-bonds established between these two HABPs are shown in the box. (6) The SERA-5 recombinant fragment's 3D structure is shown in green (PDB code 3CH2) and the localization of HABPs 6746 (dark blue) and 6754 (golden). In the middle, the superimposition of HABP 6746 is shown in purple[87] in the corresponding SERA-5 sequence. Two H-bonds from the catalytic triad present in this recombinant fragment are shown in the box. (7) The Pf EMP1 (DBL3X) (PDB code 3CPZ) domain displayed in the box shows the region for 6573 (red), 6583(dark fuschia), and 6584 (orange) HABP binding to C32 amelanotic melanoma cells. In the middle, HABPs 6583 (dark blue) and 6584 (yellow) are superimposed on their corresponding sequences. Boxed, 6584 CSA binding residues and their intricate H-bond network are shown in green. (8) The Pf EMP1 (DBL6ε) domain (PDB code 2WAU) is shown in white, displaying RBC-binding HABP 6621 in fuschia and 6622 in green in the boxed area and their corresponding H-bonds. In the middle, the 6622 HABP 3D structure is shown in dark blue superimposed on its corresponding green sequence. The H-bond between 6621 and 6622 is shown in the box. All chemically synthesized native HABPs display a 3D structure, as determined by ^{1}H NMR superimposing perflectly well on their corresponding X-ray crystalographically determined sequences in the recombinant protein (having <1.00 rmsd values), being β-turns, α-helixes, or random structures demonstrating the atomic fidelity of such chemically synthesized native HABPs (Reprinted with permission from refs88 and 93, Copyright 2010 Elsevier, and ref 172, Copyright 2008 American Chemical Society). (B) Functional−structural compartmentalization of conserved HABPs. (1) *P. vivax* AMA-1 3D structure (PDB code 1W81) showing the short prodomain fragment at the botton of the molecule in fuschia, Domain I in white, Domain II in pink, and Domain III in yellow, localizing the aforementioned RBC-binding HABPs 4313 (red) and 4325 (fuschia). The prodomain fragment localizing hepatocyte binding HABP 4310 in close proximity to 4332 is shown in the box in gold, localized in Domain III in green. At the top, the amino acid sequence of these two HABPs is shown with the H-bond established between them, and this molecule's cleavage sites are indicated by arrows. **2**) The EBA-175 RII region (PDB code 1ZRO) displaying the localization of RBC-binding HABP 1779 in pink and 1783 in red and *hepatocyte*-binding HABP 1780 in gray establishing H-bonds with 1781 in orange and 1779 in pink establishing H-bonds with 1782 in gray. Fundamental binding residues are colored. (C) Immune evasion mechanisms. The filled blue surface areas correspond to regions having high amino acid sequence variability in all figures (the darker, the more variable) located far away from the conserved HABPs, colored according to the color code described above and filled suggesting an immune distraction strategy. No amino acid sequence variability is found in conserved HABPs, by definition, as stated beforehand.[16,18,36]

the native protein's 3D structure have cast some doubts on the minimal subunit-based synthetic vaccine concept.[69] The 3D structures of our native conserved HABPs obtained by ^{1}H NMR were compared to their corresponding segments in the few malarial recombinant proteins (or their fragments) which have been analyzed by X-ray crystallography to date to test whether conserved HABPs showed the same structural conformation displayed by the native protein's original sequence (Figure 2).

Chronologically, the first malarial protein 3D structure was that of the 19 kDa fragment of the MSP-1 described in 2003 (MSP-1 residues M1628 to I1744)[70] containing HABP 5501[18] (HABPs are numbered according to our institute's sequential system for all synthesized peptides) in its N-terminus region (residue M1628, exactly where this molecule is cleaved to generate the 19 kDa fragment) (Figure 2A1 and C1, shown in light brown). The totally random structural configuration displayed by this protein fragment confirmed our previously described CD spectra and ^{1}H NMR results on this HABP.[71]

The 3D structures published in 2005 for AMA-1 ectodomains I and II[72,73] showed that the short α-helical or β-turn segment between residues 384 and 387, where our HABP 4325 was located (residues M374−H393), was similar to the ^{1}H NMR structure previously determined by us for this native HABP between residues 13 and 16[74] in 2002 (Figure 2A2 and B, in red and green, respectively, and C in red); a 0.99 root-mean-square deviation (rmsd) was found when the two structures were superimposed. A random coil conformation was suggested in the same molecule in the non-well-defined region by X-ray crystallography where our HABP 4313 was located (residues D134−F152), in complete agreement with what we had previously demonstrated by CD and ^{1}H NMR studies for this peptide.[75]

The X-ray crystallographic structure of the EBA-175 region II (RII)[76] recombinant fragment described in 2005 showed an α-helical region between residues H436 and K455 which completely corresponded to our ^{1}H NMR 3D structure for HABP 1783 described in 2003 between residues 5 and 20,[77] giving a 0.89 rmsd when the two structures were superimposed (Figure 2A3 in red and dark blue, respectively). Similarly, our studies with HABP 1779 (insoluble by ^{1}H NMR studies) localized between residues N356 and I375 from the same RII recombinant fragment showed a distorted α-helical structure by X-ray crystallography, completely agreeing with our CD deconvolution analysis[26] (Figure 2A3, B, and C in pink).

The 3D structure of the *Plasmodium knowlesi/Plasmodium vivax* **D**uffy **b**inding-**l**ike (DBL) protein described by Singh et al., in 2006,[78] which contained our HABPs 1629 (residues K89−G107 in yellow) and 1639 (residues L277−R296 in purple)[79] within subdomain 2, showed that such a subdomain formed a trough (Figure 2A5 in yellow and fuschia, respectively) where the N-terminal sequence of the **D**uffy **a**ntigen **r**eceptor for **c**hemokines (DARC) bound.[80,81] Both fully conserved HABP 1639 and semiconserved HABP 1629, containing DARC binding residues Y94, N95, K96, F98, I102, and R103 (Figure 2A5, residues in red in the yellow ribbon), shown to interact with DARC Y41[80] (sulfation of this residue increased DARC affinity by 1,000×), were exposed on the surface of this

dx.doi.org/10.1021/cr100223m |*Chem. Rev.* 2011, 111, 3459–3507

trough.[82] HABP 1639 had random configuration in this trough, as determined by CD and ^{1}H NMR and confirmed by the 3D structure of DBL, while superimposing our ^{1}H NMR determination of HABP 1629's α-helical structure showed that the 3D structure of the corresponding DBL fragment had an almost identical α-helical configuration (0.95 rmsd) (Figure 2A5 in gray).

Likewise, the β-turn type II structure described in 2007 for the MSP-2 molecule's recombinant fragment (residues 1−25) by ^{1}H NMR[83] showed a very similar 3D structure to that described by us for MSP-2-derived HABP 4044 in 2003[84] (Figure 2A4). More recently, in 2008, this protein's complete 3D structure was published,[85] being described as an **i**ntrinsically **u**nstructured **p**rotein (IUP), where only some regions displayed α-helical propensity, among them being the N-terminal region where our HABP 4044 was located. These results were in complete agreement with previous NMR and X-ray crystallography determinations of the recombinant MSP-2 or complete protein[83] and our previous ^{1}H NMR studies of HABP 4044. [Please note that the order of these two last structures (DBL and MSP-2) has been slightly changed to allow a better fit in Figure 2A.]

The 3D structure of a 284-amino-acid-long recombinant fragment (residues N564−N828) included in the SERA-5 protein's catalytic 50-kDa cleavage product was published in 2009.[86] Our results published in 2003 for HABP 6746[87] located in this fragment displayed the same α-helical structure as that for the corresponding segment of the recombinant fragment (residues M589−I608) (0.95 rmsd) (Figure 2A6 in dark blue and fuschia, respectively) while HABP 6754 (residues K749−G768) had a completely random structure, in total agreement with the structure described by our CD and ^{1}H NMR studies for these HABPs[88] (Figure 2A6 in pale brown).

Likewise, the 3D structures of three domains from the very large (∼350 kDa) and highly variable PfEMP-1 binding to human amelanotic melanoma C32 cells, human placenta proteoglycans, CD36 molecules, *etc.*, have been described during the last two years. Our HABPs 6583 (residues K1455−A1475) and 6584 (residues C1501−W1519) displayed an α-helical structure in this protein's recombinant DBL3X domain, as determined by X-ray crystallography and confirmed by us through CD and ^{1}H NMR studies (Figure 2A7 in fuschia and pale brown, respectively) (Cifuentes et al., submitted for publication). These two HABPs had 0.89 and 0.92 rmsd, respectively, when they were superimposed on the corresponding amino acid sequences in PfEMP-1. Meanwhile, HABP 6573 (residues H1257−G1275), also binding to C32 melanoma cells and mediating the same function, displayed a random structure as determined by CD and ^{1}H NMR and confirmed in the 3D structure of this DBL3X domain[89,90] (Figure 2A7 in red).

Another very recent publication (2010) determined the 3D structure of this DBL3X domain from the VARCSA clone; more exactly, the **c**hondroitin **s**ulphate **A** (CSA) minimal binding site was confirmed in subdomain 3.[91] This region corresponded exactly to our above-mentioned 6584 HABP, which displayed an α-helical structure by ^{1}H NMR which had 0.89 rmsd when superimposed on this new DBL3X domain subdomain 3 structure (Figure 2A7, orange and yellow, respectively) (Cifuentes et al., submitted for publication).

It was found in the 3D structure obtained during the last months of 2010 for the DBL6ε domain of PfEMP-1[92] implicated in binding to **c**hondroitin **s**ulfate **p**roteo**g**lycans (CSPG) and containing our RBC-binding HABPs 6621 (residues S2446−R2463)

Table 1. Amino Acid Sequences of Conserved Native HABPs from the 10 Most Relevant *P. falciparum* Merozoite Proteins Involved in RBC Invasion and Endothelial Cell Attachment and Their Modified Immunogenic Protection-Inducing Analogues. Each native HABP (labeled in Arabic numbers) with their critical binding residues highlighted in bold. The same amino acids in their corresponding peptide analogues are represented by a dashed line. Modified peptides are labeled in bold type, and their changes are highlighted in bold. II and III: Antibody titers (in parentheses) assessed by IFA 15 days after the second and third immunizations, respectively. The prefix corresponds to the total number of monkeys that developed these antibody titers; Prot: number of monkeys that were fully protected against experimental intravenous infection with a 100% infective *Aotus*-adapted *P. falciparum* strain, being the same ones that developed antibody titers. DR: HLA-DRβ1* allele with which each HABP was found to have high binding capacity. The big black dots indicate those native or modified HABPs for which their 3D structure was assessed by ^{1}H-NMR. Note that only the most representative from each family of modified analogues is shown in the following tables and figures. REF: References to studies where these HABPs were reported. Subm: Submitted article. Only immunogenic protection-inducing modified HABPs are shown in this table

	PEPTIDE	SEQUENCE	II	III	Prot	DR	3D	REF
MSP-1	1513	GYSLFQKEKMVLNEGTSGTAG	0	0	0/5	8	•	
	9882	----------ET----------	0	1(160)	1/5	ND		133
	13946	----------MKT---------	2(320)	2(320)	2/12	?	•	
	1522	QIPYNLKIRANELDVLKKLV	0	0	0/5	3,11	•	
	9782	----------GG--GG------	0	2(2560)	1/3	11	•	221
	9548	----------GG----------	0	1(1280)	1/5	11		
	1585	EVLYLKPLAGVYRSLKKQLE	0	0	0/5	?	•	
	13450	-----LD---------------	2(2560)	1(2560)	2/4	3	•	
	10014	----HV----------------	2(640)	1(640)	2/4	11	•	134
	11860	----HM--G----A------	1(1280)	1(2560)	1/7	11	•	
	22770	----HL--G----A------	2(1280)	ND	2/9	ND		
	5501	MLNISQHQCVKKQCPQNS	0	0	0/5	7		
	12926	----------S----AD----	0/5	1(640)	1/5	ND		71
	17944	----------T-MMMT-----	0	1(160)	1/7	7		
	24148	-----ML-T-MMMT---K----	1(640)	ND	1/8	7	•	
MSP-2	4044	KNESKYSNTFINNAYNMSIR	0	0	0/5	?	•	
	10008	----------EV----------	2(5120)	1(5120)	1/3	4	•	
	13464	IM--WG----EV----------	0	1(320)	1/6	ND		
	15502	IM--WA----NI------N---	1(160)	1(320)	1/5	ND		
	15504	-I--WA----NI------N---	2(320)	2(320)	1/3	ND		84
	22774	I---WA----EV------VN--	4(320)	1(2560)	1/10	?		
	24112	----------NI------V--RSM	2(5120)	ND	2/15	4	•	
	24180	-M-M---A-DI-----AN-R--	1(2560)	ND	1/9	4	•	
ABRA	2150	KMNMLKENVDYIQKNQNLFK	0	0	0/5	?		
	24922	----HL---PW-MNK-------	1(320)	ND	2/7	?		194
AMA-1	4313	DAEVAGTQYRLPSGKCPVFG	0	0	0/5	?		
	10022	----------FH-----S-----	0	1(5120)	1/5	7	•	
	22780	----------FH-----V-----	2(2560)	ND	2/10	7	•	75
	22782	----------WFV----V-----	1(2560)	ND	1/10	7	•	
	4325	MIKSAFLPTGAFKADRYKSH	0	0	0/5	3,11	•	
	13486	---AS-D------SP-------	3(2560)	2(1280)	2/5	ND	•	
	15514	---A--H------S--W-----	1(160)	1(160)	1/4	7		74
	15516	---A--H------MS--W----	1(1280)	1(160)	1/4	ND		
	20034	---A----------M-------	2(320)	1(160)	2/8	4,7	•	
	4337	WGEEKRASHTTPVLMEKPYY	0	0	0/5	?		
	14044	YS-M----L------K------	1(160)	1(320)	1/5	7	•	
	22822	HTTYS-M----L------K----	1(1280)	ND	1/8	7		122
	24926	---YSMM----L------K----	1(320)	ND	1/7	ND	•	
EBA-175	1758	KSYGTPDNIDKNMSLIHKHN	0	0	0	?	•	
	13790	MA--SD--D---K--D------	1(320)	1(320)	2/4	4	•	114
	24150	W---SVD---PM----------	1(1280)	ND	2/7	4	•	
	1779	NIDRIYDKNLLMIKEHILAI	0	0	0 /5	11		
	9794	-GG-------G-----------	0	1(320)	1/3	ND		
	22812	-N-------M-H-----M----	1(2560)	ND	1/9	11	•	103
	23386	-NP------M-H-----M----	5(640)	ND	1/7	11		
	1783	HRNKKNDKLYRDEWWKVIKK	0	0	0/5	3, 11	•	
	9928	----------------Y--N---	1(2560)	3(2560)	3/11	3	•	
	9930	----------------T-----	0	2(2560)	1/5	ND		77
	22814	---------M-Y--T---DVW	2(5120)	ND	2/10	3	•	
	1815	YTNQNINISQERDLQKHGFH	0	0	0/5	?	•	
	24292	L---------D--FN-M-----	2(320)	ND	2/7	3	•	220
	1818	NNNFNNIPSRYNLYDKKLDL	0	0	0/5	?		
	24166	----------------M-P-DD	1(320)	2(640)	2/5	1,11	•	111
RESA-155	6671	MTDVNRYRYSNNYEAIPHIS	0	0	0/5	4,7		
	9948	----------------EQ----	0	1(1280)	1/4	4	•	
	13492	-----I----------------	2(5120)	0	1/6	4	•	129
	22720	----------V---SN--K---	0	1(5120)	1/10	4	•	
HRP II	6786	KSKKHKDHDGEKKKSKKHKD	0	0	0/5	?		
	12934	-----MI---------I--L---	0	1(160)	1/4	3		130
	24224	-----M-L---MMMA-------	3(640)	ND	1/8	?	•	
	6800	NNSAFNNNLCSKNAKGLNLN	0	0	0/5	?		
	10004	----------S-----M--I---	0	2(2560)	1/4	ND		
	22228	----DD--TAM--M--I--KR	1(320)	ND	1/8	7		131
	24230	------DD--TAA--M--I---	1(320)	ND	2/7	7	•	
SERA	6725	LKETNNAISFESNSGGSLEKK	0	0	0/5	3		
	23422	----------M--A--------	1(640)	ND	1/8	11	•	142
	6737	YDNILVKMFKTNENNDKSELI	0	0	0/5	3	•	
	22834	-----H-----VI----------	1(2560)	ND	2/9	11	•	
	22796	----------VI----------	1(5120)	ND	2/9	11		143
	13844	-----H-----VIM---------	1(320)	ND	1/6	11		
	24096	-----H-----VI----------	1(5120)	ND	2/8	ND		
	6746	DQGNCDTSWIFASKYHLETI	0	0	0/5	3, 11		
	23230	-----SI----R-----L-----	1(320)	0	1/9	3	•	
	24214	-----SI----R-A-F------	1(320)	ND	1/6	3		87
	24216	-----TI----NR-A-F------	5(320)	ND	2/9	11	•	
	6754	KKVQNLCGDDTADHAVNIVG	0	0	0	ND	•	Subm
	23426	----------T-----L-T----	0	3(320)	1/9	4	•	
	6762	NEVSERVHVYHILKHIKDGK	0	0	0/5	?	•	
	22462	--T--F----------------	0	ND	1/9	ND		144
	24210	-M----------M---------	1(160)	ND	2/8	ND	•	
	24310	-M----------N-M-------	2(160)	ND	2/8	3	•	
PfEMP-1	6505	ESAKHMFDRIGKDVYDKVKE	0	0	0	?	•	
	12722	-----K----------M-----	2(320)	2(320)	3/12	?	•	237
	23410	-----K--F---I---M---R	4(1280)	ND	1/8	?		
	6583	KEWGEQFCIERLRYEQNIREA	0	0	0		•	
	6584	CKRKCEKYKKYISEKKQEW	0	0	0		•	Subm
	6622	KKWWDMNKYHIWESMI	0	0	0		•	

dx.doi.org/10.1021/cr100223m |*Chem. Rev.* 2011, 111, 3459–3507

Table 2. Representative Members from Each Group of Conserved HABP Amino Acid Sequences and Their Modified Analogues (Labeled According to Our Institute'S Serial Numbering System) Used for Immunizing *Aotus* Monkeys and Whose 3D Structures Were Determined by ^{1}H-NMR[a]

	Peptide	P_1 P_4 P_6 P_9	PI	II_{10}	II_{15}	III_{15}	Prot	Group
EBA-175	1815	YTNQNINISQERDLQKHGFH	0	0	0	0	0/5	A
	24292	LTNQNINIDQEFNLMKHGFH	0	1(320)	1(640)	ND	1/9	B
	1783	HRNKKNDKLYRDEWWKVIKK	0	0	0	0	0/5	A
	9928	HRNKKNDKLYRDEYWKNIKK	0	ND	1(2560)	2(2560)	2/4	E
	22814	NDKLYRMEYWKTIKKDVW	0	0	2(5120)	ND	2/10	B
	17914	NDKLYRDEEWKDIKK	0	0	0	0	2/7	E
MSP-1	1585	EVLYLKPLAGVYRSLKKQLE	0	0	0	0	0/5	A
	13450	EVLYLLDLAGVYRSLKKQLE	0	1(5120)	1(2560)	1(5120)	2/4	B
	15484	EVLYHMPLAGVYRALKKQLE	0	3(320)	1(320)	0	0/5	D
SERA	6762	NEVSERVHVYHILKHIKDGK	0	0	0	0	0/5	A
	24310	NMVSERVHVYHNLMHIKDGK	0	1(320)	1(320)	ND	1/6	B
	13782	VMNSERVHVYHILKHIEDGK	0	0	2(320)	2(640)	0/5	C
	24210	NMVSERVHVYHILMHIKDGK	0	0	0	ND	2/8	E
	6746	DQGNCDTSWIFASKYHLETI	0	0	0	0	0/5	A
	23230	GNSITAWIRASKYLLET	0	0	1(320)	ND	1/9	B
	21742	DQGNSDTSYIFASKYHH	0	0	2(320)	0	0/8	D
HRP-I	6786	KSKKHKDHDGEKKKSKKHKD	0	0	0	0	0/5	A
	24224	KSKKHMDLDGEMMMAKKLKD	0	3(640)	ND	ND	2/8	B
MSP-1	1522	QIPYNLKIRANELDVLKKLV	0	0	0	0	0/5	A
	9782	QIPYNLKIRAGGLDGGKKLV	0	2(2560)	1(2560)	ND	1/3	A
	13446	QIPYNLKIRANMLDVDKKLV	0	0	1(160)	ND	1/5	B
	15474	QIPYNLKIFAIMLDTHKMLV	0	3(1280)	6(320)	0	0/4	D
	22456	PYNLMIRANMLDVHKKG	0	0	0	0	1/8	E
EBA-175	1779	NIDRIYDKNLLMIKEHILAI	0	0	0	0	0/5	A
	22812	NNDRIYDMNHLMIKMHILAI	0	0	1(2560)	ND	1/9	B
	14012	NNPRIYDKNHLKIKMHILAI	0	0	0	1(320)	0/4	C
	6725	YLKETNNAISFESNSGSLEKK	0	0	0	0	0/5	A
	23422	KETNNAISFMSNAGSLEKK	0	1(640)	ND	ND	1/8	A
MSP-1	1585	EVLYLKPLAGVYRSLKKQLE	0	0	0	0	0/5	A
	10014	EVLYHVPLAGVYRSLKKQLE	0	2(320)	1(640)	1(640)	2/4	B
SERA	6737	DNILVKMFKTNENNDKSELI	0	0	0	0	0/5	A
	22834	DNIHVKMFKVIENNDKSELI	0	0	1(2560)	ND	2/9	B
	14096	DNIHVKMRKVIMNNDKSELI	0	2(320)	3(640)	0	0/6	D
MSP-1	1513	GYSLFQKEKMVLNEGTSGTA	0	0	0	0	0/5	A
	13946	GYSLFQKEMKTLNEGTSGTA	0	2(320)	2(320)	0	2/12	B
	15468	GYSLFQKEMKTDNEGTSGTA	0	0	1(320)	1(640)	0/6	C
	9882	GYSLFQKEKETLNEGTSGTA	0	0	1(160)	0	2/5	E
MSP-2	4044	KNESKYSNTFINNAYNMSIR	0	0	0	0	0/5	A
	24112	SKYSNTFNINAYNMVIRRSM	0	0	1(5120)	ND	1/8	B
	17920	KIMAKWANTFINNAYNMSNR	0	0	0	0	1/8	E
RESA	6671	MTDVNRYRYSNNYEAIPHIS	0	0	0	0	0/5	A
	13492	MTDVIRYRYSNNYEASDHIS	0	2(5120)	1(1280)	ND	1/6	B
	13494	MTDVIRYRYSNNYEAESHIS	0	2(5120)	2(5120)	1(320)	0/2	C
	10000	MTDVNRYRYSNNYERPHIS	0	1(160)	0	0	0/4	D
	15536	MTDVIRYRYSNNYEANPHIS	0	0	0	0	1/3	E
AMA-1	4325	MIKSAFLPTGAFKADRYKSH	0	0	0	0	0/6	A
	20034	MIKAAFLPTGAFMADRYKSH	0	0	2(320)	1(160)	2/8	B
	20032	MIKAAFLPTGAFKADRYKSH	0	0	1(160)	1(320)	0/8	C
EBA-175	1758	KSYGTPDNIDKNMSLIHKHN	0	0	0	0	0/5	A
	13790	MAYGSDDNDDKNKSLDHKHN	0	1(320)	1(320)	ND	2/4	B
HRP-II	6800	YNNSAFNNNLCSKNAQGLNLN	0	0	0	0	0/5	A
	24230	SAFDDNLTAANAMGLILNKR	0	0	1(320)	ND	1/7	B
MSP-1	5501	MLNISQHQCVKKQCPQNSY	0	0	0	0	0/5	A
	24148	MLNISMLQTVMMMTPQK	0	3(2560)	3(2560)	ND	3/16	B
	23754	MHNISQLQVVKKMVPQK	0	0	1(320)	ND	0/8	C
AMA-1	4337	WGEEKRASHTTPVLMEKPYY	0	0	0	0	0/5	A
	14044	YSEMKRASLTTPVLKEKPYY	0	0	1(160)	1(320)	1/5	B
	14048	YSEMKRASLTTPVLKEMPWY	0	0	0	2(320)	0/5	C
	23776	YSEMKRASLTTPVLMMKPYY	0	0	0	0	1/7	E
	4313	DAEVAGTQYRLPSGKCPVF	0	0	0	0	0	A
	10022	DAEVAGTQYFHPSGKSPVFG	0	0	0	1(5120)	1/5	B
	13766	DAEVAGTQWFDPSGKSPVFG	0	1(640)	3(640)	2(1280)	0/5	C
EBA-175	1818	NNNFNNIPSRYNLYDKKLDL	0	0	0	0	0	A
	24166	FNNIPSRYNLYDKMLPLDD	0	1(320)	1(320)	2(640)	2/15	B
	23390	NNIPSRYNLYDKMLDLDDL	0	0	2(320)	9(320)	0/8	C

[a] Peptides are aligned according to the HLA-DRβ1 molecule's pockets 1, 4, 6, and 9 (shadowed), to which *immunogenic protection-inducing peptides* (placed in group **B**) bound and are assigned according to their corresponding binding motifs and binding registers. PI, II_{10}, II_{15}, and III_{15} are the days when monkeys were bled and their antibody titers were determined by IFA (shown in brackets). The prefix corresponds to the total number of *Aotus* that developed these antibody titers. Prot: total number of *Aotus* that were protected against experimental challenge with a 100% infective *Aotus*-adapted *P. falciparum* FVO strain. HABPs are grouped according to their immunological activity: A = native HABPs; B = modified HABP high antibody titer and *protection* inducer; C = *non-protective* modified HABPs high *long-lasting* antibody titer inducer; D = nonprotective high *short-lived* antibody titer inducers; E = inducers of *cellular immunity* with no associated antibody production. Experiments with modified *immunogenic protection-inducing* HABPs were repeated twice or three times with similar results. Only the most representative ones are shown for brevity. Since the allele frequency for each of these HLA-DRβ1* *Aotus*-related alleles is ~25%, it is not unexpected that this is the maximum number of monkeys being protected per group.

dx.doi.org/10.1021/cr100223m |*Chem. Rev.* 2011, 111, 3459–3507

and 6622 (residues K2464−L2479) that the α-helical 3D structure of the latter HABP determined by ^{1}H NMR superimposed perfectly well on the corresponding amino acid sequence in this domain, giving a 0.93 rmsd (Figure 2A8 in green and dark blue, respectively). Meanwhile 6621 (which was not suitable for ^{1}H NMR studies, since it displayed a random coil structure) had a distorted α-helical formation, as determined by CD deconvolution, the same as in the recombinant DBL6ε structure (Cifuentes et al., submitted for publication) (Figure 2A8 in fuschia).

All this structural data obtained by completely different techniques, such as ^{1}H NMR compared to X-ray crystallography, has demonstrated the complete agreement of α-helices, β-turns, and random structures between conserved HABPs and their corresponding sequences within the recombinant proteins (rmsd <1.0). These results strongly demonstrated, beyond any doubt, that short HABPs (15−20-mer long) displayed the same structural conformation as they showed in their native proteins and that, therefore, they could be performing or were involved in similar biological functions, such as host cell binding,[93] enzymatic activities, protein−protein interactions, *etc*.

2.1.2. H-Bonds between Conserved HABPs in the Formation of Functionally Relevant Structures. Conserved HABPs' critical residues in binding to host cells have been determined by glycine (Gly) analogue scanning in most of our studies (defined as a >50% reduction in their capacity to bind host cells when the corresponding residue has been replaced by Gly), finding that they were extremely relevant for these peptides' function, since their activity became dramatically reduced or lost when they were replaced by Gly. Moreover, their polarity has to be inverted to render them immunogenic-protection inducers, as will be described later on.

Very recently we have shown[88] that conserved HABPs establish H-bonds with other conserved HABPs located very distantly in a protein's amino acid sequence (according to their 3D structure). Such H-bond formation between conserved HABPs, together with other electrostatic forces such as disulfide bonds, is important for shaping a protein's proper folding to generate a niche, trough, or channel formed by these conserved HABPs in parasite−host cell protein interactions.

It should be stressed that the residues establishing H-bonds between conserved HABPs in all the structures analyzed so far have been previously identified as *critical binding* residues (by Gly analogue scanning as described above) and are named *fundamental residues* here, since their modification breaks conserved HABPs' immunological code of silence, rendering them capable of inducing *sterile* protective *immunity*. Such *fundamental* residues are displayed in Figure 2A and B in the far right-hand boxes showing enlarged segments of the molecule.

Supporting this conclusion, it was found in our assays that the 19 kDa MSP-1 cleavage product (the only fragment of this protein remaining anchored as a stub on the merozoite membrane) was detected inside recently infected RBC[94] participating in the formation of the parasitophorous vacuole (PV)[95] while the other processed fragments of this protein (83, 38, 33, and 33 kDa cleavage products) were released into the milieu. Our HABP 5501 was located in the 19 kDa MSP-1 fragment's N-terminal portion,[96] displaying a whole array of H-bonds between its critical binding residues, which, when properly modified, made this important conserved HABP one of the most immunogenic and protection inducing peptides studied to date (Tables 1 and 2). H-bonds were established in this HABP between H5 with R20, K9 with E24, K10 with E26, K9 also with E26, N15 with L35, and S16 with G17 (Figure 2A1 boxed), as determined by X-ray crystallograhpy.[88]

Critical binding residues D134 and R143 in conserved HABP 4313 (D134 to F152) located in the AMA-1 domain I established H-bonds with residues K391 and Y390, respectively, from conserved HABP 4325 (located between residues M374 and H393 inside domain III). These H-bonds formed a channel or trough where a still nonidentified RBC receptor bound (Figure 2A2 in the box).[97] These H-bond-forming residues in HABPs 4313 and 4325 rendered these peptides highly immunogenic and protection-inducing when properly modified (Tables 1 and 2).

By the same token, and very important for developing a pre-erythrocytic stage vaccine and therefore a multiantigenic, multistage, fully effective antimalarial vaccine, is the fact that two H-bonds were established between T79 of HABP 4310 and Y532 of HABP 4332 (Figure 2B) in AMA-1 (a type I transmembrane protein, also expressed in sporozoite membrane and involved in hepatocyte invasion). Our HABPs binding to hepatoma-derived HepG2 cells, named HABP 4310 (residues Q74−M106), located in this molecule's prodomain, and 4332 (residues A514−Y532) had 85% identify with the *P. vivax* domain.[97,98] Moreover, the latter HABP was the stub fragment remaining anchored to the merozoite's membrane during AMA-1 processing being carried inside recently infected RBC (Cifuentes et al., submitted for publication), whereas the remaining portion of AMA-1 containing domains I and II is released to the milieu after protein processing, as elegantly shown by others.[73]

It has been described that the EBA-175 molecule is directly involved in RBC invasion[99−101] via a panel of conserved HABPs that include previously mentioned HABPs 1779 and 1783[20] (located in the recombinant RII region and whose 3D structure has been determined). H-bonds were established in these two HABPs between fundamental binding residues N433 from 1783 and fundamental binding residue V435 from 1783 from another antiparallel EBA-175 molecule orientated in a handshake-like manner.[76] This allowed this protein's dimerization and its binding to glycophorin A glycans present on the RBC membrane.[76,93] In the same way that the fundamental binding residue R446 of 1783 established an H-bond with the distant D30 residue from the recombinant RII fragment of EBA-175 to allow the docking of two antiparallel EBA-175 molecules (Figure 2A3 and B, boxed), the same HABP 1783 also established H-bonds and van der Waals forces through critical binding residues K439 and D442 with the Neu5Ac1 glycan atoms of the RBC receptor glycophorin A molecule[93,102] (Figure 2A3, boxed).

Conserved HABP-mediated sporozoite binding to hepatic cells was identified in EBA-175 for developing a multiantigenic, multistage, fully protective antimalarial vaccine: i.e. HABPs 1780 (residues A376−V395), 1781 (residues C396−Y415), and 1782 (residues W416−V435) (Cifuentes et al., submitted for publication). H-bonds have been established among these HABPs between critical binding residues D358 and K363 from RBC-binding HABP 1779, with K423 and T430 from hepatocyte-binding HABP 1782 (Figure 2B, boxed). When residues D358 and K363 were properly modified, HABP 1779 became a highly immunogenic peptide analogue capable of inducing protection against experimental infection by intravenous inoculation of *P. falciparum* iRBCs, as we have previously described[103] (Tables 1 and 2). By the same token, H-bonds were established between residues D392 K393 and E394 from 1780 with C396, K397, and

I398 from 1781 (Figure 2B, boxed). The appropriate modification of these residues rendered these modified HABPs highly immunogenic in *Aotus* monkeys, as shown by the high antibody titers against sporozoites detected by immunofluorescence assays (IFA) and Western blot (Cifuentes et al., submitted for publication).

MSP-2 is one of the most abundant merozoite surface proteins. This molecule has the tendency to become polymerized when produced as a recombinant protein, producing amyloid-like microfibrils (some of them aggregating in solution); such an observation has led to suggesting that polymerization could also occur on the merozoite surface to form a niche or trough where a still unknown RBC receptor binds. Recent studies by Adda et al., using selective enzymatic digestion with protein kinase (PK),[104] have shown that such polymerization-associated residues were in the MSP-2 N-terminal portion, exactly in the region where our HABP 4044 was located.[84] Since MSP-2 has the tendency to bind to lipid membranes, ^{1}H NMR studies were performed with the complete recombinant MSP-2 molecule using a micelle forming phosphorylcholine analogue (dodecylphosphocholine $^{2}H_{38}$) to simulate the RBC lipid bilayer. ^{1}H NMR signal displacements have been found in our previously described critical binding residues K**NE***SK**YS***NTF**IN**NA**Y***NM**SI***RRSM (critical binding residues are shown bold and underlined, with the most displaced ones being marked by an asterisk), suggesting that they could be establishing strong electrostatic forces with the phosphorylcholine moiety of the RBC membrane, also partly explaining our difficulty in recognizing a particular receptor for this HABP on erythrocytes via **b**is **s**ulfo**s**uccinimidyl **s**uberate (BS3) cross-linking.[84]

Fundamental binding residue S596 established H-bonds with fundamental binding residues H762 and A763 from conserved HABP 6754 (K749 to G768) (Figure 2A6, boxed) in the recently described 3D structure of the recombinant SERA-5 fragment[88] (residues N564 to N828) including our conserved HABP 6746 (residues M589−I608), which together with N787, forms this molecule's noncanonical serine active catalytic triad, deeply involved in processing merozoite proteins during parasite egress and invasion.

The same situation holds true for the relevant PfEMP-1 molecule, one of the mediators of *P. falciparum* malaria parasite pathogenesis[105−107] and virulence, involved in pregnancy-associated malaria (PAM), cerebral malaria (CM),[108] and severe malaria.[109,110] The structural localization of several conserved HABPs binding to amelanotic melanoma C32 cells was identified in the recently described 3D structure of one of its domains, DBL3X (C1251−Y1530), which has been shown to bind to the **ch**ondroitin **s**ulfate **A** (CSA)[90] ligand expressed on placental and vascular endothelial cells. These HABPs corresponded to 6573 (residues H1257−G1275), 6583 (residues K1455−A1475), and 6584 (C1501−W1519). According to the DBL3X 3D structure, H-bonds were established between residues W1457 and E1464 from conserved HABP 6583 with E1518 and Y1511, respectively, from conserved HABP 6584 (Cifuentes et al., submitted for publication) to create the channel or trough where CSA bound through residues R1503, K1504, K1507, and K1510 present in HABP 6584 (in Figure 2A7 boxed; these residues are displayed in green).

Similarly, in the very recently described 3D structure for the PfEMP-1 DBL6ε domain[92] (residues D2350−K2634) binding to **c**hondroitin **s**ulfate **p**roteo**g**lycans (CSPG)[92] and also to RBCs, an H-bond was established between N2460 from HABP 6621 with K2464 from HABP 6622; both of them bound strongly to RBCs (Figure 2A8, boxed) (Cifuentes et al., submitted for publication).

Deeper analysis of these malarial proteins for which the 3D structure has been determined and for which conserved HABPs have been identified and modified in critical binding residues to render them highly immunogenic and protection-inducing peptides has led to finding that H-bonds were established in the following:

- MSP-1 19 kDa fragment (PDB code 1CEI) between HABP 5501 residue V8 (HN) and EGF-1 domain atom Oε1 as well as HABP 5501 residue H5 (O) and EGF-1 domain (HN) R20;
- AMA-1 recombinant protein (PBD code 1Z40) between conserved HABP 4325 residue Y390 (O) and HABP 4313 (HH21) R143;
- EBA-175 RII fragment (PDB code 1ZR0) between HABP 1779 residue K363 (HN) and HABP 1782 (Oγ1) T430; and
- SERA-5 fragment (PDB code 3CH2) between HABP 6746 residue S596 (O) and HABP 6754 (Nδ1) H762.

This data clearly shows that the fundamental residues which had been shifted to render the conserved HABPs into highly immunogenic-protection inducing peptides were those establishing hydrogen bonds between their backbone atoms (O or NH) and other conserved HABP residues' lateral chains from with which they form the troughs or channels where the receptor molecules bind or were involved in the formation of these molecules' catalytic sites.

Such very recent data is of the utmost importance due to its theoretical and practical implications. First, since conserved HABPs perform vital functions in processes important for parasite survival such as invasion of host cells, enzymatic activity, evading immune surveillance by clearance organs (such as the spleen) via binding to vascular endothelial cells, rosetting, and other escape mechanisms, then the most likely explanation for conserved HABPs' unmodifiable structure is that microbes cannot tolerate mutations in these regions at the risk of losing such a particular critical function; these critical HABPs MUST therefore be conserved. As a consequence of this, conserved HABPs have to be immunologically silent to avoid the host's strong immunological pressure and such immunological pressure must therefore be resisted somewhere else in the molecule, in areas not critical for parasite survival.

Second, conserved HABPs' localization in corresponding proteins' 3D structures show that they are forming nonsequential functional structures such as the DARC region in the DBL protein,[92] the binding trough or channel in AMA-1,[73] the dimerization and glycan 5 binding site in EBA-175,[76] the catalytic triad in SERA5,[86] the PV-forming structure in 19 kDa MSP-1,[70] the CSA binding pocket in DBL 3X,[91] the CSPG binding site in DBL6ε PfEMP-1,[92] and many more, suggesting the existence of functionally relevant discontinuous structures, and since these HABPs mediate vital functions for parasite survival, *etc.*, then their activities can be blocked by inducing an appropriate immune response against any one of these HABPs, thereby strongly supporting this strategy for a logical and rational approach to vaccine development.

Third, the elusive long-postulated and sought-after "conformational epitopes" could be partially explained by these distantly conserved HABPs' interactions via H-bond-forming fundamental residues placed in specific localizations of the molecule to perform a specific function.

Fourth, these previous findings make it clear that critical binding residues have to be identified and modified to elicit a

protective immune response in which the most relevant or fundamental residues for inducing sterile immunity are those establishing H-bonds between different HABPs and, more specifically, residues establishing H-bonds between their backbone atoms and amino acids present in other conserved HABPs or receptor molecules, thereby forming molecules' catalytic sites.

This so exquisite and specific a problem can be partially explained and solved by working with short (~15−20 amino acids long) conserved HABPs to design components for a minimal subunit-based multiantigenic fully effective antimalarial vaccine.

As experimental support for selecting these minimal amino acid sequences or HABPs for designing a fully protective antimalarial vaccine, it should be mentioned that adding most of these conserved HABPs has proved to block invasion of new RBCs *in vitro*; however, the same biological function (binding and inhibition) has not been blocked by their corresponding scrambled peptides (peptides having the same amino acid composition but different amino acid sequence). Furthermore, most conserved HABPs bind specifically and strongly to specific receptor molecules on the host cell membrane; it can be further added in support of such a minimal subunit-based approach that most of these HABPs lose their ability to bind specifically to RBCs when host cells are enzymatically treated, as has been extensively shown by us,[16−20,25,36] suggesting that host cell receptor molecules have been cleaved or removed by this enzymatic treatment.

When HABPs were analyzed, both the monomers and their corresponding polymers displayed very similar secondary structural characteristics (as assessed by CD spectra),[103,111,112] thus making them excellent tools for studying the immunological responses induced by these HABPs.

All these findings rule out the possibility that solvents such as TFE (in which these peptides are dissolved in a low ratio (30/70 v/v TFE/water) for CD and ^{1}H NMR analysis) *induce* conformational structures different from those displayed by these conserved HABPs under natural conditions[113] or in their corresponding crystallographic stuctures, therefore confirming previous reports on this solvent showing that TFE only acts by *stabilizing* structural components such as α-helices in solution.[75,111,114,115]

All the chemical, structural, and biological information mentioned above provides strong structural and immunological support for consolidating the minimal subunit-based, multiantigenic, multistage, synthetic vaccine concept long sought for by us.

2.2. Structural Functional Compartmentalization in Multifunctional Proteins

It has been clearly documented by transcriptional and immunological analysis that some proteins involved in merozoite invasion of RBCs are also transcribed in hepatic stages during *P. falciparum* development inside human liver cells as well as in salivary gland sporozoites inoculated by *Anopheles* mosquitoes while feeding on human blood and invading hepatic cells. The most studied ones have been EBA-175,[116] AMA-1,[113] MSP-2, MSP-5, RAP-1, RAP-2, and SERA-5.[117]

We have previously reported AMA-1 conserved HABPs 4313, 4325, 4337 binding to RBCs and their highly immunogenic, protection-inducing modified peptides (Figure 2A and B) as components of a chemically synthesized, minimal subunit-based, antimalarial vaccine. However, we have recently reported finding AMA-1 conserved HABPs binding to hepatic cells (HABPs 4310 and 4332).[118] These HABPs correspond to amino acid sequences used by the sporozoite when invading liver cells.

Interestingly, while *fundamental* H-bonds were established between conserved HABPs 4313 and 4325 localized in this

Table 3. Structural Features of Native Conserved HABPs and Their Modified Analogues, as Determined by ^{1}H-NMR, Associated with Their HLA-DRβ1*-Binding Capacity and Their Immunological Activity (Groups A−E)[a]

Protein	Peptide	Structural features	Distance (Å), from P1 to P9	Haplotypes: DR1 0101	DR52 0301	DR52 1101	DR53 0401	DR53 0701	TCR contact resid.	Grp.
				%Binding to HLA-DRβ1						
	1815	α-helix Q4-L14	17.7	-2	-10	-10	30	45		A
	24292	α-helix I6-F12	19.6	-4	**51**	42	16	27	3,7,8	B
EBA-175	1783	α−helix N6-K20	16.5	3	**49**	**65**	-2	7		A
	9928	α−helix N6-I18	17,8	4	**51**	22	4	ND	3,7,8	B
	17914	α−helix D2-I13	15,1	-3	**54**	1	14	8		E
	1585	α-helix Y4-Y12	14,3	5	18	15	7	37		A
MSP-1	**13450**	α-helix L5-Q18	20,2	12	**47**	20	-8	33		B
	15484	α-helix A9-K17	13,3	16	21	**58**	0	10	3,7,8	D
	6762	α-helix E2-K20	13,5	2	-5	3	3	28		A
	24310	α-helix M2-H15	18,5	-1	**60**	35	17	13	3,7,8	B
	13782	α-helix S4-M17	14,0	10	21	41	10	20		C
SERA	**24210**	α-helix M2-D18	18,4	1	31	**50**	11	30		E
	6746	α-helix (CD)	—	12	**55**	**76**	5	42		A
	23230	αhelix N9-H16	20. 0	2	**84**	37	13	17	3,7,8	B
	21742	α−helix N4-A12	12.7	6	13	**51**	7	20		D
	6786	Random + turn (CD)		1	29	10	10	ND		A
KHARP	**24224**	α-helix D7-G10, M13-K16	20,3	-3	53	31	34	ND	3, 7	B
	1522	α-helix Q1-V20	16.9	1	**88**	**91**	-3	23		A
MSP-1	**9782**	α-helix P3-N11	20,2	-1	16	**50**	-14	0		B
	15474	α−helix K7-K17	15.2	18	**73**	45	37	23		D
	22456	α−helix L4-H14	17,8	4	-2	**70**	6	29		E
	1779	α-helix (CD)	—	12	**55**	**76**	5	31		A
EBA-175	**22812**	α-helix N9-H16	17,7	1	0	**67**	-1	ND	3,7,8	B
	14012	α−helix P3-L11	14,1	5	0	23	-8	19		C
SERA	6725	α-helix (CD)	—	2	33	**66**	**71**	22		A
	23422	α-helix I7-A13	18,5	3	37	**83**	51	ND	3,7,8	B
MSP-1	1585	α-helix Y4-Y12	14,3	5	18	15	7	37		A
	10014	α-helix A9-Q18	20,6	-4	30	**61**	-5	21	3,7,8	B
	6737	α-helix I3-N14	14.2	0	**79**	38	0	15		A
SERA	**22834**	α-helix V5-V10	21.0	-3	4	**54**	**51**	19	3,7,8	B
	14096	α−helix V5-M12	14.2	-3	**65**	**78**	14	35		D
	1513	α-helix L4-E14	13,5	-1	**43**	**46**	-4	7		A
MSP-1	**13946**	α-helix K7-N13	19,9	9	-3	12	11	16		B
	15468	α-helix K7-T12 and N13-S17	17,2	-4	**80**	23	1	-11		C
	9882	α-helix S3-E10 and N13-G18	17,9	-1	**55**	10	-4	14		E
	4044	Classical type III' β−turn S7-F10	19,0	5	0	-60	38	39		A
MSP-2	**24112**	Distorted Type III' β-turn Y3-T6 and Classical type III β−turn A11-M14	26,5	9	1	0	**53**	46	2,3,8	B
	17920	Distorted Type III' β-turn A7-F10	20,8	-3	1	10	**61**	40		E
	6671	β-turn + Random	—	24	45	16	**61**	**55**		A
	13492	α-helix V4-R8	26,1	-5	33	16	**50**	16	2,3,8	B
RESA	**13494**	α−helix M1-Y9	21.2	6	**83**	16	32	15		C
	10000	α−helix T2-Y9	18.4	3	17	**73**	11	29		D
	15536	α−helix M1-Y7	18,2	28	43	21	**65**	**96**		E
	4325	β-turn and Short α-helix K13-R16	21.5	18	**83**	**74**	28	**48**		A
AMA-1	**20034**	α-helix K3-F6 and A11-R16	25.5	40	34	7	**69**	**64**	2, 3, 8	B
	20032	α-helix K3-F6 and K13-R16	20.6	17	**80**	37	31	30		C
	1758	Distorted α-helix I9-H17	20,9	6	34	38	5	6		A
EBA-175	**13790**	Distorted Type I β-turn N12-L15	27,1	10	27	16	17	0		B
	6800	Random	—	3	10	15	16	40		A
HRP-II	**24230**	α-helix F3-N6 and N11-L17	23.7	0	37	6	27	**50**	2, 3, 8	B
	5501	Random	—	3	5	10	-12	**58**		A
MSP-1	**24148**	Short α-helix S5-V10	25.1	13	3	3	-13	**65**	2, 3, 8	B
	23754	Short α-helix Q6-K12	19.3	-1	0	11	-11	20		C
	4337	Random	—	-17	12	-6	4	28		A
	14044	Short α-helix K5-T10	23.1	4	19	39	7	**79**	2, 3, 8	B
	14048	Short α-helix R6-L9 and V13-E16	17.9	-2	29	**53**	-1	5		C
AMA-1	**23776**	Classical type III β−turn V13-M16	18,8	6	15	30	4	**55**		E
	4313	Random	—	0	20	26	9	23		A
	10022	Distorted type III' β−turn T7-F10	25.0	9	7	4	2	**42**	2, 3, 8	B
	13766	Distorted type III β−turn T7-F10	19.3	1	22	**44**	-2	26		C
	1818	Distorted α-helix	—	2	33	6	11	36		A
EBA-175	**24166**	Classical type III β−turn S9-N12 and Distorted type III β−turn Y14-M17	24.9	**53**	5	**69**	18	38	3, 8	B
	23390	Distorted Type III β-turn S9-N12 and 3_{10}-helix D19-L23	20.3	-6	**52**	24	15	4		C
ABRA	2150	α-helix N8-Y11 and Q13-N17	15,6	5	**47**	10	4	ND		A
	24922	3_{10}-helix L6-V9	25,2	5	41	13	9	71	2, 3, 8	B
	6505	α-helix F7-E20	17,5	20	41	**44**	33	24		A
Pf-EMP-1	**12722**	α-helix A3-E20	20,5	5	30	6	3	10	3, 7	B

[a] The table shows structural features: distance (in Å) between HABP residues fitting inside HLA-DRβ1* molecule's pockets 1−9 and the percentage of these HABPs' binding capacity to these Class II molecules (HLADRβ1* molecules to which they bound with ≥ 50% of affinity are shown in bold). Solvent-exposed, putative TCR contact residues were assigned based on the ability shown by these HABPs to bind to HLA-DRβ1* molecules, the motifs to which they were associated, and their corresponding binding registers. Groups are the same as in Table 2, based on the immunological activities induced by these HABPs. Ref refers to studies where 3D structures were reported. New = 3D structures reported in this review for the first time.

protein's domains I and II for RBC binding, as previously described,[88] hepatocyte-binding conserved HABP 4310 localized in the pro-domain sequence, and HABP 4332 located in domain III,[118] localized one in front of the other (according to the *P. vivax* AMA-1 3D structure), established H-bonds among them, despite their very long amino acid sequence distance (approximately 420 residues apart), to form a trough or channel[73] where a 50 kDa hepatocyte membrane protein bound[118] (Figure 2B, boxed).

Likewise, EBA-175 has been thoroughly shown to be involved in RBC invasion via binding to glycans present in RBC Glycophorin A molecules through HABPs 1814, 1815, 1818, 1758, 1779, and 1783,[20] all of which have been shown to become highly immunogenic and protection inducers in vaccinated *Aotus* monkeys after having been properly modified.[77,93,103] The same panel of synthetic peptides (20 mer-long) spanning the entire EBA-175 amino acid sequence (FCR-3 strain) showed a completely different binding profile when they were analyzed for their ability to bind to hepatic cells (HepG2). These results showed that HABPs binding to RBCs did not bind to hepatocytes and *vice versa* (Cifuentes et al., submitted for publication); it was observed that *most* hepatocyte-binding HABPs were located in the F1 region and the variable extra amino acid sequence (segment F) while a large number of RBC-binding HABPs were located toward this protein's C-terminus. Furthermore, analysis of the segment localized in RII (residues S140−K599), the only one where both functions were present (RBC binding and hepatocyte binding), showed that none of these binding functions or HABPs overlapped each other, therefore suggesting different modes of structural and functional compartmentalization for multifunctional malarial proteins (Figure 2B, boxed).

HABPs 6573, 6583, and 6584, strongly binding to amelanotic melanoma C32 cells and located in the DBL3X domain, showed no RBC binding activity at all in the very recently described 3D structure of DBL3X and DBL6ε domains from PfEMP-1. By contrast, HABPs 6621 and 6622 localized in the DBL6ε domain have been found to bind strongly to RBC but not to C32 cells (Cifuentes et al., submitted for publication); such observation has led to suggesting a clear functional compartmentalization of these domains in PfEMP-1.

Such data could have a great impact on vaccine development, since it could reduce the number of HABPs required to induce fully protective sterile immunity against malaria when binding is properly blocked in the pre-erythrocytic or early stages of malarial invasion.

2.3. Conserved HABPs' Structural Compartmentalization in Native Proteins

Some structural principles for developing chemically synthesized, minimal subunit-based, multiantigenic vaccines began to emerge after 20 years' efforts[14] and hundreds of trials on large numbers of *Aotus* monkeys. The almost ninety (90) native and modified HABPs derived from the ten (10) most relevant *P. falciparum* merozoite proteins participating in the different steps of RBC invasion (structurally analyzed by ^{1}H NMR and thoroughly studied in the immunization experiments mentioned above) are displayed in this manuscript's tables and figures. Moreover, it is worth mentioning that the identification of an additional sixty (60) conserved HABPs derived from the above HABPs (Table 1) and a large number of other merozoite proteins has been described elsewhere very recently,[36−44] and this data has not been included in this manuscript due to limitations of space.

Native and modified HABPs are arranged in Tables 2 and 3 according to their ability to bind to purified HLA-DRβ1* molecules. However, this manuscript will first discuss those structural characteristics most clearly related to and associated with HABPs' function in merozoite invasion of RBCs, since doing it the other way around will make this manuscript very confusing.

Conserved HABPs derived from proteins containing a glycosyl phosphatidylinositol (GPI) tail anchoring them to the merozoite membrane have all been found to display β-turns and/or a very high percentage of unordered structures, as determined by CD and confirmed in some cases by ^{1}H NMR and X-ray crystallography.

Examples of such merozoite membrane native conserved HABPs would be the following:

- HABP 4044 located in the MSP-2 N-terminal region;[19,83,84]
- HABP 5501 located in the MSP-1 19 kDa fragment N-terminal region;[18,71]
- HABP 24115 located in the MSP-7 N terminal region;[119]
- HABP 26373 identified in MSP-8;[120] and
- MSP-10-derived HABPs[121] 31122 and 31132 located in this molecule's N-terminal portion preceding the epidermal growth factor-like (EGF-like) domains.

It has been clearly demonstrated that the MSP-1−19 kDa fragment, which contains our HABP 5501 and remains anchored to the merozoite membrane via a GPI-anchor tail, is the only fragment drag inside recently invaded RBCs and is also involved in PV formation.[95]

Likewise, HABPs 4313,[75] 4325,[74] and 4337[122] derived from AMA-1, which is originally deposited in merozoite micronemes and the apical region to be translocated to the merozoite membrane later on, also displayed β-turn or unordered structures (Table 3).[26]

HABPs found in the N-terminal region immediately before the ***P**lasmodium* **e**xport **e**lement (PEXEL) motif[123,124] characteristic of proteins transported from the merozoite to the PV, Maurer's clefts, and RBC cytosol and, sometimes, to the RBC membrane during early stages of parasite intraerythrocytic development via a putative transportome machinery,[125−128] and involved in parasite nutrition, secretion, and even remodeling of infected RBC, also display β-turn or unordered structures. Some examples would include the HABPs found in **r**ing-infected **e**rythrocyte **s**urface **a**ntigen 155 or RESA-155 (6671),[129] **k**nob-**a**ssociated **h**istidine-**r**ich **p**rotein (KAHRP) (6786),[130] and HRP-II (6800),[26,131] molecules that allowed this PEXEL motif to be identified.[123−131]

Therefore, ^{1}H NMR and CD studies clearly showed that conserved HABPs in most proteins anchored to the parasite membrane via GPI tails' PEXEL motif displayed unordered or β-turn type structural configurations. Furthermore, it has been very recently described that many of the proteins analyzed in the *P. falciparum* proteome are completely unordered or display large unordered regions and that these proteins are often involved in key biological processes such as membrane fusion, protein transport, translation, signaling, and large multiprotein complex self-assembly regulation.[132] RESA, MSP-2, KAHRP, and HRP-II (from which the previously mentioned HABPs were derived) have been reported among them.[132]

In another scenario, conserved HABPs contained in MSPs or their cleavage fragments involved in merozoite recognition of and or binding to the RBC membrane, or which were not transported inside the RBC during invasion but were rather

released to the milieu, or did not contain a GPI tail, preponderantly displayed α-helical structural features (Table 3), as determined by CD[26] and ^{1}H NMR.

Examples of such conserved surface protein derived HABPs are as follows:

- Conserved HABPs (1513, 1522, 1585) derived from MSP-1 83 kDa and 33 kDa soluble cleavage fragments,[26,133,134]
- HABPs (31193, 31202, 31209) from MSP-3,[135]
- HABP (20494) from MSP-4,[119]
- HABP (31191) from MSP-6,[136]
- HABPs (26101, 26107, 26114) from MSP-7,[119]
- HABPs (26361, 26368, 26369) from MSP-8,[120]
- HABPs (2148, 2149) from MSP-9 or acid-basic repeat antigen (ABRA),[137]and
- HABP (31121) derived from MSP-10.[121]

These proteins or their cleavage products altogether form large macromolecular complexes essential for the merozoite's initial contact with RBC membrane proteins. As an example, the 33 kDa and 19 kDa cleavage fragments derived from the 42 kDa MSP-1 cleavage fragment (where conserved HABPs 1585 and 5501 were localized)[18] associate with MSP-9 to form a stable complex that binds to the band 3 RBC protein.[138] Similarly, MSP-1 83 (where conserved HABPs 1513 and 1522 are localized) 30 and 38 kDa soluble cleavage products also establish noncovalently associated macromolecular complexes with MSP-6 and MSP-7 and/or their cleavage fragments during invasion.[139,140]

Following the same trend, soluble protein-derived HABPs from proteins that remain loosely bound to the merozoite membrane[141] to perform some enzymatic-like activity, such as the serine-rich antigen or SERA 5 protein (where conserved HABPs 6725, 6737, 6746, and 6762 are located) not found inside recently invaded RBCs, all had α-helical structural features, as determined by CD[26] (Table 3) and ^{1}H NMR for 6725,[142] 6737,[143] 6746,[87] and 6762.[144]

Similar structural patterns were observed for some of the micronemal proteins involved in the initial steps of RBC invasion.[145] All HABPs localized in the F1 and or F2 regions highly similar to the Duffy binding-like (DBL) domains of erythrocyte binding-like (EBL) proteins, which have been shown to act as contact sequences for RBC membrane sialoglycoproteins, also displayed α-helical structural patterns, as determined by CD spectra analysis (namely HABPs 1779, 1783, and 1815 from EBA-175, HABPs 30031, 30042, and 30051 from EBA-181, HABPs 26135, 26144, and 26147 from EBA-140, and HABPs 29903, 29907, 29923, 29924, 30009, and 30018 from the erythrocyte binding ligand EBL-1 protein)[26] or ^{1}H NMR and X-ray crystallography as in the case of HABPs 1783 and 1779. Some other structures have been determined by ^{1}H NMR analysis, as will be shown later on.

It has been shown that membrane-anchored EBA and EBL proteins were processed by rhomboid-like enzymes from the subtilisin-like family (PfSUB1), named sheddases,[146] during the last seconds preceding merozoite penetration into RBC, leaving only their last 100 amino acids anchored as a *stub* to the merozoite membrane by their transmembrane fragments. The remaining portion of the molecule (where the aforementioned HABPs are located) was released into the *milieu* after having fulfilled its function in RBC adhesion and was *not* carried into the recently invaded RBCs.

It is equally interesting that all conserved HABPs derived from rhoptry proteins which have been shown to be involved in RBC invasion, probably mediating PV formation, clearly displayed α-helical structures, as shown by CD spectroscopy for rhoptry-associated proteins RAP-1 (HABPs 26188, 26201, 26202, and 26204) and RAP-2 (HABPs 26220, 26225, 26229, and 26235), normocyte-binding protein 1 (NBP-1) (HABP 26332), and reticulocyte-binding protein 2 homologue a (RBP-2Ha) (HABPs 26752, 26794, 26796, 26803, 26805, 26807, and 26818).[26]

Furthermore, working with the pathologically relevant *P. falciparum* malarial molecule PfEMP-1 has led to showing that HABP 6621 displayed a classical α-helix while 6622 had a distorted α-helix structure in semiconserved RBC-binding, as determined by CD and ^{1}H NMR studies and confirmed by superimposing their 3D structures on the crystallographic structure described for DBL6ε, as shown in Figure 2A8 (Cifuentes et al., submitted for publication).

We have very recently described that PfEMP-1 HABPs 6583 and 6584, which bound strongly to CSA in the placenta and to C32 melanoma cells, also displayed α-helical structures, as determined by CD and ^{1}H NMR studies (Cifuentes et al., submitted for publication), which was confirmed when superimposed on the corresponding sequence in the DBL-3X domain's 3D X-ray crystallographic structure[89,90] (Figure 2A7). This PfEMP-1 molecule involved in virulence functions, together with others, acts as a pathogen secretion system.[147]

It can thus be suggested that α-helical structures were displayed by a considerable number of conserved HABPs derived from molecules involved in initial loose contacting phases between merozoites and RBCs or endothelial cells, such as cell recognition and binding (as occurs with MSPs, micronemal protein EBAs and EBL,[145] and RAP, NBP, and RBP rhoptry proteins), enzymatic processing of molecules involved in RBC adhesion, and penetration (some of which were loosely bound to the merozoite membrane, as in the case of SERA). All these HABPs and their corresponding protein fragments were released into the *milieu* after they had fulfilled their function, possibly acting later on as immune response decoys to deviate deleterious cytolytic activity which could otherwise be induced against the merozoite protein fragment remaining anchored to the merozoite membrane, which could lead to the parasite's destruction and demise.

In another scenario, most conserved HABPs whose fragments remain anchored to the merozoite membrane via GPI tails or transmembrane segments (such as those remaining anchored to the membrane of iRBCs or having PEXEL motifs) displayed β-turn or unordered structures. Such structures could be clue targets for triggering an effective induced sterile immune response, since a lytic activity directed against them could lead to the merozoite's destruction via immune effector mechanisms.

This manuscript presents an extensive analysis of the secondary structures of ∼200 conserved and modified HABPs (some of them shown in Table 3) determined by CD spectral analysis[26,36] and the ^{1}H NMR 3D structures elucidated for ∼90 of these native conserved HABPs (since their number is growing systematically) or their nonimmunogenic, nonprotection-inducing analogues. This information clearly shows that the functional *compartmentalization* of proteins involved in merozoite invasion of RBCs to perform specific biological functions is associated with specific features of native conserved HABPs' 3D structures.

Consequently, such association between the α-helical structure displayed by HABPs remaining loosely bound to the merozoite membrane and those membrane-anchored HABPs mainly displaying β-turn or random conformations opens the

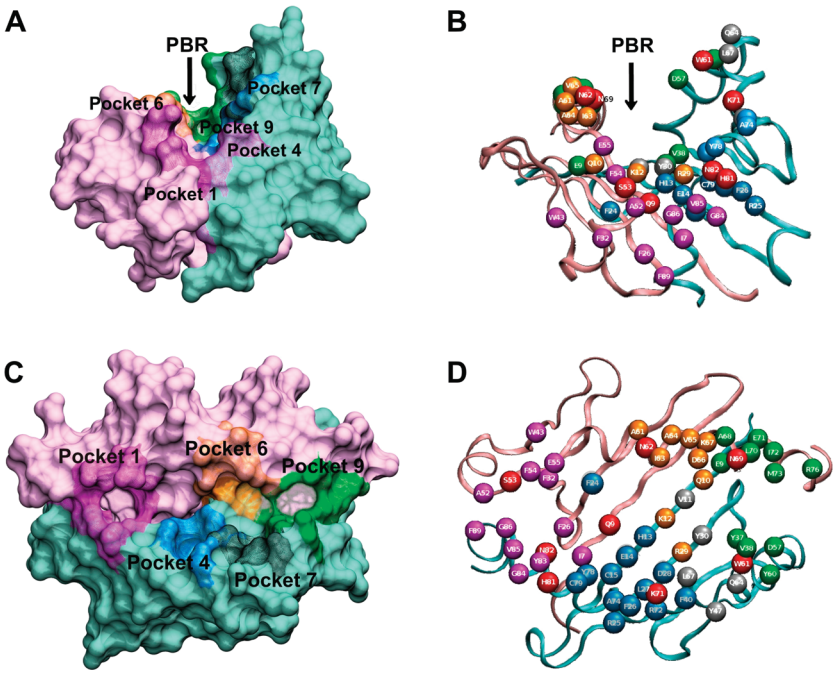

Figure 3. (A) Front-view, Connolly surface representation of the HLA-DRβ1*0101 molecule's 3D structure (PDB code: 1DLH)[185] showing the α-chain region (pink) and the β-chain region (pale blue) forming the groove or the PBR where peptides fit by accommodating their side chains inside pockets 1 to 9 (displayed in different colors according to the color code mentioned below and from here on) to be properly presented to the TCR. (B) Front-view, ribbon representation of the HLA-DRβ1*0401 molecule (PDB code: 1FYT)[182] showing the α-chain as a clear pink ribbon and the β-chain as a pale blue ribbon. Residues are shown as colored balls according to the following color code: pocket 1, fuchsia; pocket 4, dark blue; pocket 6, light brow; pocket 9, green. Red balls correspond to those HLA-DRβ1*0401 residues establishing H-bonds with the peptide's backbone. (C) Top-view, Connolly surface representation of the HLA-DRβ1*0101 3D structure[185] highlighting deep pocket 1 (fuchsia), which anchors the peptides, and pocket 9 (green), which stabilizes such anchoring, as well as the more shallower pocket 4 (dark blue) and pocket 6 (light brown), which provide allele and antigenic specificity. (D) Top-view, ribbon representation of the HLA-DRβ1*0401 molecule displaying the amino acids from both chains forming the different pockets colored according to the previously described color code (Reprinted with permission from ref 172. Copyright 2008 American Chemical Society).

door for a simple technique such as CD spectroscopy to establish new principles for the logical and rational molecular design of subunit-based, multiantigenic, synthetic vaccines, with an antimalarial one being of vital importance.

3. GENETIC CONSTRAINTS REGARDING *AOTUS* MONKEYS' IMMUNE RESPONSE TO MINIMAL SUBUNIT-BASED, CHEMICALLY SYNTHESIZED VACCINES

3.1. Genetic Control of the Immune Response

The large scale phase II and phase III field trials for the first chemically synthesized, multiantigenic, multistage, subunit-based antimalarial vaccine **SPf66**[4−11] performed 22 years before showed that ~25% of the vaccinated population did not produce any detectable antibody levels against this vaccine,[148,149] nor were they protected against natural infection. The binomial (Gaussian) distribution pattern of antibody titers clearly suggested genetic control of an immune response elicited by SPf66[148,149] mediated by HLA-DR genetic-region encoded molecules. The HLA typing of these vaccinated populations disclosed that most nonresponsive individuals harbored the HLA-DRβ1*04 genetic marker.[150] Similarly, analysis of the TCR molecules activated by HLA-DRβ1*0401-presenting molecules revealed preferential use of TCR β chain Vβ3, Vβ10, and Vβ11 *variable* regions[151] in nonresponsive individuals, suggesting that such nonresponsiveness was probably associated with an imperfect fit of this vaccine's molecular components that hampered appropriate MHCII/pTCR complex formation.

Since this data, and some by other authors, clearly shows that genetic control of the immune response against malarial vaccines is mediated by these MHCII molecules,[150−154] a tripartite association was sought between these peptides' induced immunological responses, HABPs ability to bind to purified HLA-DRβ1* molecules, and their 3D structure.

The genetic region encoding human MHCII molecules needs to be described at this point. This genetic region is located in the short arm of chromosome 6 in position 6p21.3 and encodes the synthesis of three types of membrane proteins, or isotypes, named HLA-DP, -DQ, and -DR. These MHCII molecules are heterodimers formed by two heavy chains: the alpha (α) chain (pink ribbon in Figure 3B and D) encoded by the almost monomorphic HLA-DRA region and the beta (β) chain (pale blue ribbon in Figure 3B and D) encoded by the highly polymorphic HLA-DRB genetic region.[155]

This HLA-DRB genetic region (represented by capital letter B) contains nine genes (represented by numbers 1−9), five of which are pseudogenes while the other four (HLA-DRB 1, 3, 4, and 5) are transcribed, with HLA-DRB1* being the most polymorphic one. The molecules encoded by these genes, named HLA-DRβ1* as in HLA-DRβ1*0401, are in charge of presenting peptide antigens to the TCR, a necessary step in forming the MHCII/pTCR complex to induce an appropriate immune response (the expressed protein product is represented by the

dx.doi.org/10.1021/cr100223m |*Chem. Rev.* 2011, 111, 3459–3507

Greek letter beta, or β, followed by the numeral 1, corresponding to the product expressed by gene 1 from region B, while the number following the asterisk differentiates the allele).

In an effort to better understand the great impact of the HLA-DRB genetic region on vaccine design, it should be mentioned that 16 HLA-DRβ1* *alleles* (or genetic traits) following a Mendelian segregation pattern have been identified to date, along with their ~400 genetic variations. These *alleles* have been serologically, molecularly, and phylogenetically grouped into five large groups or *haplotypes*[156] that share common serological, functional, and evolutive characteristics (please note that the haplotypes are *not* written with the letter β or an asterisk). These *haplotypes* are as follows: HLA-DR1 (including HLA-DRβ1*01, 10, and 103 alleles), HLA-DR51 (including the HLA-DRβ1*15 and 16 alleles), HLA-DR52 (containing the HLA-DRβ1*03, 11, 12, 13, 14; 1403 and 1404 alleles), HLA-DR8 (exclusively with the HLA-DRβ1*08 allele), and HLA-DR53 (including HLA-DRβ1*04, 07, and 09 alleles).[155,156]

HABP ability to bind to a particular HLA-DRβ1* allele is based on their capacity to bind to purified HLA-DRβ1 molecules, as determined by competition assays, by measuring the ability to displace the control peptide by $\geq$50%,[157] as well as the presence of preferred binding motifs (specific amino acids that fit perfectly well into each of these molecules' characteristic pockets)[158] and their corresponding binding registers.[155−158]

3.2. Reasons for Conducting Immunization Trials in *Aotus* Monkeys

After decades of "very disappointing malarial vaccine trials,"[50,159,160] performed in *humans* by other laboratories (only a few are quoted),[50,159−169] it has been very recently concluded that "even with the money pouring in from people like Bill Gates, the extremely high cost of clinical trials is an alarm sign that the world cannot afford to squander money for research into AIDS, tuberculosis and malaria vaccines that have little or no hope of succeeding" and "that therefore monkey trials had to be performed to speed up vaccine development against these scourging diseases",[170] an approach fiercely defended by our Institute for more than three decades.

For ethical reasons, starting with the identification of peptides which led to the discovery of the **SPf66** vaccine, all our immunogenicity and protection efficacy trials have been conducted first in *Aotus* monkeys,[3,23,24] before any human or field vaccination trials were performed. Furthermore, as the immune system molecules in mice, guinea-pigs, and rabbits (these being the most used experimental models) are very different from those of humans, mainly in the MHC region mediating antigen presentation and protection induction, immunogenicity studies carried out on these animal models have very limited use for human vaccine development, as has been notoriously shown by the failure to apply such results to humans. On top of this, these experimental models are not infected by human malaria parasites, limiting furthermore their use in protective efficacy studies.

Although at first glance the ideal vaccine candidates seemed to be those conserved HABPs that did not display any amino acid sequence variation between the different *P. falciparum* malarial parasite strains, hundreds of our experiments with *Aotus* monkeys showed and convinced us that conserved HABPs were inadequate for eliciting any humoral or cellular protective immune response in immunized animals; this is a phenomenon that we have named the *conserved antigens' immunological code of silence*.[36,171,172]

Apart from the ethical considerations, we have also used the *Aotus* monkey as an excellent experimental model for vaccine development due to the high similarity between *Aotus* and human immune system molecules and, therefore, their ability to mimic the human immune response against malarial infection. Such characteristics and the ones described in the previous section make this molecularly characterized primate an ideal model for breaking conserved antigens' immunological code of silence and vaccine development.

Based on this data, for developing a logical and rational vaccine methodology at the molecular level, we decided to analyze these monkeys' immune system molecules by cloning and sequencing the *Aotus* genes encoding immunoglobulins, cytokines, Class I and II molecules, and TCR α, β, δ, and δ chains, which revealed striking homology with their human counterparts.[173−181]

Sequencing studies using the genes encoding these Class II molecules (HLA-DRβ1*-like) in *Aotus* monkeys, initially undertaken in 110 *Aotus* monkeys, have revealed 88%−100% homology with human HLA-DRβ1*04, 03, 08, 11, (13, 14), 15, 16, 10, 07, and 01 molecules[181] (data recently corroborated with larger numbers of *Aotus*). These immunogenetic studies have also shown that these monkeys displayed $\geq$80%−100% homology with human TCR molecules,[176,179] therefore making it a unique and exceptional experimental model for vaccine development, given that once the conserved antigens' immunological code of silence has been broken in *Aotus* monkeys, it would be much easier to transfer such results to developing vaccines for humans.

We have previously reported that the allele frequency for these HLA-DRβ1*-associated genes in *Aotus* monkeys is 20%−30% in each HLA-DRβ1*0403/0407, HLA-DRβ1*0422, HLA-DRβ1*0301, and HLA-DRβ1*15-16 allele, 10%−20% in HLA-DRβ1*08-11, and 5%−10% in HLA-DRβ1*1001, HLA-DRβ1*0101, and HLA-DRβ1*0701[181] alleles. Therefore, the maximum protective efficacy that a *single* modified HABP can induce in a random population of *Aotus* monkeys when being individually used as a subunit-based synthetic vaccine component is equivalent to the frequency of that particular allele in the vaccinated population of *Aotus* monkeys (therefore, a maximum of 20%−30%). A difference regarding humans is these alleles' percentage (*frequency*) of distribution in the wild monkey population, a fact that we have taken very seriously into account for developing a fully effective vaccine for human use.

3.3. MHCII (HLA-DRβ1*) Molecular Structure

MHCII molecules are expressed on the surface of professional antigen presenting cells, such as B-lymphocytes, monocytes, macrophages, *etc.*, and they consist of two noncovalently associated polypeptides: the almost monomorphic α-chain (pink ribbon in Figure 3B and D) and the highly polymorphic β-chain (pale blue ribbon in Figure 3B and D, adapted from PDB code 1FYT).[182] The characteristic amino acid sequence of each chain displayed in their heterodimer's association dictates their antigen specificity.

The elegant 3D structural work performed by Don Wiley,[182−185] Ian Wilson,[186,187] Daved Fremont,[188] John Kappler and Pipa Marrack,[189] Roy Mariuzza's groups,[190] and some others laboratories[191] has shown that both chains have a large extracellular region, a single transmembrane fragment, and a short cytoplasmic tail. These two chains combine to form a membrane-distal **p**eptide **b**inding **r**egion (PBR) or groove (Figure 3A and B) formed by a floor or platform of eight β-strands derived from both α- and β-chains and two α-helical walls, one formed

dx.doi.org/10.1021/cr100223m |*Chem. Rev.* 2011, 111, 3459–3507

by the α-chain and the other one by the β-chain (Figure 3B and D).[182−191]

A peptide fitting into the PBR (residues 1−9 of the peptide's binding register) is bound into this groove in an extended configuration that is stabilized by 11 H-bonds between the *peptide's backbone atoms*[182−191] and the *lateral chain atoms* of conserved and a couple of variable MHCII *residues* located on the walls and platform of the PBR (red balls in Figure 3B and D).

According to the canonical binding pattern, the side chains of the peptide's amino acids must fit inside two deep pockets (Figure 3C) formed by amino acids (represented as colored balls in Figure 3B and D) from both the MHCII α (pink) and β (pale blue) chains, named pocket 1 (displaying the Glyβ86Val dimorphism), which is of the utmost importance because this pocket anchors the peptide to the PBR (fuchsia pocket in Figure 3C and fuchsia balls in Figure 3B and D) and pocket 9, which also displays limited polymorphism on the basis of the presence of an Asp (D) residue in position 57 of the β chain. Here, the β57D positive variant establishes a salt bridge with an Arg (R) located in position 76 of the α-chain, whereas the β57D negative variant does not do so (β57Asp can be replaced by Ser, Thr, Ala, Val). This pocket 9 reaffirms the peptide's anchoring to the PBR (green pocket in Figure 3C and green balls in Figure 3B and D). The difference between these PBRs is that these pockets are wider, deeper, and positively charged in alleles carrying the β57D negative characteristic (β57D), since the salt bridge with α76Arg is not formed, thereby allowing the preferential fit of small negatively charged residues such as D and E or small neutral or apolar residues such as N, A, or S,[192] to establish H-bonds with the now free α76Arg.

Two other shallower pockets (Figure 3C) are pocket 4, which is mainly formed by the β-chain highly polymorphic amino acid sequence (dark blue pocket in Figure 3C and blue balls in Figure 3B and D), and pocket 6 (light brown pocket in Figure 3C), which is formed by residues from both α- and β-chains but mainly from the α-chain (light brown balls in Figure 3B and D).[182−191] These two pockets play an extremely critical role in the peptide's specific binding to the PBR, with the

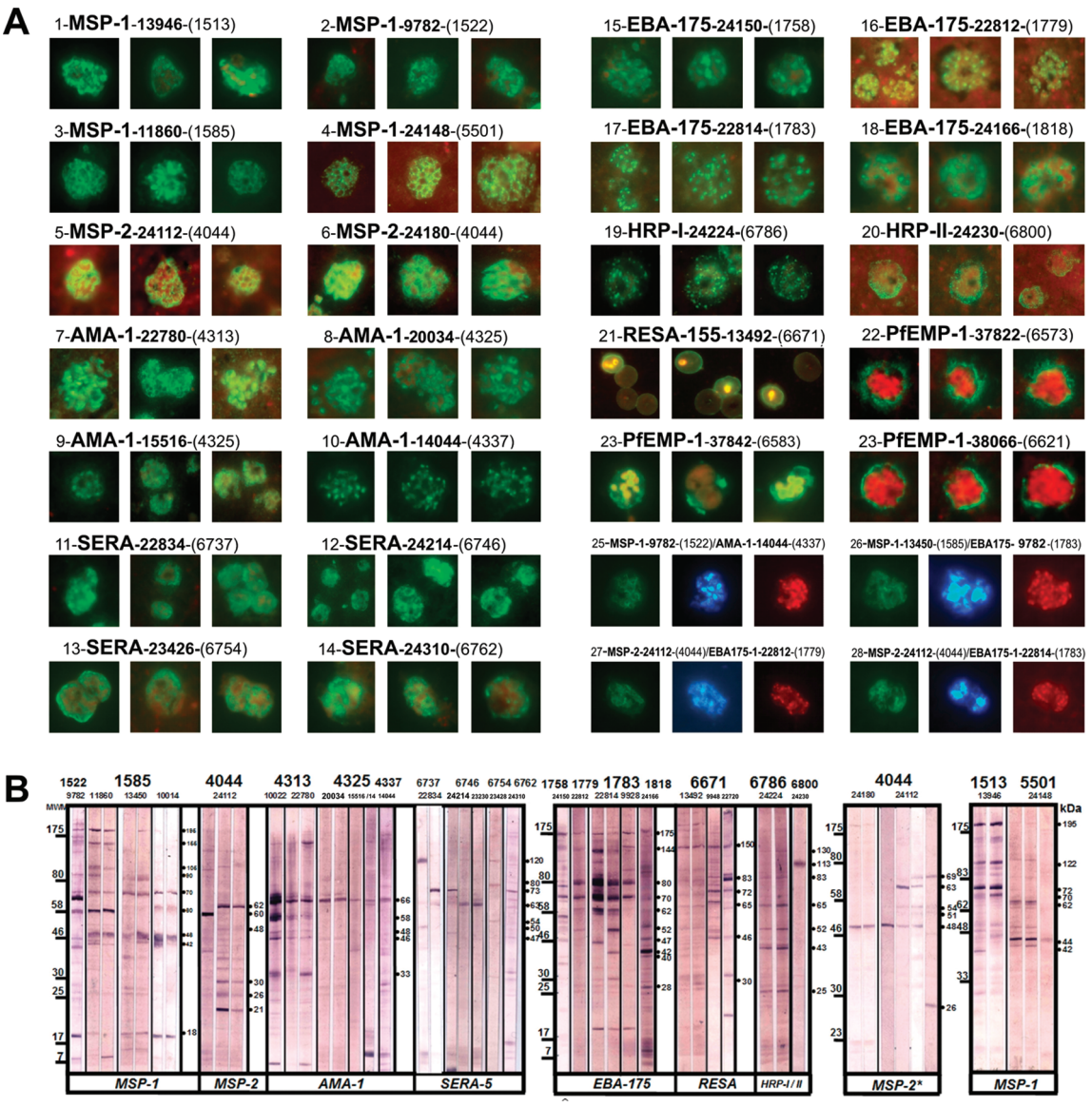

Figure 4. Continued

dx.doi.org/10.1021/cr100223m |*Chem. Rev.* 2011, 111, 3459–3507

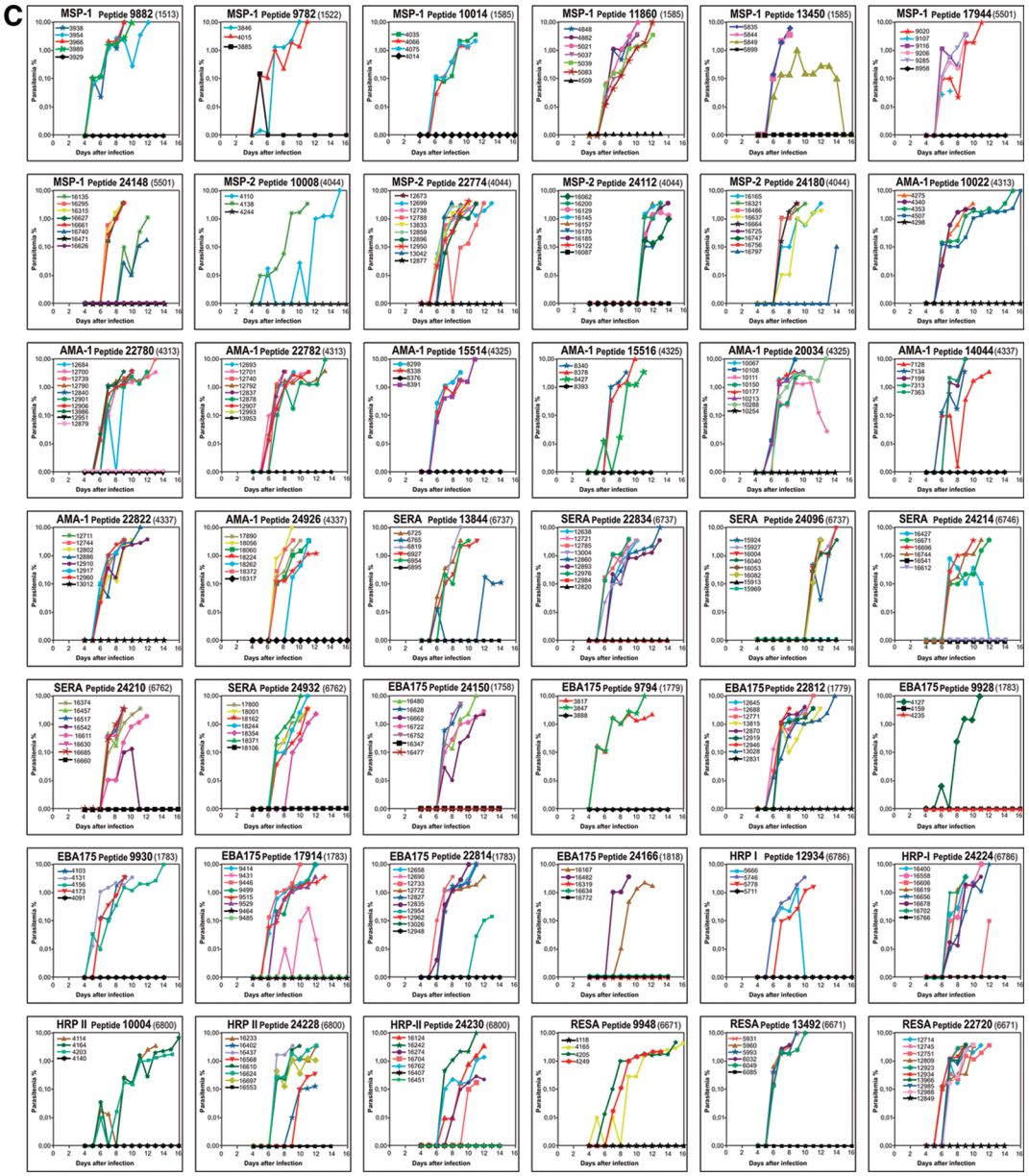

Figure 4. (A) Immunofluorescence of asexual erythrocyte stage staining patterns. Immunofluorescence patterns shown by sera from protected *Aotus* monkeys immunized with their corresponding protein (shown in bold letters) modified analogues (shown in bold) derived from conserved HABPs (shown inside parentheses), completely agreeing with the localization of *P. falciparum* proteins from which these modified HABPs were derived. This immune *Aotus* sera showed membrane, micronemal, diffuse intraplasmatic schizont, ring infected erythrocyte membrane, dotted erythrocytic membrane, and double fluorescence staining patterns, as described in great detail in the text (see section 4.2). (B) Western blot analysis of *P. falciparum* merozoite protein lysates with sera from protected *Aotus* monkeys immunized with modified analogues (as indicated on top of each membrane strip) derived from conserved HABPs (as indicated on top in bigger bold numbers), showing the recognition of protein bands, agreeing with the theoretical weights of the proteins from which their amino acid sequences were derived (indicated below each membrane panel) or their cleavage products. Molecular weight markers are shown to the left in kDa, while the molecular weights of the recognized bands are shown to the right. For a full description of these clear and specific reactivities, see section 4.2. (C) The course of parasitemia in *Aotus* monkeys immunized with fully protection-inducing peptides. Due to space limitations, ~60 more modified HABPs, derived from these and some other proteins are not shown (see Tables 1 and 2); those for which the 3D structure has been determined have mainly been selected. The course of parasitaemia displayed on a semilogarithmic scale was quantified daily by the highly specific and sensitive Acridine Orange staining method with a fluorescence microscope; it was determined in individual monkeys intravenously inoculated with 100,000 infected erythrocytes (freshly obtained from another infected monkey) 20 days after the last immunization. Ten thousand (10,000) RBCs were counted daily to determine their percentage of infection (%), and the complete slide (~1,000,000 RBCs) was read in fully protected monkeys to exclude the presence of small parasitaemias (breakthrough) potentially developing into fully blown disease later on. Nonprotected and control monkeys (not shown) displayed patent parasitaemia by days 4−6, reaching very high levels (≥5%) by days 8−10 that required immediate treatment. All monkeys still receiving treatment by day 14−15 were kept in quarantine for 20−30 more days to ensure their complete cure and released back into the Amazon jungle in excellent physical and behavioral conditions.

former displaying the main and most important genetic variations. Antigen specific residues enter inside a sort of cave or cap (clearly seen in Figure 3D), where a peptide's specificity is scanned in terms of its binding capacity and the peptide is

dx.doi.org/10.1021/cr100223m |*Chem. Rev.* 2011, 111, 3459–3507

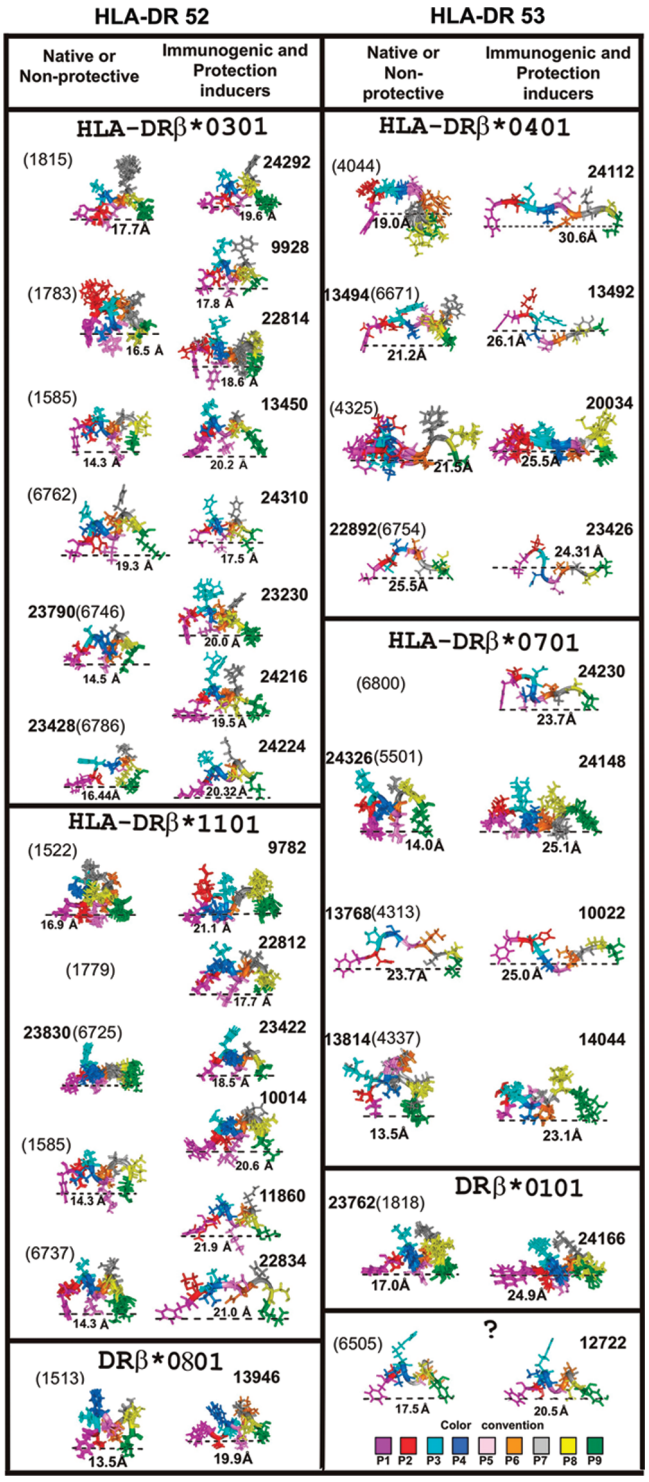

Figure 5. Comparing the ^{1}H NMR structures of native and modified HABPs according to their immunological characteristics: native or nonprotective versus *immunogenic protection-inducers*, grouped according to the HLA-DRβ1* binding characteristics of the immunogenic, protection-inducing HABP. The 3D structures of native HABP (labeled in parentheses) or nonimmunogenic, nonprotective (when native 3D structure was not available) are shown to the left of their corresponding modified *immunogenic protection-inducers* (written in *bold*). The amino acid-color code is based on HLA-DRβ1* binding activities, binding motifs, and binding registers as follows: pocket 1, fuchsia; P2, red; P3, turquoise; pocket 4, dark blue; P5, rose; pocket 6, light brown; P7, gray; P8, yellow; pocket 9, green. The distances between the farthest atoms of residues fitting inside pockets 1 and 9 are measured in angstroms (Å). There is a striking and very visible ~3.0 Å difference between the *immunogenic protection-inducing* modified HABPs binding to HLA-DR52 (HLA-DRβ1*0301 and HLA-DRβ1*1101) and HLA-DR8 molecules when compared to those binding to HLA-DR53 (HLA-DRβ1*0401 and HLA-DRβ1*0701) and HLA-DR1 molecules. There is also a clear difference in structural and residue orientation between these two haplotype lineages from binding peptides, suggesting haplotype structural compartmentalization of the protective immune system. These differences in distance, conformation, and residue orientation are very clearly observed when comparing native, nonimmunogenic, nonprotection-inducing HABPs versus immunogenic protection-inducing modified HABPs (Reprinted with permission from the following references (Copyright): 122 (2002); 74, 77, 87, 143 (2003); 129, 133, 142 (2004); 130, 220 (2005); 131 (2007) Elsevier. 71, 221 (2003); 171 (2008) John Wiley and Sons. 84 (2003); 111(2004) American Chemical Society. 238 (2008) Bentham Publishers. 237 (2007) De Gruyter. 134 (2001) Wiley-VCH).

stabilized via H-bond formation to be presented to the TCR and induce the appropriate immune response, or is otherwise released.

The antigen's residues fitting into these positions are called *anchoring residues* because they stabilize the peptide interaction with the MHCII molecule via an H-bond network and some other weaker electrostatic forces, such as van der Waals forces. The binding pockets are mainly characterized by the properties of the amino acids conforming P1, P4, P6, and P9 (Figure 3B and D) in the canonical structure of MHCII molecules, given that they provide the appropriate electrostatic environment and space needed for the peptide's anchoring residues to fit inside MHCII[182−191] molecules.

If a peptide is anchored in a firm and stable way, most of the other peptide side chains are directed outside the PBR for their scanning and interaction by the TCR to establish an appropriate MHCII/pTCR complex.

4. TOWARD THE DEVELOPMENT OF A STERILE IMMUNITY-INDUCING VACCINE

4.1. Shifting the Polarity of the Critical Binding Residues

It has been clearly established that conserved HABPs are immunologically silent given that they are poorly antigenic or *nonantigenic* (i.e., they are weakly recognized or not recognized at all by antibodies in the sera of people who have had one or several episodes of *P. falciparum* malaria); they are also *not immunogenic* (i.e., they do not induce antibody production upon immunization), and therefore, most of them do not induce protection against a malarial challenge.[71,74,75,77,84,87,103,111,112,122,129,130,133,134,143,171,172,193,194]

Our institute has been working to break the immunological code of silence of these conserved HABPs during the last 20 years. Conserved HABPs derived from 50[36−41,43,44] out of the 58 proteins involved in merozoite invasion of RBCs were thus identified and synthesized, and their critical RBC binding residues were identified (by Gly analogue scanning for most of them) and replaced by other residues having different physicochemical properties.

These native and modified HABPs (15−20-mer long) were polymerized via adding Cys to their N- and C-terminal regions. They were then homogenized in Freund's adjuvant and administered subcutaneously twice or three times (as minimal subunit-based components of a chemically synthesized antimalarial vaccine) on days 1, 20, and 40 in mice, rabbits, goats, and *Aotus* monkeys to determine their ability to induce antibodies against the parasite by IFA (Figure 4A1−A28) as well as Western blot

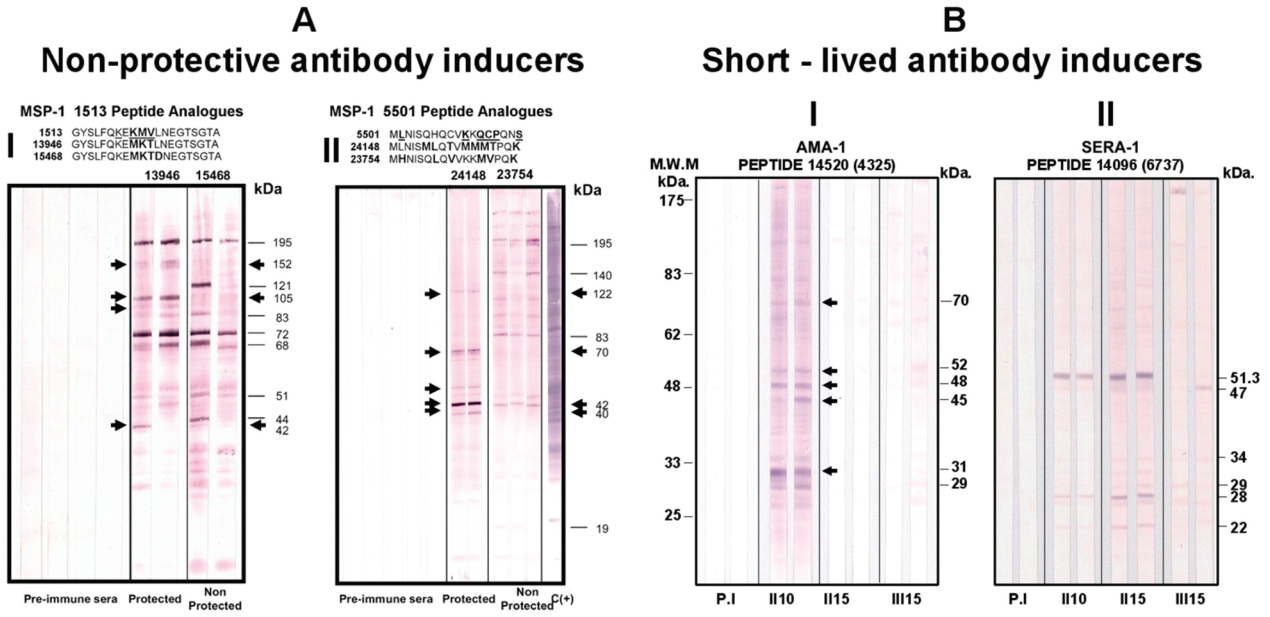

Figure 6. Western blot analysis of *Aotus* monkey sera immunized with immunogenic and protection-inducing or solely immunogenic *non*-protection-inducing modified HABPs. The arrows highlight differences in reactivity by comparing (AI) 1513 native (nonimmunogenic, nonprotective) derived peptides with its protective (**13946**) and immunogenic nonprotective (**15468**) analogues and (AII) 5501 native (nonimmunogenic, nonprotective) derived peptides with their protective (**24148**) and immunogenic nonprotective (**23754**) analogues. Two different patterns of reactivity may be observed: AI shows recognition of extra MSP-1 protein cleavage products (arrows) by sera from protected *Aotus* monkeys, and AII shows reactivity associated with a different MSP-1 protein processing pattern (arrows). All of them have been described as MSP-1 195 kDa precursor protein cleavage products. The critical binding residues are shown in bold in their corresponding amino acid sequences, and amino acid replacements rendering them immunogenic and protection-inducing or only immunogenic are highlighted, with L12D being the only difference between protection and nonprotection inducers. BI and BII: Western blot analysis of *Aotus* monkey sera immunized with modified short-lived antibody response-inducing modified HABPs. (BI) Peptide **14520** derived from AMA-1 protein HABP (4325) induced antibodies that appeared only 10 days after the second dose (II10) and then disappeared (arrows). (BII) Peptide **14096** (derived from SERA protein HABP 6737) induced short-lived antibodies lasting a little longer (II10, II15) and which then disappeared (arrows). Both short-lived antibodies are associated with nonprotection (Reprinted with permission from ref 195. Copyright 2006 Elsevier. Reprinted with permission from ref 196. Copyright 2005 American Chemical Society).

analysis with parasite lysates (Figure 4B). Furthermore, their protection-inducing ability was also determined in *Aotus* monkeys by the most stringent challenge methodology, the experimental intravenous inoculation (performed 20 days after the last immunization) of a 100% infective dose of 100,000 iRBCs freshly obtained from another nonimmune *Aotus* monkey previously infected with the *Aotus*-adapted *P. falciparum* (FVO) strain.

Protection has been defined in such studies as being the *complete* absence of parasites in the blood (determined daily by counting more than 10,000 RBCs and sometimes the complete slide) of challenged monkeys during the 15-day period of the experiment. Controls and nonprotected *Aotus* began showing parasites in their blood by days 4−6 when reading the same number of RBCs and developed very high parasitemia (≥5%) by days, thus requiring treatment.

This endeavor, involving testing thousands of synthetic peptides in large numbers of *Aotus* monkeys, revealed that most modifications were immunologically silent, since they did not induce IFA or Western blot reactive antibodies nor protection, while other modifications induced *high antibody titers associated with protection* against experimental challenge (Table 1, in Tables 2 and 3, group B, and Figure 5). This has been thoroughly shown with some of the 10 most relevant proteins derived from different evolutive and functional origins (shown in Tables 1 and 2). A certain number of modifications were able to induce high *nonprotective* antibody levels[195] (group C in Tables 2 and 3, and Figure 6A), others induced high nonprotective *short-lived* antibody titers[196] (group D in Tables 2 and 3, and Figure 6B) and very few induced *protective cellular immune response* without antibodies but with high cytokine production[197] (group E in Tables 2, 3, and 5).[171,172]

These large series of experiments involving replacing the critical binding residues by others having different physicochemical characteristics (such as charge, volume, and surface) led us to conclude that the *polarity of some critical binding residues had to be shifted* in the native conserved HABPs to render them immunogenic and capable of inducing protection, maintaining the same or similar masses, surfaces, and volumes.

Such a phenomenon, which has been deeply studied by our institute and will be analyzed in detail later on in this manuscript, led us to a partial understanding of the structural mechanisms (analyzed at the atomic level) used by microbes to evade the protective immune response and therefore set the basis for breaking the immunological code of silence, which could lead to developing synthetic vaccines against infectious and transmissible diseases, malaria being perhaps the best model for achieving this goal.

But the most striking result, a consequence of these numerous unique specific and selective substitutions that have to be performed in *some critical binding residues* to render these immunologically silent conserved HABPs into highly immunogenic and protection-inducing peptides, was that only phenylalanine (F) could replace arginine (R) and *vice versa* (amino acids

dx.doi.org/10.1021/cr100223m |*Chem. Rev.* 2011, 111, 3459–3507

are noted according to their one letter code), W ↔ Y, L ↔ H, I ↔ N, P ↔ D, M ↔ K, C ↔ T or V, Q ↔ E, A ↔ S. G has special physicochemical properties.[71,74,75,77,84,87,103,111,112,122,129,130,133,134,143,171,172,193,194]

4.2. Immunological Evidence

As protection against *P. falciparum* erythrocytic stage is mediated by the humoral immune response as shown 50 years ago by S. Cohen and I. McGregor[198−200] by transfusing either whole blood or isolated gamma globulins from recovered individuals to patients suffering from severe *P. falciparum* malaria, we decided to pursue such pathway and work with *Aotus* monkeys' antibodies induced after immunization with native HABPs or their modified analogues, rather than with the more difficult and still not well-defined cellular immune responses.

IFA and Western blot analysis were thus chosen rather than the more widely used and simple to perform ELISA test to avoid peptide−antipeptide reactivity (suggestive of an appropriate immunization regime but not conclusive of reactivity with terciary structures or the native protein), neo-antigen formation reactivity (consequence of different 3D structures adopted by the immunizing peptides), different monomer peptide antibody binding ability, conformational modification of the peptides regarding the reaction platform, and many other problems associated with ELISA methodology.

Immunological results can be semiquantitatively determined with these two serological methodologies (IFA and WB) in terms of antibody titers (the reciprocal of the dilution factor), and the pertinent molecules can be topographically localized in the merozoite by IFA (as shown in the whole of Figure 4A). By the same token, the original molecules or their cleavage fragments from which the amino acid sequences of native HABPs were derived can be recognized by WB, as observed in Figure 4B.

Western blot analysis was performed (due to the large number of samples to be analyzed), with different *P. falciparum* schizonts' protein lysate batches solubilized in Laemmli buffer and containing the denaturing reagent sodium dodecyl sulfate (SDS). Protein lysates were then separated by polyacrylamide gel electrophoresis (PAGE) and transferred to different nitrocellulose membrane strips to react with the corresponding antibodies in the immunized monkeys' sera (such minimal batch-to-batch variability can partly explain the small differences in mobility and molecular weights observed in Figure 4B).

An approximate correlation that *protection* achieved in these immunized monkeys (semiquantitatively determined as antibody titers) was the result of antibodies induced against the corresponding parasite's molecules was thus obtained, since IFA recognized native undenatured proteins as well as their cellular localization while WB led to identifying epitopes in these SDS-denatured molecules (separated by PAGE), which mainly recognized amino acid sequences and secondary structures. Therefore, a careful analysis of these serological data deserved thorough analysis, since they provided strong experimental support for this work. These immunological results were further associated with protection in challenge with the most lethal *P. falciparum* strain (FVO) adapted to *Aotus* monkeys.

Please note that hereinafter native HABPs will be shown in parentheses after their modified analogues shown in bold (the effect of modified HABPs being the main emphasis of this paper) to facilitate reading and understanding the basic concept implied in their use.

IFA analysis of sera from protected *Aotus* monkeys immunized with MSP-1 HABPs **13946** (1513), **9782** (1522), **11860** (1585), **13450** (1585), and **10014** (1585) showed immunofluorescence patterns suggestive of the presence of this protein on the mature schizont and merozoite surface (Figure 4A1−A3 for the first three HABPs and 4A25 and 4A26 for **9782** and **13450** double labeling). These sera were also seen to react by Western blot with 195 kDa molecules corresponding to the complete MSP-1 molecule from which this native HABP amino acid sequence was derived, as well as with its 155, 105, 90, 70, 67, 60, 46, 42, and 19 kDa cleavage fragments (Figure 4B). This was consistent with studies conducted by Chulay et al., using monoclonal antibodies[201,202] where MSP-1 was described as being proteolytically processed into 155, 112, 101, 90, 70, 67, 55, 45, 42, and 19 kDa fragments completely corresponding to the cleavage products recognized by *Aotus* sera immunized with the immunogenic modified HABPs described herein.[202]

Please note that despite the identical IFA membrane patterns and some similarities in Western blot reactivity between the complete MSP-1 molecule and some of its cleavage fragments, the antibodies induced by different analogues from the same conserved HABP derived from the same protein (MSP-1) induced very clear and visible Western blot differences (Figure 4B) associated with these peptides' ability to bind to different MHCII molecules. Modifications performed on **13450** (1585), which strongly bound to HLA-DRβ1*0301, resulted in a different molecular recognition pattern by Western blot to that induced when modifications were performed on peptide **11860** (1585), which displayed high HLA-DRβ1*1101 binding capacity (Tables 1 and 3).

Conserved HABP 1585 (residues E1367−E1386) was localized close to the cleavage site for the first MSP-1 cleavage process, producing 83, 38, 33, and 42 kDa fragments,[96] more specifically 17 residues downstream of the N terminus of the large 42 kDa fragment. This 42 kDa MSP-1 recombinant fragment has induced growth and intraerythrocytic maturation inhibition antibodies against the parasite when used as a vaccine candidate in humans[203,204] but has not been associated with clinical malaria protection.

This data shows a common reactivity pattern that we have observed in most malarial proteins analyzed so far where small modifications performed in different parts of the same conserved HABPs have induced different immune responses associated (as we show here) with their ability to bind to different HLA-DRβ1* molecules or displaying different motifs and/or binding registers which could lead to different MHCII/pTCR complex formation, a topic analyzed in more detail in sections 5 and 6.

It should be stressed that all these immune responses induced by MSP-1 derived HABPs located in this protein's soluble cleavage fragments which are released to the milieu are associated with binding to molecules belonging to the same HLA-DR 52 haplotype allele (Table 1 and Figure 3).

Based on the different reactivities induced by the same peptide, following different modifications, it is not difficult to envision the tremendous problems in designing a vaccine using complete proteins or their recombinant fragments, a problem which becomes even worse when working with complete microorganisms.

The problem of choosing the appropriate mixture or combination of these individually highly immunogenic, protection-inducing modified HABPs to produce a fully protective, chemically synthesized, minimal subunit based, multiantigenic, multistage, antimalarial vaccine also did not escape our attention. This problem, currently being resolved in our institution, is

nevertheless less complex than developing a vaccine involving a large group of complete molecules (either DNA, vector-based or recombinant) or entire microorganisms (dead or attenuated), which can partly explain the very few vaccines obtained throughout the last 120 years working with the above-mentioned methodologies, thereby providing a stronger reason for continuing the search for a logical and rational methodology for vaccine development via synthetic peptide chemistry.

IFA analysis of *Aotus* monkey sera producing high antibody titers against the parasite and being protected upon immunization with 19 kDa MSP-1 **24148** (5501) revealed a grapelike merozoite membrane pattern in mature schizonts (Figure 4A4). Such sera also displayed reactivity (Figure 4B, far right panel) with this molecule's ~62, 44, and 42 kDa cleavage fragments, as well as weak reactivity with a 122 kDa fragment, corresponding to the MW from proteolitic fragments derived from MSP-1 from which the amino acid sequence was obtained.

Likewise, the same IFA grapelike (Figure.4A5) pattern of merozoite membrane proteins was displayed by the thoroughly studied MSP-2 **24112** (4044), as previously described.[84] Due to this HABP's great relevance in inducing protective immunity, monkey trials were repeated several times with **24112** and other 4044 analogues such as **24180**, with the same IFA pattern being found (Figure 4A6) and these protected *Aotus* sera's strong reactivity with 63, 60, 48, 30, 23, 21 kDa molecules by Western blot, corresponding to the molecular weight of native MSP-2 and its cleavage products from which our HABP's amino acid sequence was derived (Figure 4B).

The AMA-1 protein[205] is synthesized in the merozoite's Golgi apparatus to be stored in the micronemes and later on translocated to the merozoite membrane,[206] where it performs a central role in the merozoite's binding, mediating apical reorientation to allow the formation of the **t**ight **j**unction (TJ) during RBC invasion.[207,208] It is visualized by IFA as large dots inside mature schizonts[209] and in the apical pole of free merozoites (Figures 4A7−4A10). Such a fluorescence pattern confirmed AMA-1's micronemal origin and translocation to the apex to allow TJ formation. Sera from *Aotus* immunized with AMA-1-derived immunogenic and protection-inducing **10022** (4313), **22780** (4313) (Figure 4A7), **20034** (4325) (Figure 4A8), **15516** (4325) (Figure 4A9), and **15514** (4325) and **14044** (4337) (Figure 4A10) all recognized a 66 kDa molecule by Western blot (Figure 4B), corresponding to the AMA-1 fragment that is cleaved in the rhoptry's neck to be later redistributed on the merozoite's surface, which is where these HABPs are located (AMA-1 domains I, II, and III, respectively).

However, sera induced by **10022** and **22780** (4313) localized in AMA-1 domain I not only recognized the 66 kDa fragment but also showed strong reactivity with previously described 58, 48, 46, 33, and 10 kDa cleavage fragments; the latter reactivity was also recognized by *Aotus* antisera **14044** anti-4337. This probably corresponded to a ~110-amino-acid-long stub where this HABP was located which remained anchored to the merozoite membrane and was the only AMA-1 processed fragment carried inside recently infected RBC.

As before, with all processed MSP-1 merozoite molecules, AMA-1 modified HABPs strongly bound to different HLA-DR53 haplotype alleles (Tables 2 and 3) so that **10022** (4313), **22780** (4313), **15516** (4325), and **14044** (4337) all bound to HLA-DRβ1*0701 and **20034** (4325) bound to both HLA-DRβ1*0701 and 0401 with similar binding capacity, confirming a similar pattern of compartmentalization but with a different HLA-DR haplotype allele, thereby providing a possible mechanism for dealing with the numerous evasion strategies microorganisms display during the invasion process.

SERA-5 is a member of the papain-like family which is essential for *P. falciparum* protein processing during all developmental stages; it is synthesized in the Golgi apparatus and stored in the rhoptries to mediate merozoite egress from infected RBC[210] after being processed by the merozoite membrane-bound multifunctional enzyme from the subtilisin-like family named PfSUB1.[211−213] It displayed a diffuse intracytoplasmic fluorescence pattern in mature schizonts, as shown by IFA analysis with sera from monkeys immunized with this protein's **22834** (6737) (Figure 4A11), **24214** (6746) (Figure 4A12), **23230** (6746), **23426** (6754) (Figure 4A13), and **24310** (6762) (Figure 4A14). Western blot revealed strong reactivity between sera from protected monkeys immunized with **22834** (6737) with a 116-kDa molecule corresponding to the complete SERA protein precursor and its 73 kDa fragment (Figure 4B) as well as recognition of 73, 56, and 50 kDa fragments by sera from *Aotus* immunized with **24214**, where HABP 6746 was located together with **23230** and **23426** (6754).[88] Meanwhile, **24310** (6762) mainly reacted with the 73-kDa fragment where this HABP was located, all processing previously described SERA-5 fragments.

The thoroughly analyzed RBC invasion-mediating, highly relevant micronemal protein EBA-175 was detected by IFA as big fluorescent dots[214] inside mature schizonts when sera from protected monkeys immunized with **24150** (1758) (Figure 4A15), **22812** (1779) (Figure 4A16), **22814** (1783) (Figure 4A17), and **24166** (1818) (Figure 4A18) was used. Such sera also recognized a 175 kDa molecule by Western blot and its 145, 80, 70, 62, 52, 46, 42, 40, and 28 kDa cleavage fragments (Figure 4B) while protected *Aotus* monkeys who had been immunized with **24166** (1818) displayed strong reactivity only with the 175, 52, 47, 42, and 28 kDa cleavage fragments (Figure 4B), suggesting that cleavage processing this conserved HABP is only present in these fragments in EBA-175.

The RESA-155 molecule synthesized during the early stages of *P. falciparum* infection of RBC was visualized by IFA reactivity (Figure 4A21) of sera from protected *Aotus* monkeys immunized with **13492** (6671) as a green fluorescence pattern on the iRBC membrane identified by the intracytoplasmic presence of *P. falciparum* rings shown as yellow fluorescent rings inside iRBC. This phenomenon led to this molecule being named **r**ing **e**rythrocyte **s**urface **a**ntigen (RESA). The same sera from protected *Aotus* monkeys immunized with **13492** (6671), **9948** (6671), and **22720** (6671) showed a ~150 kDa molecule (its name thus being RESA-155) by Western blot reactivity and 83, 72, 66, 46, 32, and 20 kDa cleavage fragments (Figure 4B).

KAHRP, also called HRP-I, contains a PEXEL motif[126] and is transported from the Golgi apparatus to the PV and from there to the cytosol and iRBC membrane. We visualized it as small intraerythrocytic fluorescent dots (Figure 4A19) when reacting with sera from protected *Aotus* monkeys immunized with the **24224** (6786). Such sera also recognized 83, 65, 52, 43, and 25 kDa molecules which corresponded to these native proteins' molecular weights and their cleavage fragments (Figure 4B).

HRP-II, which is synthesized in the merozoite's cytoplasm throughout the intraerythrocytic cycle and carried to the RBC cytosol to perform transport functions through its PEXEL motif,[215] was visualized by IFA as fluorescent microdots intracytoplasmatically located inside iRBCs when sera from protected *Aotus* immunized with **24230** (6800) were used (Figure 4A20). Western blot showed

that these sera also recognized a ~113 kDa molecule from which the **24230** amino acid sequence was derived (Figure 4B).

A recently reported experiment performed with a group of HLA-DRβ1*0403-genotyped *Aotus* monkeys which were protected upon immunization with **24112** (MSP-2-derived 4044) showed that Western blot recognized serological reactivity with 68, 62, 54, 51, 48, and 26 kDa molecules (Figure 4B far right) corresponding to MSP-2 and its cleavage fragments.[216] This demonstrated the complete reproducibility of these results in completely different groups of *Aotus* monkeys caught in the wild when comparing these sera's reactivity with that of others shown in Figure 4B.

As reference, Western blot showed that the reactivity of sera from *Aotus* protected against *P. falciparum* by immunization with **13492** (MSP-1 N-terminal-derived 1513) had strong reactivity with a 195 kDa molecule, corresponding to the molecular weight of the complete MSP-1 native molecule and its 122 and 70 kDa cleavage fragments where this HABP has been reported to be located. Please note the difference in reactivity induced by peptides modified from 1585 and 5501 derived from amino acid sequences located toward the C-terminal portion of MSP-1 (in the 42 kDa and 19 kDa processed fragments), when compared to the reactivity induced against **13492** (1513), which was more similar to **9782** (1522); the last two HABPs were located in this protein's N-terminal region, which includes the 83 kDa fragment, completely agreeing with Chulay's studies[201,202] performed with monoclonal antibodies.

We have recently identified 6573, 6583, and 6584 in PfEMP-1, which were located in the C32-cell binding domain DBL3X, as well as 6621 and 6622 located in the RBC binding domain DBL6ε. Modifications performed on these HABPs' H-bond residues yielded highly immunogenic **37822** (6573) (Figure 4A22), **37838** (6584), and **37842** (6583) (Figure 4A23), which reacted with a membrane protein present in trophozoites and early schizonts in IFA studies performed with **unfixed** iRBCs,[217] revealing quite interesting reactivity patterns which were very different from the homogeneous RESA pattern which was detected on early trophozoites or recently invaded iRBCs. By the same token, sera from *Aotus* monkeys immunized with **38066** (DBL6ε-derived 6621) induced very high antibody titers associated with iRBC membranes (Figure 4A24). All these sera reacted very strongly with a very high ~350 kDa molecular weigh protein in Western blot assays (data not shown) performed with different *P. falciparum* isolates (FCB-2, NF54, HB3, 3D7 PAS) and the *Aotus*-adapted *P. falciparum* FVO strain where this molecule is abundantly expressed.[110]

Colocalization studies for these molecules were also performed with anti-*Aotus* IgG goat antisera labeled with either of two different fluorochromes: fluorescein-isothiocyanate (FITC), which gives a green-yellow fluorescence, and rhodamine isothiocyanate (RITC), which gives red fluorescence when being observed by immunofluorescence (UV) microscopy. A DNA-binding fluorochrome (DAPI) emitting blue fluorescence was used for identifying the parasites' nuclei to help in locating subcellular structures.

In these few examples of colocalization studies, **9782** (derived from N-terminal MSP-1 HABP 1522) displayed green fluorescent reactivity on the merozoite membrane (Figure 4A25), as shown by others with antibodies against the complete MSP-1 83 kDa recombinant fragment,[218,219] while sera from *Aotus* monkeys immunized with **14044** (AMA-1-derived 4337) displayed bright red-dotted fluorescence inside the merozoites, consistent with this molecule's micronemal and apical location (Figure 4A25).

Such reactivity was very similar when using MSP-1 1585-derived **13450** *Aotus* antisera as the first antibody, giving green membranal fluorescence while antibodies against **22814** (EBA-175-derived 1783) displayed an intense red intracytoplasmic fluorescence on red dots, indicative of its micronemal origin (Figure 4A26). The immunofluorescence pattern was quite similar when *Aotus* immune sera against **24112** (MSP-2-derived 4044) was used, which gave a very bright green membranal fluorescence pattern characteristic of this molecule while **22812** (EBA-175-derived 1779) induced antibodies displaying a dotted intracytoplasmic red fluorescence pattern coherent with what has been previously described (Figure 4A27). The same reactivity pattern was observed when working with **24112** (MSP-2-derived 4044) induced antibodies as the first reagent and **22814** (EBA-175-derived 1783) *Aotus* antibodies as the second antibody layer.

It should be stressed that *all* these studies (including serological analysis performed with polyclonal sera) were carried out with outbreed populations of wild *Aotus* monkeys caught at different sites in the Colombian Amazon basin at different times during our studies and that *all* these sera were previously heat-inactivated, absorbed with *Escherichia coli* and mycobacterial lysates covalently coupled to Sepharose beads to remove nonspecific cross-reactivity in sera from immunized animals, or cross-reactive antibodies induced against the dead *Mycobacterium tuberculosis* bacilli present in complete Freund's adjuvant.

It should also be stressed that sera from these *Aotus* monkeys immunized with *chemically synthesized* specifically modified conserved HABPs recognized *native* nonstructurally modified merozoite molecules in air-dried parasites in IFA tests, as well as their subcellular location as described for these proteins. Furthermore, they reacted with denatured original molecules and/or their cleavage fragments when analyzed by Western blot, as elegantly shown by many other groups.

4.3. Evidence of Induced Sterile-Immunity

However, more important is the fact that all the modified HABPs reported here (Table 1) induced complete *sterile immunity* in some monkeys when vaccinated, understanding *sterile immunity* to be the *complete absence* of parasites in immunized monkeys' blood during the 15 days the experiment lasted after the intravenous injection of 100,000 freshly obtained iRBC. Those monkeys developing complete sterile immunity were the same animals having high IFA antibody titers and corresponding protein reaction seen by Western blot. All *Aotus* controls and nonprotected monkeys developed very high parasitaemia (>5%) by days 8−10 that required immediate treatment to save their lives and then keep them in excellent health (Figure 4C and Table 1).

The course of parasitaemia in monkeys immunized with some of the fully protection-inducing modified peptides (*shown here for the first time*) stresses the importance of the very thorough and careful modification of conserved HABPs which was performed on hundreds of peptides tested in large numbers of *Aotus* monkeys (during the last 20 years) to finally obtain such highly immunogenic and protection-inducing modified HABPs, in our endeavor to develop a fully effective anti-*P. falciparm* malaria vaccine and to establish the rules or principles for a logical and rational methodology for vaccine development using chemically

synthesized minimal subunit based peptides, the *raison d'être* of this research.

Some other modifications which induced high antibody titers, as determined by both methods, did not induce any protection against the same experimental challenge (shown later on). Hundreds of modified peptides that induced high antibodies levels but maintained low parasitaemia ($\leq$0.1%) for some time ($\geq$15 days) were not included (or their information was used for further modification), since these monkeys developed high parasitaemias that required treatment later on (a phenomenon called semi-immune reactivity by others). Information gleaned from them was thus used for making further modifications to peptides; however, they were not considered to be protection-inducing modified HABPs. But many modifications did not induce any antibody production nor protection in large numbers of immunized monkeys, as has been reported in the corresponding publications.

The reproducibility of these results in different groups of *Aotus* monkeys caught in the wild ruled out the possibility of confounding factors in these trials, such as previous exposure to related malarial parasites (ruled out by the *absence* of positive IFA and Western blot reactivity in their preimmune sera), unspecific stimulation by Freund's adjuvant (since these sera were previously absorbed by tuberculosis and *E. coli* lysates, and furthermore, the control monkeys also immunized with saline solution and Freunds Adjuvant were never protected), monkey blood incompatibility between donor and recipient monkeys during challenge (since there was clear correlation with their serological reactivity), and specific genetic variants or mutants in challenge studies, since synthetic modified HABP amino acid sequences were derived from worldwide *P. falciparum* merozoite protein conserved sequences obtained from strains published in the PlasmoDB database (mainly from the *African* 3D7 strain). Furthermore, IFA and Western blot analysis were performed with the *Colombian* FCB-2 strain, and challenges were made with the *Vietnamese* FVO strain, thereby avoiding the strain-specific immunity induced by their products which has often been found by other groups.

Work has almost been completed to determine the role of amino acid side chain stereospecific constraints such as *gauche*$^+$, *gauche*$^-$, *trans*, *etc*. in peptide structure to further modify HABPs according to their HLA-DRβ1* allele binding characteristics (see below) and to provide most of the rules and principles required for designing desperately needed minimal subunit-based, multiantigenic, multistage synthetic vaccines, one of them being an antimalarial one.

4.4. Compartmentalizing the Immune Response

Our Institute's work during the last 20 years attempting to break the immunological code of silence of conserved antigens has revealed some other very striking findings; *compartmentalizing a protective immune* response against *P. falciparum*-modified merozoite proteins has been seen to be associated with HLA-DR genetic characteristics.

Protective immunity associated with high antibody titers induced by the modified conserved HABPs shown in Table 3 was found to be associated with a preferential binding of these modified peptides to HLA-DR52 haplotype alleles (HLA-DRβ1*03 and HLA-DRβ1*1101) from native and modified HABPs: **24292** (EBA-175-derived 1815),[220] **9928** (EBA-175 1783),[77] **22814** (EBA--175 1783), **13450** (MSP-1 1585),[134] **24310** (SERA 6762),[144] **24214** (SERA 6746),[87] and **24216** (SERA 6746), **24224** (KAHRP 6786),[130] **37842** (PfEMP-1 6583), **37838** (PfEMP-1 6584), **38070** (PfEMP-1 6621) (Cifuentes et al., submitted for publication), **9782** (MSP-1 1522),[221] **22812** (EBA-175 1779),[103] **23422** (SERA 6725),[142] **10014** (MSP-1 1585),[134] and **11830** (MSP-1 1585) (this review) and **22834** (SERA 6737).[143]

13946 (MSP-1-derived 1513) located in this protein's N-terminus[133] strongly bound to HLA-DR8 (HLA-DRβ1*08) (Pluschke G. Swiss Tropical Institute, Basel, Switzerland, personal communication), this being the only modified HABP so far found to bind to HLA-DRβ1*0801 molecules, a genetic trait having low prevalence in both humans ($\sim$10%) and monkeys.[181]

It has been postulated that the HLA-DRβ1*08 molecule might have originated from a gene-contraction event occurring in an HLA-DR52-like primordial gene about 100,000 to 20,000 years ago, since this gene resembles the DRB1 gene at the 5′-end and the DRB3 gene at the 3′-end.[156,222] Therefore, HLA-DR8 binding could be associated with HLA-DR52-derived haplotype binding activity.

All these HABPs were derived from merozoite protein soluble fragments, remaining loosely bound to each other or to other proteins on the merozoite membrane[139,141] and/or were involved in protein enzymatic processing during parasite invasion of RBCs or endothelial cells. Therefore, all these protection-inducing modified HABPs displayed HLA-DR52 and/or HLA-DR8 haplotype binding characteristics (Tables 2 and 3, group B).

A protective immune response associated with HLA-DR53 binding capacity, particularly with HLA-DRβ1*0401, has also been induced by modified conserved HABPs derived from native membrane-anchored molecules or their fragments. Among these HABPs were **13492** (6671) and **22720** (6671) from RESA-155,[193] which is anchored and exposed on the iRBC membrane (Figure 4A21) during early stages of parasite invasion[129] 50 residues downstream of a PEXEL motif[124] and MSP-2-derived **24112** (4044) and **24180** (4044),[172] which were attached (4044) to the parasite's membrane via a GPI-tail,[84] being located in this molecule's N-terminal region, one residue upstream of a degenerate PEXEL motif (RxL/MxE).

AMA-1-derived peptides such as **20034** (4325),[74] which was translocated to the merozoite membrane during reorientation and TJ formation during RBC invasion,[208] were also associated with HLA-DR53 haplotype's alleles. It has been shown that EBA-175-mediated invasion of RBC was facilitated by the N-terminal portion of EBA-175 inside which **24150** (1758)[114] was included; **23426** (SERA-5 6754) was also associated with binding to DRβ1*0401 molecules (Bermudez et al., submitted for publication).

By the same token, **24148** (5501),[71] corresponding to the 19 kDa-MSP-1 fragment's N-terminal, the only fragment of this protein remaining anchored to the merozoite membrane via a GPI-tail and carried inside the recently invaded RBC and located five residues upstream of a PEXEL motif, was also associated with HLA-DR53 (HLA-DRβ1*0701) binding activity. AMA-1-derived peptides **22780** (4313), **10022** (4313),[42] **15516** (4325), and **14044** (4337)[110] were all located in different domains of the AMA-1 protein; they also bound strongly to HLA-DRβ1*0701 purified molecules, as occurred with **24230** (6800)[193] two residues upstream of a PEXEL motif. All the foregoing peptides thus displayed HLA-DR53 (HLA-DRβ1*04 and HLA-DRβ1*07 alleles) haplotype binding characteristics (Tables 2 and 3, group B).

EBA-175 **24166** (1818)[111] located in the protein's C-terminal fragment, in the so-called region III−V, which remained anchored to the merozoite membrane during RBC invasion, also

induced IFA antibodies (Figure 4A18), recognizing the EBA-175 protein and its cleavage products, as confirmed by Western blot (Figure 4B). Interestingly, these immunological properties were associated with haplotype HLA-DR1 (HLA-DRβ1*01) binding ability (Tables 2 and 3), this being the only HABP found to have high binding to this molecule, which also displayed ~10% HLA-DRβ1*01 allele frequency in humans and *Aotus* monkeys.[181]

The protective immunity induced by modified HABPs against these merozoite and/or iRBC membrane-anchored protein peptides was therefore associated with HLA-DR53 or HLA-DR1 haplotype-related immune responses (Tables 2 and 3, group B).

The data gathered for the HABPs derived from the ten (10) most relevant *P. falciparum* proteins involved in different steps of merozoite invasion of RBCs (MSP-1, EBA-175, SERA, RESA, MSP-2, AMA-1, HRP-I, HRP-II, ABRA, and PfEMP-1)[26] led us to suggest that *genetic control of the immune response* against *P. falciparum* malaria was also *functionally and structurally compartmentalized*.

Recent studies performed by our group with 100 new conserved HABPs derived from 40 more of the proteins involved in RBC invasion (such as EBA-181, EBA-140, MAEBL, EBL, CLAG, RAMA, RAP-1, RAP-2, RAP-3, Rh-1, -2, -4, -5, REX, *etc.*), analyzing their ability to bind to purified HLA-DR molecules, confirmed this conclusion.[26] Table 3 also shows the association between parental HABP secondary structure and the HLA-DR binding capacity shown by their modified immunogenic protection-inducing HABPs.

4.5. Immunological Escape

An interesting finding by Holder et al.[50] was that only two of the large panel of monoclonal antibodies (MoAb) raised against the MSP-1 19 kDa fragment were able to inhibit merozoite invasion of RBCs, thus being called inhibitory antibodies (our HABP 5501 was located in this fragment and is shown as an orange surface in Figure 2C1). They showed that the reactivity of inhibitory MoAb 12.8 and 12.10 was specifically directed against two amino acids in the HABP 5501 C-terminus (MLNISQHQCVKKQCPQNS), while the reactivity of all neutralizing inhibitory antibodies as well as blocking antibody activity (MoAbs 7.5, 1E1, 2.2, 111,4, 2F10, *etc.*) was targeted at regions outside HABP 5501 (EGF domains, *etc.*). A large number of them did not have any inhibitory activity despite being seen to react with recombinant molecules by ELISA or WB and the *P. falciparum* parasite by IFA (therefore named neutralizing and blocking, depicted by a blue surface in Figure 2C1). This observation suggested the absence of antibody reactivity against conserved HABPs and, therefore, such relevant merozoite structures' immunological silence.

These elegant results clearly confirmed our previous findings related to the immunological silence of conserved HABPs at the single amino acid level (detected by PEPSCAN),[223] suggested the induction of useless (neutralizing) or even deleterious (blocking) immune responses induced by the *P. falciparum* parasite as a strategy to escape immune pressure, and led us to propose a compartmentalization of immunological escape mechanisms. Accordingly, the immunological relevant sequences or residues would be located far away in the molecule's 3D structure to hide conserved HABPs from persistent immune response surveillance. This can be clearly observed in all structures in Figure 2C (in blue), where the darker the color, the more relevant antigenic variation was or more variable the residues were, as a way to distract the immune response by changing the most antigenic residues, but NOT involving any conserved HABPs.

By the same token, mapping *P. vivax* DBL polymorphic amino acids from Colombian[224] and Papua New Guinean[225] isolates has revealed that conserved RBC-binding HABPs 1629 (yellow ribbon in Figure 2C2) and 1639 (Fuschia ribbon in the same figure), forming the channel or trough where the DARC receptor binds, were situated at opposite sites of these polymorphic residues (depicted as blue balls; the darker, the more variable) displayed on the Connolly surface.

Similarly, the amino acid sequencing of EBA-175 RII in isolates from different parts of the world has shown that this fragment's genetic variability is located in areas which were very distant from the 100-amino-acid-long segment where RBC-binding HABPs 1779 and 1783 and hepatocyte-binding HABPs 1780, 1781, and 1782 were located (as clearly seen in Figure 2C3, dark blue surfaces) and that such genetic variations[226] did not affect the binding interaction of conserved HABPs 1779 (depicted in pink) and 1783 (red surface in Figure 2C3).

The very relevant AMA-1 protein involved in RBC invasion by merozoites as well as hepatocyte invasion by merozoites,[113] shown by us[118] and others, contains conserved HABPs 4313 located in domain I (red surface in Figure 2C4) and 4325 located in domain II (fuschia surface, Figure 2C4), both strongly binding to RBCs, establishing H-bonds creating troughs or channels for as yet unknown receptors on these cells, as we have previously shown.

Extensive and deep analysis of such an important protein for merozoite reorientation and formation of the moving tight junction with RBC membrane to allow parasite penetration has revealed extensive genetic polymorphism having more than 200 genetic variations in single amino acids and ~24 genetic combinations of two or three genetic variants in different amino acids, named haplotypes. Most of these genetic polymorphisms were located in domain I, known to be involved in strain-specific immunity against *P. falciparum*,[227,228] hence suggesting that these allelic polymorphisms were responsible for immune evasion.[229] These genetic variations acting together formed *clusters* C1−C7, containing so-called antigenic escape residues (AER) identifying five highly polymorphic residues in C1 located in an α-helical region in domain I[230] and a second cluster or C2 localized in domain II. The AERs located in domain III enhanced the inhibitory function of those located in domain II.[231] All these strain-specific genetic variations were located in distant parts of AMA-1, far away from where HABPs 4313 and 4325 were located (identified as dark blue surfaces in Figure 2C4: the most variable residues are shown in dark blue), suggesting a mechanism for distracting the immune system by localizing the most variable and immunogenic variations of this strain-specific immunity far away from the place where conserved HABPs were localized.

Altogether, data obtained from different proteins involved in RBC or hepatocyte invasion, from different evolutive origins, clearly suggested these molecules' structural compartmentalization to enable them to perform different functions; some these **mu**lti**fu**nctional proteins **d**omains (MUFUCIDs) involved in receptor−ligand interactions essential for parasite survival were structurally distant from other areas involved in immune distraction, as a way of evading immune pressure.

Table 4. Alignment of Modified Immunogenic and Protection-Inducing HABPs Derived from Different Proteins According to Their HLA-DRβ1* Molecule's Binding Registers[a]

	Peptide/pocket	P1	P2	P3	P4	P5	P6	P7	P8	P9
DRβ1*0301	**24292** (1815)	I	N	I	D	Q	E	F	N	L
	9928 (1783)	L	Y	R	D	E	Y	W	K	N
	13450 (1585)	Y	L	L	D	L	A	G	V	Y
	24310 (6762)	V	Y	H	N	L	M	H	I	K
	23230 (6746)	W	I	R	A	S	K	Y	L	L
	24224 (6786)	M	D	L	D	G	E	M	M	M
	Average in volume (Å^3)		158.2	166.7				164.9	153.2	
DRβ1*1101	**9782** (1522)	Y	N	L	K	I	R	A	G	G
	22812 (1779)	L	M	I	K	M	H	I	L	A
	23422 (6725)	I	S	F	M	S	N	A	G	S
	10014 (1585)	Y	R	S	L	K	K	Q	L	E
	Average in volume (Å^3)		135.8	153.0				122.0	113.4	
DR8	**13946** (1513)	Y	S	L	F	Q	K	E	M	K
DRβ1*0401	**24112** (4044)	Y	N	M	V	I	R	R	S	M
	13492 (6671)	Y	R	Y	S	N	N	Y	E	A
	20034 (4325)	F	L	P	T	G	A	F	M	A
	13790 (1758)	Y	G	S	D	D	N	N	D	K
	Average in volume (Å^3)		129.5	142.1				168.7	125.4	
DRβ1*0701	**24230** (6800)	F	D	D	N	L	T	A	A	N
	24148 (5501)	T	V	M	M	M	T	P	Q	K
	14044 (4337)	T	T	P	V	L	K	E	K	P
	10022 (4313)	F	H	P	S	G	K	S	P	V
	Average in volume (Å^3)		130.1	129.8				109.6	130.9	
DR1	**24166** (1818)	Y	D	K	M	L	P	L	D	D

[a] P2, P3, P7, and P8, pointing in the opposite direction to the binding groove and, thus, available for interaction with the TCR, are shadowed in gray. The table shows the average residue's volume for each HLA-DR allele set. Residues are written in the one-letter code used throughout this review.

4.6. Structural and Immunogenetic Compartmentalization of the Immune Response

It was also striking to observe in Table 3 that all modified HABPs inducing a protective immune response associated with HLA-DR52 or HLA-DR8 haplotypes [viz. **24292** (1815), **9928** (1783), **22814** (1783), **13450** (1815), **24310** (6762), **23230** (6746), **24124** (6746), **24224** (6786), **37842** (6583), **37838** (6584), **38070** (6621) (Cifuentes et al., submitted for publication), **9782** (1522), **22812** (1522), **23422** (6725), **10014** (1585), **11860** (1585), **22834** (6737), and **13946** (1513)] displayed an α-helix structure, with the exception of peptide 6786, which displayed a random tendency (Table 2, group B).

Similarly, **24112** (4044), **13492** (6671), **22720** (6671), **20034** (4325), **23426** (6754), and **13790** (1758), shown to induce high antibody titers and protective immune responses associated with HLA-DR53 (HLA-DRβ1*0401) binding capacity, all displayed *β-turn* or random coil structures in their native peptides. Likewise, highly immunogenic, protection-inducing peptides **10022** (4313), **22780** (4313), **15514** (4325), **14044** (4337), **24230** (6800), and **24148** (5501), associated with high HLA-DRβ1*0701 binding capacity, *all* displayed random coil structural characteristics. The HLA-DR1 (HLA-DRβ1*0101) haplotype binding peptide **24166** (1818) displayed classical type III β turn structural features associated with a distorted β turn, as determined by ^{1}H NMR, as well as distorted α-helical and unordered elements, as assessed by CD spectroscopy in native HABP 1818 (Table 3).

All of these secondary structural elements were determined by CD analysis; the 3D structure was confirmed by ^{1}H NMR for thirty-two (32) of these *immunogenic, protection-inducing* modified HABPs, twenty five (25) of which are shown in Figure 5 (due to space limitations).

It can thus be suggested that *tailor-made* synthetic vaccines can be easily designed based on native HABPs' secondary structure (simply determined by CD spectra analysis); for example, native α-helical HABPs can be more suitably modified to obtain HLA-DR52 (DRβ1*0301 and DRβ1*1101) or HLA-DR8 (DRβ1*0801) alleles binding-associated protective immune responses while β-turns and random structural conformations in these HABPs may be more easily modified to induce HLA-DR53 (HLA-DRβ1*04 and HLA-DRβ1*07) or HLA-DR1 (DRβ1*0101) alleles' binding-associated protective immunity. Moreover, if predictive algorithms such as TEPITOPE,[232] Net MHCII,[233,234] *etc.* and the identification of binding motifs and binding registers[67,70] are associated with the methodology herein described, then this approach will pave the way for an *easier design* for *minimal subunit-based, multiantigenic, fully effective vaccines.*

The Dictionary of Secondary Structure of Proteins (DSSP)[235,236] has so far defined 10 different types of secondary structure: three helix types (3_{10} or G; α or H; π or I), turns (T), strands (E), bridges (B), bends (S), and other secondary structures (L). This leaves enough room for improving the characterization of such association, a goal pursued in our institution for providing more physicochemical rules for vaccine design.

4.7. Immunogenic, Protection-Inducing, Modified HABP Binding to HLA-DR Molecules and Their Pertinent Binding Motifs and Binding Registers

Based on our experimental data, we can state that native HABPs are neither immunogenic nor protection-inducing. Native HABPs 1815, 1585, 6762, 6754, 6786, 4044, 1758, 6800, 4337, 4313, 1818, and 6786 did not bind to any of the HLA-DRβ1* purified molecules tested so far (Table 3). Meanwhile, native peptides 1783, 6746, 1522, 1779, 1513, and 4325 showed promiscuous binding to HLA-DRβ1*0301 and HLA-DRβ1*1101 (both HLA-DR52-related), the same as 6725, which showed promiscuity in binding to HLA-DRβ1*1101 and HLA-DRβ1*0401. Similarly, HABP 6671 displayed high HLA-DRβ1*0401 and HLA-DRβ1*0701 binding capacity (both belonging to the HLA-DR53 haplotype) whereas 6737 bound exclusively to HLA-DRβ1*0301, 5501 to HLA-DRβ1*0701, and 6505[237] to HLA-DRβ1*1101.

The modifications displayed in Table 2 show that changes made in **24292** (1815),[220] **9928** (1783),[77] **22814** (1783), **13450** (1585),[134] **24310** (6762),[238] **23230** (6746),[87] **24214** (6746), **24224** (6786), **37842** (6583), **37838** (6584), and **38070** (6621) (Cifuentes et al., submitted for publication) rendered them immunogenic and protection-inducing and thus capable of eliciting high antibody titers against the parasite, as determined by IFA (1:320, 1:2560; 1:640; 1:2560, 1:320, 1:320, 1:640, 1:640, 1:1280, 1:640, 1:280 sera dilutions, respectively) (Table 1 and group B in Table 2) and Western blot analysis, showing recognition of the native proteins or their cleavage fragments by these immune sera (Figure 4B) (as thoroughly analyzed in a previous section and published in papers corresponding to each one).

The aforementioned immunogenic protection-inducing modified HABPs binding selectively and specifically to

HLA-DRβ1*0301 (Table 1 and group B in Tables 2 and 3) displayed specific DRβ1*0301 binding motifs (shadowed in Table 2), as follows: I, L, Y, V, W, M for pocket 1; D, D, D, N, A, D for pocket 4; E, Y, A, M, K, E for pocket 6; L, N, Y, K, L, M for pocket 9[155,158] (group B in Tables 2 and 3). The number of peptides included in Table 2 and Figure 5 has been reduced due to space limitations, but they are available on request.

Besides these modified HABPs having been identified for their high specific binding capacity to HLA-DRβ1*0301 purified molecules and their appropriate binding motifs and binding registers, structural conformation analysis also revealed that the distance between the farthest atoms of those residues fitting inside pockets 1 and 9 of a determined binding register was 19.2 ± 1.5 Å for immunogenic protection-inducing modified HABPs (group B in Tables 3 and 4 and Figure 5).

9782 (1522),[221] **22812** (1779),[103] **23422** (6725),[142] **10014** and **11860** (1585),[134] and **22834** (6737),[143] showing high HLA-DRβ1*1101 binding capacity and inducing considerable antibody titers in *Aotus* monkeys, as determined by IFA (1:2560, 1:2560, 1:640, 1:640, 1:640, and 1:2560, respectively) (Tables 1 and 2, group B), conferred protection against experimental challenge on monkeys and raised antibodies that recognized native MSP-1, EBA-175, or SERA proteins from which the peptide sequence had been derived, as assessed by Western blot analysis (Figure 4B).

These peptides exhibited characteristic HLA-DRβ1*1101 allele binding motifs: L, L, I, Y, and I in pocket 1; R, K, M, P, and N in pocket 4; G, H, N, A, and K in pocket 6; D, A, S, Y, and L in pocket 9 (shadowed in Table 2). The distance between the residues fitting into pockets 1 and 9 in the classical binding register for modified HABPs binding to the HLA-DRβ1*1101 allele was 20.2 ± 1.5 Å (group B in Table 3 and Figure 5).

Similarly, high antibody titers were induced in some of the monkeys immunized with immunogenic protection-inducing **24112** (4044),[84] **24180** (4044), **13492** (6671),[129] **22720** (6671), **20034** (4325),[74] **24150** (1758),[114] and **23426** (6754) (1:5120, 1:1280, 1:5120, 1:5120, 1:1280, and 1:320, respectively), all of which bound to HLA-DRβ1*0401 with high capacity (shadowed in Table 2). These peptides contained the characteristic motifs shown by peptides binding to this molecule: Y, Y, F, Y, and L in pocket 1; V, S, T, D, and D in pocket 4; R, N, A, N, and T in pocket 6; M, A, A, K, and L in pocket 9.[155,158] A very notable 26.3 Å ± 1.5 Å distance could be observed between the residues fitting into pockets 1−9 of the putative register associated with binding to these HLA-DRβ1* haplotype alleles (Table 3, group B and Figure 5).

^{1}H NMR analysis of **24230** (6800),[239] **24148** (5501),[71] **10022** (4313),[75] and **14044** (4337)[122] (all having random structures) showed that they all adopted short α-helical or distorted β-turn structures, inducing considerably high antibody titers (1:320, 1:2560, 1:5120, and 1:320, respectively) which were protective against experimental challenge (Table 3, group B). These modified HABPs bound with high affinity to HLA-DRβ1*0701 and displayed the characteristic binding motifs for this HLA-DR haplotype allele. The distance between the farthest atoms of the residues fitting into pockets 1 to 9 was 24.2 ± 1.2 Å (Table 3, group B, and Figure 5).

The highly immunogenic (IFA titer 1:640) **24166** (1818)[111] was the only one that did not just bind exclusively and strongly to HLA-DRβ1*0101 molecules but also to HLA-DRβ1*1101. It displayed classical and distorted type III β-turn structures and presented classical HLA-DRβ1*0101 binding motifs (Y in pocket 1, M in pocket 4, P in pocket 6, and D in pocket 9), having a 24.9 Å distance between the farthest atoms in pocket 1 and pocket 9. Intriguingly, this distance was around 4.0 Å longer than that of residues fitting into HLA-DRβ1*0301 and HLA-DRβ1*1101 molecules, for which ∼20.0 ± 1.5 Å distances had been registered (group B in Table 3 and Figure 5), suggesting that some modified HABPs might have different binding capacities, binding motifs, and binding registers.

5. MODIFIED HABPS' STRUCTURAL FEATURES ALLOWING THEM TO FIT INTO MHCII MOLECULES

5.1. Differences in the Distance between Modified HABP Residues Fitting inside Pockets 1−9 Associated with Different Haplotype Binding Characteristics

Although ^{1}H NMR reliability for determining side-chain conformation has been limited by the relatively high conformational freedom, clear structural differences could be observed among immunogenic protection-inducing modified HABPs, their native precursors, and their immunogenic nonprotection-inducing analogues.

The first appreciable difference when comparing the 3D structures dealt with the distance and conformational features associated with HLA-DRβ1* binding capacity, MHCII binding motifs, and binding registers (Table 3 shadowed residues and Figure 5). Most modified immunogenic protection-inducing HABPs binding to HLA-DRβ1*03, HLA-DRβ1*011, and HLA-DRβ1*08 (DR-52 haplotype-related alleles) had a 20.0 ± 1.5 Å distance between the most distant atoms of the residues fitting into pockets 1−9 (group B in Table 3, and Figure 5).

The same experimental data showed that protection-inducing modified HABPs binding to HLA-DR53 haplotype-related alleles (HLA-DRβ1*0401 and HLA-DRβ1*0701) and HLA-DRβ1*01 had 25.5 ± 1.5 Å between the same atoms. This suggested differences in the distance between the boundaries of pockets 1 to 9 among these haplotype's molecules (group B in Table 3, and Figure 5). Such data showed that there was a striking ∼3.0 Å difference between the peptide atoms fitting into pockets 1 to 9 of HLA-DR52 and HLA-DR8 molecules when compared to HLA-DR53- and HLA-DR1-related ones; this difference can be very clearly seen in Figure 5, displaying the ^{1}H NMR 3D structure of thirty-two (32) immunogenic protection-inducing modified HABPs having the aforementioned MHCII binding characteristics.

Based on the same structural information, it can also be seen that there were marked differences between the peptides fitting inside the PBR and the pockets of a specific HLA-DRβ1* allelic molecule, as has been found by other authors for several HLA-DRβ1* alleles.[155,158] For example, the peptide binding motifs in HLA-DRβ1*0801 defined a pocket 5 inside which amino acids H, K, and R fit; this is a specific characteristic of this allele that leaves HLA-DRβ1*0801 exclusively formed by pockets 1 and 5.[158] Similarly, pockets 1, 3, 6, and 9 have been defined for HLA-DRβ1*1201 with specific amino acids fitting inside a putative pocket 3 instead of the canonical pocket 4. A pocket 7 has been defined as being one of the main pockets in the HLA-DRβ1*1501 allele together with pockets 1 and 4.[184,240] Pocket 9 in HLA-DRβ1*0901 displayed the unique Kβ9E or W replacement which, being shared with pocket 6, can swing into this pocket, thereby promoting the anchoring of acidic residues (such as D) in pocket 6 and causing complete permissiveness or residue promiscuity in pocket 9 of HLA-DRβ1*0901 molecules.[241] This could be why NO particular binding motifs have been identified for this HLA-DR53 allele in these pockets. All

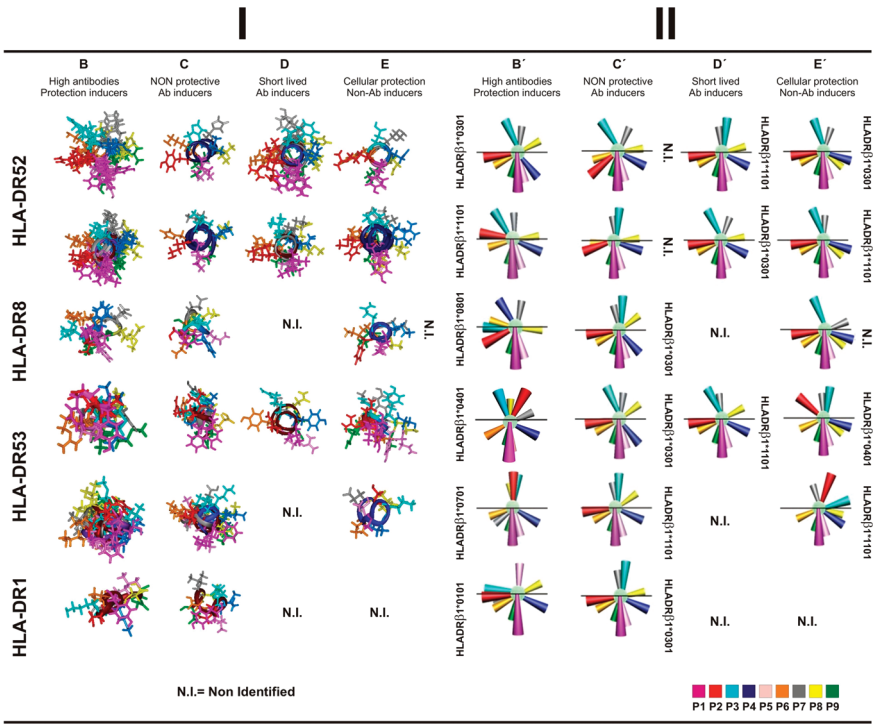

Figure 7. Left-hand panel (I). Front view of overlapping ^{1}H NMR-derived structures of modified HABPs grouped according to their HLA-DR binding capacities and immunological inducing characteristics. **HLA-DRβ1*0301** is associated with **13450** (1585), **22814** (1783), **23230** (6746), **24292** (1815), and **24310** (6762) in group B, in C with **13782** (6762), in D with **15484** (1585) and **21742** (6746), and in E with **17914** (1783). **HLA-DRβ1*1101** is associated with **10014** (1585), **13446** (1522), **22812** (1779), and **22834** (6737) in B, with **14012** (1779) in C, with **14096** (6737) and **15474** (1522) in D, and with **22456** (1522) and **24210** (6762) in E. **HLA-DRβ1*0801** is associated with **13946** (1513) in B, with **15468** (1513) in C, and with **9882** (1513) in E. **HLA-DRβ1*0401** is associated with **13492** (6671), **20034** (4325), and **24112** (4044) in B, with **13494** (6671) and **20032** (4325) in C, with **10000** (6671) in D, and with **15536** (6671) and **17920** (4044) in E. **HLA-DRβ1*0701** is associated with **10022** (4313), **14044** (4337), **24148** (5501), and **24230** (6800) in B, with **13766** (4313), **14048** (4337), and **23754** (5501) in C, and with **23776** (4313) in E. **HLA-DRβ1*0101** is associated with **24166** (1818) in B and with **23390** (1818) in C. Right-hand panel (II). Diagrammatic representation of the modified HABPs according to the lateral chain orientation of 3D structures shown in panel A. N.I. = not identified to date. Diagrams are labeled B′, C′, D′, and E′ for better identification in the text, thereby corresponding to their respective 3D structures in panel I.

this evidence supports the fact that marked differences have been observed regarding canonical pocket configuration in different HLA-DRβ1* alleles and their interactions during antigen presentation.

5.2. Residue Orientation in Immunogenic Protection-Inducing Modified HABPs

^{1}H NMR structural analysis of these thirty-two (32) protection-inducing immunogenic modified HABPs led to identifying that P1 (i.e., the amino acid residue fitting into pocket 1) (fuchsia in Figure 3), P2 (red), P4 (dark blue), P5 (pink), P6 (light brown), and P9 (green) side chains had large atomic groups pointing downward in all modified HABPs binding to HLA-DR52 haplotype alleles and the only one binding to HLA-DRβ*08. The foregoing structural data for the fifteen (15) immunogenic protection-inducing modified HABPs binding to HLA-DR52 molecules clearly suggested the existence of pocket 2 (P2, red) in HLA-DR52 (HLA-DRβ1*0301 and HLA-DRβ1*1101) and HLA-DR8 alleles, as shown in the lateral views of ^{1}H NMR analysis (Figures 5 and frontal views shown in Figure 7IB) and the diagrams summarizing side-chain orientation in the residues fitting inside the HLA-DRβ1* pockets and making contact with the TCR (Figure 7 IIB′).

Following the same methodology, in the nine (9) immunogenic protection-inducing modified HABPs binding to HLA-DR53 (HLA-DRβ1*0401 and HLA-DRβ1*0701) and the only one binding to HLA-DR1 (HLA-DRβ1*0101), the downwardly pointing residues have been shown to be as follows: P1 (fuchsia), P4 (dark blue), P6 (light blue), and P9 (green). The difference between these two HLA-DR53 alleles was that P3 (pale blue) was upwardly or horizontally orientated in HLA-DRβ1*0401 and that P7 (gray) in HLA-DRβ1*0401 was orientated toward the right-hand side in modified HABPs while being orientated toward the left-hand side in modified HABPs binding to HLA-DRβ1*0701 (Figure 5 and Figure 7I and II, panels B and B′). Please note the following observation. Residue orientations in HLA-DR53 have to be taken very cautiously due to the tremendous polymorphism in HLA-DRβ1*04 alleles where >60 variants have been described so far, this being the most polymorphic allele in the MHC II system. In spite of these constraints, we concluded that there were striking differences in pocket distances and structural formations between the different HLA-DRβ1* alleles and their haplotypes, as determined by immunogenic protection-inducing modified HABPs.

By the same token, the theoretically solvent-exposed residues from peptides binding to HLA-DR52 haplotype-related alleles probably establishing contact with the TCR in terms of the orientation of overlapped upwardly pointing ^{1}H NMR structures of high antibody titer protection-inducers were P3 (pale blue), P7 (gray), and P8 (yellow) for this haplotype (Figure 7 IB and

dx.doi.org/10.1021/cr100223m |*Chem. Rev.* 2011, 111, 3459–3507

summarized in Figure 7 IIB′). The putative TCR-contacting residues in HLA-DR8 seemed to be P3 (pale blue), P4 (dark blue), P6 (brown), and P7 (gray), but it has to be remembered that only one structure has been identified for this last haplotype.

The residues in these upwardly pointing immunogenic protection-inducing peptides binding to HLA-DR53 and theoretically making contact with the TCR could be P2 (red), P3 (pale blue), P7 (gray), and P8 (yellow) (Figures 7IB and 7IIB′). The same residues plus an additional upwardly orientated P3 (pale blue) have been found for HLA-DRβ1*0701.

The protection-inducing modified HABP residues binding to HLA-DR1 (HLA-DRβ1*01) could be P1, P2, P4, P6, and P9, while the putative upwardly orientated TCR contacting residues could be P5 and P8. Unfortunately, there was only one modified HABP having this immunological characteristic from which to draw such a conclusion.

5.3. Evolutionary Evidence Supporting Haplotype and Allelic Structural Differences

Differences in the binding motifs, binding registers, pocket distances, residue orientations, *etc*. can also be partly explained by the information gleaned by comparing the nucleotide sequence of the different haplotype's genes between humans, primates, and a large number of other species.[222] For instance, elegant and extensive phylogenetic molecular analysis of Class II molecules has led to estimating that the highly polymorphic HLA-DRβ1*04 allelic lineage in the HLA-DR53 haplotype (having more than 60 genetic variants) arose more than 85 million years ago (mya), as HLA-DRβ1*04-like allelic molecules have been found in pro-simian species[156,222] and the alleles in this lineage have always clustered together in all mammals studied so far, thus implying a common ancestral origin representing a distinct main evolutionary branch.

It has also been found that the DRB genes from the HLA-DR52 haplotype (of which HLA-DRβ1*0301 and HLA-DRβ1*1101 have been included in this study) probably originated by two successive gene duplication events estimated to have occurred 60 mys and 40 mys ago, respectively.[156]

As mentioned before, the single complete DRB gene in the HLA-DR8 haplotype was probably generated by a gene contraction event in the HLA-DR52 haplotype occurring about 100,000−20,000 years ago after hominoid speciation (~6 mys ago), which is one of the reasons for grouping HLA-DRβ1*08 together with HLA-DR52.

Furthermore, the *Aotus* MHC-DRβ1*0301 group B converged with human HLA DRβ1*08/11/12/13/14 in our study of monkeys, providing additional support for our grouping HLA-DRβ1*0801 together with the HLA-DR52 haplotype.[181]

The HLA-DR51 haplotype contained two polymorphic and functional DRB genes: DRβ1* (containing HLA-DRβ1*15 and 16 alleles) and DR*β5 (the former displaying a closer relationship to HLA-DR1 when compared to other HLA-DR haplotypes[222]). These two haplotypes showed greater evolutionary closeness to HLA-DR53 than HLA-DR52 and HLA-DR8. Therefore, the structural conformation of HLA-DR1 could be more related to HLA-DR53 than HLA-DR52, as we found for modified HABP **24166** binding to HLA-DRβ1*0101 (Table 3).

Unfortunately, we have no information about modified HABPs' structural and functional characteristics in the HLA-DR51 haplotype due to difficulties in obtaining purified native HLA-DR51 (HLA-DRβ1*1501, 1601) molecules for experimental binding studies.

Such structural, functional, and phylogenetic analysis has strongly supported our suggestions that the striking differences between haplotype and allele peptide binding characteristics arose throughout millions of years of Class II molecules' evolution in different scenarios and, therefore, these structural differences should be considered very seriously when designing vaccines.

5.4. Binding Specificities Suggesting a Haplotype- and Allele-Conscious Tcr Mode of Interaction

Experimental work has shown that peptides binding to Class II molecules can be bound and read according to different functional binding registers within different scenarios. For instance, some peptides are bound and read within the context of different Class II molecule isotypes from the same individual, as occurs in the murine system with peptide Hb (amino acids 64−76 from hemoglobin), which is read from I68 to K76 by mouse I-E^k molecules (more similar to HLA-DRβ) and from V67 to I75 by mouse I-A^k molecules (more related to HLA-DQβ).[242]

It has also been shown that the same peptide can be presented within the context of different alleles from the same HLADRβ* molecules, as happens with the myelin basic protein peptide (MBP 84−102). Such peptide has been found to bind to HLA-DRβ5*0101 and DRβ1*1501 molecules according to two totally different binding registers.[190]

The same Class II molecule can read the same peptide using two totally different functional registers, as happens with the OVA 323−339 peptide and the I-A^d molecule in which the binding register is 323−335 or, alternatively, 325−336. Nevertheless, the former is unable to activate a T-cell hybridoma, whereas the same T-cell response can be activated by the latter. This data suggests that a single peptide can bind to Class II molecules having different functional registers to induce totally different immune responses.[240,243]

Experimental and structural studies with murine wild-type and mutated I-E^k Class II molecules have shown that the reorganization of some H-bonds allows peptides to escape from these mutated Class II molecules, thereby leading to their lower immunogenicity in mutated I-E^k mice. Elegant experiments performed by Kersh et al.,[244] with the Hb 64−76 hemoglobin peptide binding to the I-E^k molecule, found that a single modification made to this peptide in residue E73D (*i.e*. shortening only one methyl group by switching E for D) fitting into this molecule's pocket 6 altered peptide distances between residues P6 and the orientation of P7 and P8, causing a 1,000-fold reduction in this modified peptide's ability to induce antibodies. Therefore, a single shortening of a methyl group in an amino acid drops these peptides' immunogenicity 1,000-fold, so it is not difficult to envision the consequences of shifting the polarity of conserved HABPs' critical and fundamental binding residues, as we have thoroughly shown and discussed in previous sections.

The data provided by other groups regading human and murine species could also provide a partial explanation for the different reactivity we have previously found by Western blot for sera (Figure 4B) from *Aotus* monkeys immunized with slightly modified 1585 peptides, where such modified HABPs were read in different binding registers by the different HLA-DR52 alleles to form different MHCII/pTCR complexes. This situation was clearly seen in **11860** binding to HLA-DRβ1*1101 and **13450** binding to HLA-DRβ1*0301, both of which were found to be highly immunogenic protection-inducers. However, the former strongly recognized the 195 kDa precursor molecule and high molecular weight 105, 90, and 60 kDa cleavage fragments while

the latter reacted very strongly with 70, 46, 42, and 19 kDa fragments. Western blot reactivity of the sera raised against **13946** (1513) located in the MSP-1 N-terminus and binding to the HLA-DRβ1*0801 allele was completely different from the reactivity induced against the same protein fragments by **24148** (5501) located in the MSP-1 molecule C-terminus and binding to HLA-DRβ1*0701. This data showed the *structural compartmentalization* of *P. falciparum* proteins as well as the immune system's *functional compartmentalization*.

Moreover, this data suggested the existence of different TCR contact residues in the immunogenic protection-inducing modified HABPs binding to different alleles from the same haplotype, therefore suggesting that there is also a haplotype- or allele-conscious TCR, or different TCR preferential modes of interaction with the peptide, as clearly shown in Figure 7, panels IB and IIB′.

Besides *class-conscious TCRs*,[245,246] the existence of *haplotype- and allele-conscious TCR* modes of interaction was therefore deduced from the peptide's structural and functional point of view in a thorough analysis of thirty-two (32) immunogenic, protection-inducing modified HABPs.

As thoroughly shown by other groups, a single peptide can also have different TCR interaction modes that would allow it to induce different types of immune response, e.g. canonical diagonal,[247−250] orthogonal,[191] N-terminal,[251] C-terminal,[252] or class-conscious[245,246] signatures supporting our finding that all these structural features determining *haplotype and allele-conscious TCR* recognition have to be very seriously taken into account when developing vaccines capable of inducing a protective immune response.

6. STRUCTURAL AND IMMUNOLOGICAL MECHANISMS USED BY *P. FALCIPARUM* PARASITES FOR EVADING PROTECTIVE IMMUNE PRESSURE

6.1. Inducing Long-Lived Nonprotective Antibodies

6.1.1. Striking Differences in Antibody Recognition Patterns Revealed by Immunological Analysis. In our attempt to identify the principles or rules for a logical and rational vaccine development methodology, using *Plasmodium falciparum* malaria as our model disease, we have found that *Aotus* monkeys immunized with some conserved modified HABPs induced the production of *long-lasting NON-protective high* antibody titers against the *P. falciparum* parasite,[197] as assessed by IFA and Western blot. Most antibody titers became raised to ≥1:160 (protection-associated antibody level) upon second immunization and persisted after the third dose, while others were only detectable after the third dose (Tables 2 and 3, group C). These modified HABPs displayed marked structural differences (Figure 5), as can be observed in their superimposed ^{1}H NMR structures (Figure 7 IC) and the diagram summarizing them (Figure 7 IIC′).

An example of such antibody reactivity was shown when monkeys were immunized with MSP-1 high antibody titer-, nonprotection-inducing **15468** (1513) (Tables 2 and 3, group C). Western blot analysis showed that IFA positive sera (Figure 6AI) reacted with the complete MSP-1 protein (195 kDa) and its 121, 83, 72, 68, and 51 kDa cleavage fragments but *not* with the 152, 105, 100, and 42 kDa fragments, which were only recognized by sera from *Aotus* monkeys immunized with the highly *immunogenic, protection-inducing 13946*, also derived from HABP 1513.

It is worth stating that the only variation between these two peptides was L12D (Table 2, groups B and C), to which such different types of immunological reactivity could be attributable.

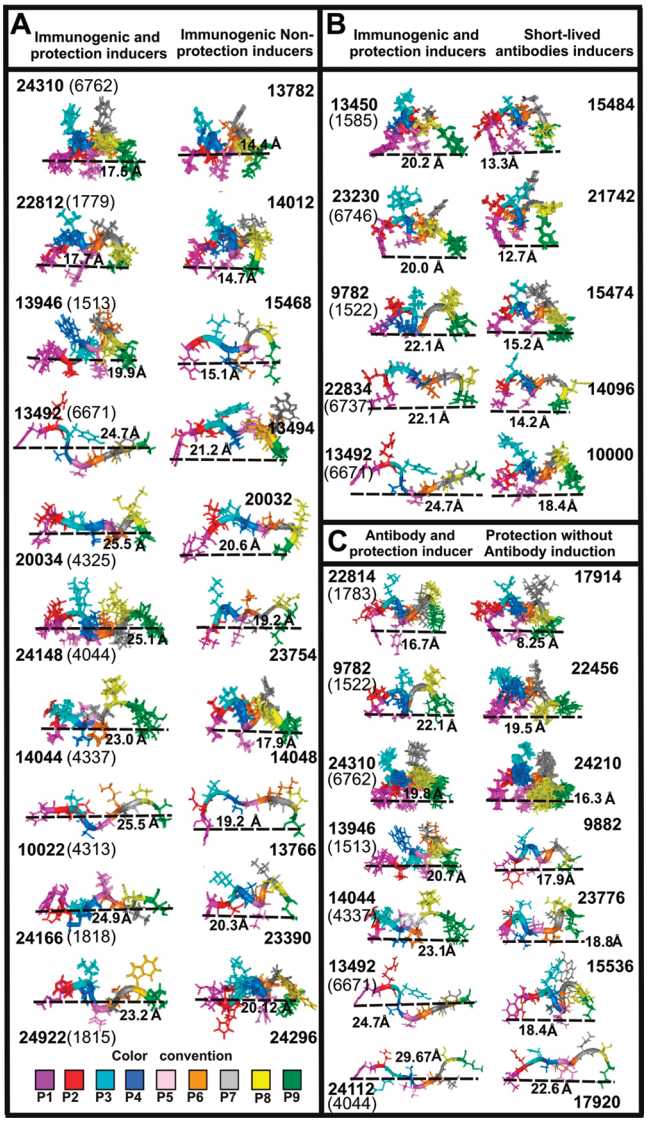

Figure 8. 3D structure of modified HABPs inducing *biased* immune responses. Residues, in the lateral view, are colored according to previous convention. (A) *Immunogenic and protection-inducing* (left-hand panel) and *solely immunogenic* (right-hand panel) modified HABPs.[197] Note the 4.6 ± 1.4 Å difference in distance between the most distant atoms of residues fitting into P1 and P9 and the residue orientation of these *immunogenic protection-inducing* modified HABPs when compared to the corresponding modified HABPs, which were *immunogenic non-protection* inducers. (B) Modified HABPs, which only induced high *short-lived* antibody titers (right-hand panel).[220] Note the 6.8 ± 0.5 Å difference between *immunogenic protection-inducing* HABPs and their corresponding *short-lived* antibody-inducing modified ones. (C) *Antibody inducer and protection-inducing* modified HABPs are shown in the left-hand panel, and modified HABPs, which only induced *protection without antibody* induction, are shown in the right-hand panel.[197] Note the upward orientation of the P8 residue (yellow) in the former and downward orientation in the latter (Reprinted with permission from refs 195 and 197. Copyright 2006 Elsevier. Reprinted with permission from ref 196. Copyright 2005 American Chemical Society).

This showed the immune system's stereospecific exquisite recognition capacity, this being the inherent problem which this characteristic adds to the development of immunogenic, protection-inducing synthetic vaccines.

dx.doi.org/10.1021/cr100223m |*Chem. Rev.* 2011, 111, 3459–3507

Another type of antibody recognition pattern was observed when *Aotus* were immunized with peptides inducing *high, long-lasting, nonprotective* antibody titers (Tables 2 and 3, group C). Nonprotection-inducing **23754** (19 kDa fragment MSP-1 HABP 5501) (Figure 6AII), which induced high antibody titers, elicited antibodies reacting with MSP-1 (195 kDa) and its 140, 120, 110, and 83 kDa cleavage fragments. On the contrary, antibodies induced by immunization with *immunogenic protection-inducing 24148* (5501) displayed a completely different reactivity pattern against 122, 70, 48, and 42 kDa (very strongly) and 40 kDa MSP-1 cleavage products.

These ten (10) high long-lasting antibody titer nonprotection-inducing modified HABPs' structural characteristics were different when compared to the twenty-four (24) high long-lasting antibody titer protection-inducing modified HABPs. There was an increase or shift in the helical region of nonprotection-inducing **13782** (α-helix S4 to M17), **14012** (P3 to L11), **15468** (K7 to T12 and N13 to S17), and **13494** (M1 to Y9) when compared to immunogenic protection-inducing modified HABPs, where there was a shortening of helical length in **20032** (K13 to R16),[197] **23754** (Q6 to K12), **24296** (N8 to N15), and **14048** (R6 to L19), a change in their type III′ β-turns compared to classical type III ones in **13766** (T7 to F10), or an induction of a 3_{10} helix in **23390** (D19 to L23) (Table 3).

6.1.2. A Shift in Residue Orientation and Shortening the Distance between Binding Residues in Immunogenic Nonprotection Inducing HABPs Is Associated with a Shift in Binding to HLA-DRβ1* Molecules from Another Haplotype. When the 3D structure of *immunogenic protection-inducing 13946* binding to HLA-DRβ1*0801 (HLA-DR8) was compared to that of **15468** (1513), which elicited a high *nonprotection-inducing antibody* response, it was found that the latter had shifted its binding preference toward the HLA-DRβ1*0301 (HLA-DR52) molecule (group C in Tables 2 and 3). The same phenomenon was observed when comparing *immunogenic protection-inducing* modified HABP binding to HLA-DRβ1*0401 (HLA-DR53) to *high nonprotection-antibody-titer-inducing* **13494** (6671) and **20032** (4325) (group C in Tables 2 and 3), in which the latter had shifted their ability to bind to HLA-DRβ1*0301 (HLA-DR52) (Tables 2 and 3, groups B versus C).

An analogous situation occurred when comparing *immunogenic protection-inducing* **10022** (4313) and **14044** (4313) binding to HLA-DRβ1*0701 (HLA-DR53) with the *high nonprotective* antibody-titer-inducing **13766** (4313) and **14048** (4337) (Table 3, groups B versus C), in which the latter had shifted their binding ability to HLA-DRβ1*1101 (HLA-DR52).

Some of the modified protection-inducing HABPs binding to HLA-DRβ1*0701 (HLA-DR53) did not bind to any of the MHCII molecules studied here while they did induce high nonprotection-antibody titers. These peptides could possibly have been binding to HLA-DRβ1*13 or HLA-DRβ1*14 (HLA-DR52) molecules or other haplotypes such as HLA DR51 (HLA-DRβ1*1501 and 1601), which are also present in *Aotus* monkeys.[181] Unfortunately, these molecules were not available for us for testing this hypothesis.

Such data show that the minimal structural differences inducing different immunological activities in these analogues were associated with a shift in their ability to bind to *allelic molecules from a different haplotype*.[197]

When these *immunogenic nonprotection-inducing* modified HABPs' 3D structures were analyzed, there was a 4.6 ± 1.4 Å shortening between the most distant atoms of the residues fitting inside pockets 1−9 when compared to *immunogenic protection-inducing* modified HABPs.[197] Tables 2 and 3 compare groups B and C, while distance differences can be clearly observed in Table 3 and Figure 8A.

When their lateral-view chain orientation (Figure 8A) and frontal 3D structures (Figure 7IC and IIC′) were analyzed, it was clear that they had *changed not only biologically* (binding to a different haplotype molecule) *but also structurally*; that is, when immunogenic protection-inducer binding to HLA-DRβ1*0701 became immunogenic-nonprotection inducers, their structures resembled the structure of HLA-DRβ1*0301 binders and they bound to purified HLA-DRβ1*0301 when assessed experimentally. This phenomenon is currently being studied in depth in our institution to better understand the as yet not well-known mechanisms used by microbes to bias immune responses and evade the shield of a completely protected host or induced sterile-immunity; understanding such a mechanism is essential for fully effective vaccine development.

6.2. Inducing Short-Lived Nonprotective Antibodies

6.2.1. Distinctive Antibody Titer Patterns and Structural Differences Compared to Immunogenic Protection-Inducing Peptides. We have also found that certain modifications performed on native nonimmunogenic, nonprotection-inducing HABPs rendered them inducers of very *short-lived* high IFA antibody titers which were *not* protective. It can be seen in Tables 2 and 3 (group D) and in the Western blot analysis shown in Figure 6B that there were structural differences between modified HABPs inducing very-early appearing antibodies (II_{10}) that disappeared definitively by II_{15} or III_{15} (Figure 6BI), compared to the modified HABPs inducing short-lived, later-appearing antibodies (which lasted 10−15 days after the second immunization and then disappeared definitively) (Figure 6BII).[196,220]

^{1}H NMR structural analysis showed clear differences in the extension and localization of α-helices between immunogenic protection-inducing **13450** (1585), **23230** (6746), **9782** (1522), **22834** (6637), and **13492** (6671), with the corresponding five (5) *short-lived* antibody-inducing **15484** (1585), **21742** (6746), **15474** (1522), **14096** (6737), and **10000** (6671) (Figure 8B and Table 3, group D). **15484** (1585) inducing short-lived antibodies had an α-helix between A9 and K17 whereas immunogenic protection-inducing **13450** (1585) presented an α-helix between V2 and Q18. **15474** (inducing short-lived antibodies) had an α-helix between K7 and K17 while its analogue (protection-inducing peptide **9782**) had a shorter α-helix between amino acids P3 and N11.

Another example of helix displacement in short-lived antibody-inducing peptides could be observed in **22834**, which displayed a shorter α-helix between residues V5 and V10 while the helical region spanned V5 to M12 in its analogue **14096** (short-lived antibody-inducing). **21742** (inducing short-lived antibodies) had a helical region between N4 and A12 which was displaced when compared to its protection-inducing analogue **23230** (6746), in which the helical region spanned residues N9 to H16 (Table 3, group D). A similar phenomenon occurred with other peptides involved in this study.

6.2.2. Structural Changes in Short-Lived, Antibody-Inducing, Modified HABPs Are Associated with a Shift in Binding to Different Alleles from the Same Haplotype. When **15484** and **21742** (Table 2), inducing *short-lived nonprotection-inducing antibody* titers, were compared to the modified immunogenic protection-inducing HABPs binding to HLA-DRβ1*0301 (**13450** and **23230**) (Table 3, groups B versus

Table 5. Cytokine Production in Monkeys Immunized with Antigenic Peptides[a]

		Th1 profile						*Th2 Profile*								
		IFN-γ			***TNF***			***IL-2***			***IL-4***			***IL-6***		
	Monkeys Code	**Peptide**	**bkg**	**PHA**	**Peptide**	**bkg**	**PHA**	**peptide**	**bkg**	**PHA**	**Peptide**	**bkg**	**PHA**	**Peptide**	**bkg**	**PHA**
15536	**440**	**157**	44	172	3.4	2.6	2.2	**25**	17	24	6.7	7.0	3.2	2.7	2.9	1.9
	481	**331**	30	88	2.7	2.8	3.2	23	23	25	4.1	6.5	3.8	2.7	4.2	3.1
	497	9.5	40	91	1.2	3.3	3.3	0	23	25	4.0	7.7	9.6	1.5	3.5	5.3
13844	**451**	**52**	27	339	**3.7**	1.8	2.1	**30**	14	17	**10.2**	6.4	6.1	**5.0**	1.8	2.2
	468	**341**	57	408	2.2	2.2	2.3	13	13	18	1.6	5.5	9.8	2.7	2.6	3.6
	510	**107**	39	129	2.5	2.2	2.9	25	22	23	**7.6**	5.5	5.5	3.0	3.4	3.2
9236	**446**	**45**	23	93	3.7	3.4	3.2	23	21	33	**9.5**	7.3	8.5	4.0	3.2	3.5
	517	35	34	290	1.8	1.6	1.6	18	17	23	**7.0**	4.2	5.2	2.4	3.2	2.5
Control	**520**	48	50	58	4.0	4.3	4.5	38	36	39	4.9	4.7	5.1	4.9	4.7	5.1

[a] Representative cytokines from Th1 (IFN-γ, TNF, and IL-2) and Th2 (IL-4 and IL-6) immune responses quantified from cell culture supernatants. The results are presented in pg/mL for each cytokine produced after the second immunization. Significant results are shown in bold, being those presenting a relevant level of cytokines after subtracting the value of their respective control (background or bkg = cells which had not been exposed *in vitro* to the peptide). Phytohemagglutinin (PHA) mytogen was used as positive control for cytokine production. Animals shown in gray are those that were protected (total control of parasitemia) during experimental challenge with a virulent *P. falciparum Aotus*-adapted strain.

D), the former had shifted their binding activity from HLA-DRβ1*1101 to HLA-DRβ1*0301. Reciprocally, *protection-inducing* modified HABPs binding to HLA-DRβ1*1101 (**9782** and **22834**) shifted their ability to bind to HLA-DRβ1*0301 when compared to their corresponding *short-lived antibody-inducing* analogues (**15474** and **14096**). It can be observed that all such shifting in binding activity occurred *within alleles* from the same HLA-DR52 haplotype, i.e. from HLA-DRβ1*0301 to HLA-DRβ1*1101 and *vice versa* (Table 3, groups B versus D).

Structural analysis (Figure 8B and Table 3, group B versus D) showed a 6.8 ± 0.5 Å shortening[196,220] in the distance between the farthest atoms of residues fitting inside pockets 1−9 from *immunogenic protection-inducing modified* HABPs when compared to those inducing high, very *short-lived nonprotection-inducing antibody* titers.

The 3D structure of these five (5) modified HABPs inducing short-lived nonprotective antibody titers was quite similar to that of immunogenic protection-inducing modified ones (Figure 7ID and IID′), with the sole difference being much shorter (Figure 8B), probably suggesting a probable unstable and perhaps short permanence inside the MHCII/pTCR complex. Even though this hypothesis still needs to be proved, the results have clearly shown that they had shifted their binding capacity to *another allele of the same haplotype* and were 6.8 ± 0.5 Å shorter (Figure 8B).

6.3. Inducing Protective Cellular Immune Responses in the Absence of Antibodies

6.3.1. Protective Cellular Immune Responses in the Absence of Antibodies. Seven (7) of the hundreds of modified HABPs assessed in large numbers of *Aotus* monkeys reproducibly induced protection against experimental challenge *without* raising any antibody response, suggesting a different protective-induced mechanism besides antibody recognition (perhaps T-cell immune response)[197] (Figures 7IE and IIE′ and 8C).

Group E in Table 2 shows the amino acid sequences of native peptides and those of their modified analogues inducing a protective cellular response in the total absence of antibodies (<1:20 titers), as determined by IFA 15 days after the second and third immunization (II_{15}, III_{15}) with sera from immunized *Aotus* monkeys protected against experimental challenge.

This phenomenon was completely reproducible when experiments were repeated (Table 5) with **9236** (6737), for which the 3D structure was not available, **13844** (6737), and **15536** (6671), thus ruling out any extrinsic or intrinsic factor that might have affected the reliability of data, such as prior exposure of *Aotus* to *P. falciparum* (discarded due to the lack of reactive antibodies in preimmune sera), absence of antibodies in sera obtained following immunization, blood group incompatibility with the *Aotus* parasite donor (which might have been preventing infection rather than inducing immune protection against the same), *etc.*

Lymphoproliferation or cellular immune response studies carried out with peripheral blood mononuclear cells (PBMCs) isolated from the sera of those *Aotus* in which assays were repeated revealed high stimulation indexes (SI) for both modified HABP monomers and their polymers, thus indicating that a specific cellular immune response was raised against modified HABPs' amino acid sequences used for immunization rather than neoantigens generated during polymerization. Even though no direct correlation was shown between SI and protection, monkeys that were fully protected against experimental challenge presented ≥5.0 SI when compared to those immunized with monomers or polymers from the respective native peptide (Table 4).[197]

On the contrary, all control monkeys simultaneously immunized with saline solution in complete and incomplete Freund's adjuvant presented ≤3.0 SI when their leukocytes were exposed to the same monomeric or polymeric peptides used in immunization, therefore showing that the lymphoproliferation response had been most likely due to a nonspecific cellular response resulting from immunizing these monkeys with Freund's adjuvant.

Although this data agrees with that supporting lymphoproliferation assays as a suitable methodology for revealing a cellular immune response's specific stimulation, it should be considered that it is not a robust test for correlating SI and protection.

6.3.2. Cytokine Production Induced by Activating Protective Cellular Immunity. The cellular immune response induced by these peptides in protected monkeys in the absence of a humoral response was further documented by determining cytokine concentrations. The different Th1/Th2 associated cytokines were quantified using a primate-cytokine-specific kit due to the difficulty of obtaining specific reagents for *Aotus* cytokines, the large quantity of lymphocytes needed for PCR quantification, and the poor or null ability of human-cytokine-specific-reagents to recognize these cellular mediators.

Table 5 shows that *Aotus* 440 immunized with **15536** (6671), as well as monkeys 510 and 446, which were immunized with

dx.doi.org/10.1021/cr100223m |*Chem. Rev.* 2011, 111, 3459–3507

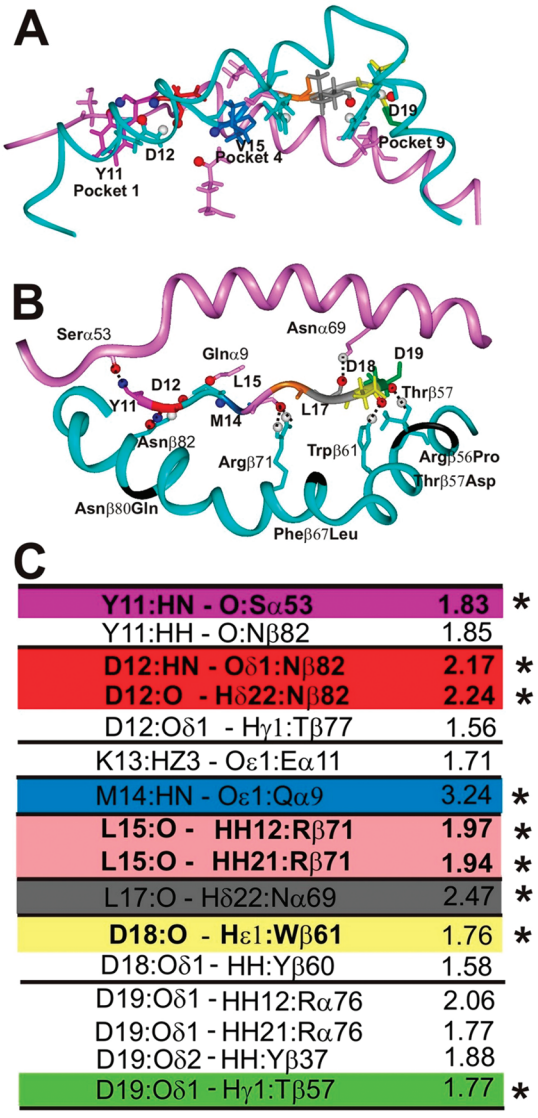

Figure 9. HABP **24166** interatomic interactions with HLA-DRβ1*01 molecules. **24166** interaction with HLA-DRβ1*0101-like from protected *Aotus* monkeys modified according to the HLA-DRβ1*0101 structure (PDB code 1DLH)[185] and Suarez et al.[181] (A) The front view shows the orientation of **24166** residues' lateral-chains (represented as sticks) and their position inside modified HLA-DRβ1*01 shown according to the same color code used in Figure 5. Panel B shows the top view of the peptide backbone displaying the H-bonds (shown as dotted lines) established between **24166** backbone atoms (represented as sticks) and HLA-DRβ1*0101 α- and β-chain residue side-chain atoms (depicted as pink and blue ribbons, respectively) in protected monkeys. The nitrogen and oxygen atoms are shown as blue and red balls, respectively. Black segments in the β-chain correspond to the residues that were modified according to the *Aotus* MHCII sequence (HLA-DRβ1*0101-like). (C) H-bond (indicated by an asterisk) and van der Waals interactions, both measured in angstroms (Å) between **24166** and HLA-DRβ1*0101 lateral chains, colored according to the color code previously established for P1 to P9.

13844 and **9236** (both derived from 6737), were protected against experimental challenge, but such protection was not associated with antibody production as assessed by IFA, Western blot, and ELISA.[197] Interestingly, these monkeys were the only ones that simultaneously produced high concentrations of IFN-α and IL-4 (although they were not the highest), which suggested that both Th1 and Th2 associated immune responses were simultaneously activated by immunization with these modified peptides. Another *Aotus* monkey (451), which was also immunized with **13844** (6737), produced IFN-γ, TNF-α, IL-2, IL-4, and IL-6, and low SI (SI $\leq$ 3.0).

6.3.3. Critical Role of P8 in Inducing a Protective Cellular Immune Response against Malaria. When these modified HABPs' 3D structures were determined by ^{1}H NMR studies and compared to immunogenic protection-inducing HABP analogous structures, we found that there was a different orientation of the P8 residue in the seven (7) modified HABPs inducing protective cellular immune responses (no antibody production, but high SI associated with high Th1 and Th2 cytokine levels). Accordingly, P8 (yellow) pointed downward or sideways, whereas the same residue had mostly an upward or different orientation in high, long-lasting antibody levels and protection-inducing modified HABPs. This orientation difference in P8 suggested that an upward-orientation in appropriately modified HABPs was required for establishing contact with the TCR, thus inducing protective antibody production[197] (Figures 7ID and IID′ and 8B).

7. MOLECULAR MODELING OF MODIFIED HABP DOCKING INTO HLA-DR AND TCR MOLECULES

Molecular modeling and docking studies were carried out for some peptides to determine how well the 3D structures of our immunogenic protection-inducing modified HABPs' (determined by ^{1}H NMR) fit inside the few previously identified HLA-DRβ1* structures (determined by X-ray crystallography), based on HLA-DRβ1* binding capacities, binding motifs, and binding registers previously demonstrated for these modified HABPs, to test these results' reliability by working with two completely different but complementary techniques: ^{1}H NMR and X-ray crystallography.

It would have been ideal to have the *Aotus* HLA-DRβ1*0403-**24112**-TCR complex crystallized to analyze its informative macromolecular complex 3D structure; unfortunately, despite the tremendous effort made by excellent groups of scientists (immunologists, crystallographers, *etc.*), very few (just 2) MHCII-pep-TCR 3D structures have been determined during the previous 12 years.

7.1. Modified HABP 24166 Docking in the HLA-DRβ1*0101 Molecule Complex

24166 (1818) was reproducibly immunogenic (Figure 4A18 and B) and induced protection in some experimentally challenged *Aotus* (Tables 1 and 2) associated with binding to HLA-DRβ1*0101 molecules (Table 3). Docking was performed by replacing the hemagglutinin (HA) peptide (residues 306-318) with **24166** into which the HLA-DRβ1*0101 molecule was cocrystallized.[185] This showed that **24166** fit very well when superimposed onto the PBR of HLA-DRβ1*0101 molecules (Figure 9A and B).

Please note that amino acids are written in one-letter code if they came from a modified peptide and three-letter code for amino acids from HLA-DR, hereinafter.

Docking **24166** inside the 3D structure of HLA-DRβ1*0101 (modified according to the amino acid sequence differences found in analogous DRβ* W4301 and W4304 *Aotus* monkeys) showed the spontaneous formation of *nine* H-bonds between this MCHII molecule and **24166** (Figure 9C). *Aotus* HLA-DRβ1*0101 Class II molecules are similar to human HLA-DRβ1*0101

according to molecular biology studies by Suárez et al.[181] as displaying nine amino acid differences in the β-chain residues forming the PBR (Trp9Lys, Cys13Phe, Asp28Glu, His30Cys, Tyr37Ser, Arg56Pro, Thr57Asp, Phe67Leu, and Asn70Gln, with the last four involved in peptide binding).

Please remember that Class II residues are written in three-letter code while peptide residues are shown in one-letter code for clarity in these sections of the manuscript.

Our previous ^{1}H NMR studies have shown that **24166** displayed two different structural families having classical β-turn type III structures, one spanning residues S9 to N12 and the second Y14 to M17; the latter was used for docking studies, as it was the most common.[111] The presence of these two families of structures could have partly explained dual binding ability (one to HLA-DRβ1*0101 and the other to HLA-DRβ1*1101), since both binding registers were present in this molecule; however, the specific methodology for isolating each isoform is not yet available.

Similarly to what occurs with the HA peptide within the HLA-DRβ1*0101's groove, the residues corresponding to the **24166**'s binding motifs and binding registers (**Y**DK**ML**P**L**D**D** in bold and underlined) fitting into P1 (Y, fuchsia) and P9 (D, green) were deeply embedded within this molecule. The residue fitting into P4 (M, dark blue) was relatively large whereas the one fitting inside P6 (P, brown) was very small, a particular characteristic of HLA-DRβ1*0101, since only small apolar amino acids such as A, G, S, P, and T could fit inside pocket 6, due to this pocket's very small size. All the amino acids corresponded to the classical binding motifs and binding registers for fitting into this Class II molecule's pockets[155,157,158] (Figure 9) and correlated very well with the binding ability found for this modified HABP when working with purified HLA-DRβ1*0101 molecules.

The *nine* H-bonds (Figure 9C) established between **24166** backbone atoms and the lateral chains of HLA-DRβ1*0101 modified residues (replaced according to the *Aotus* DRβ*W4301 sequence, as previously described) and their corresponding interatomic distances (in angstroms, shown in parentheses) are shown in Figure 9C indicated by an asterisk following the color code previously established for **24166** amino acids: Y11 (fuchsia) fitting into pocket 1, D12 (red) into P2, K13 (pale blue) into P3, N14 (dark blue) into pocket 4, L15 (pink) into P5, P16 (brown) into pocket 6, L17 (gray) and D18 (yellow) into P7 and P8, respectively, and D19 (green) into pocket 9.

These nine H-bonds were established between the backbone atoms of **24166** and lateral chain atoms of HLA-DRβ1* 0101 residues in such a way that Y11 established an H-bond with Serα53 (fuchsia, 1.83 Å), D12 established a bidentated H-bond with Asnβ82 (red, 2.13 Å and 2.24 Å), as has been thoroughly described for this Class II residue, M14 with Glnα 9 (dark blue, 3.24 Å), another bidentated H-bond was established between the double reacting N groups of Argβ71 with L15 (pink 1.97 Å and 1.94 Å, respectively), L17 reacted with Asnα 69 (gray, 2.47 Å), D18 with Trpβ61 (1.76 Å), and D19 (green, 1.77 Å) with Thrβ57.

These H-bonds were the canonical H-bonds established by the HA peptide and HLA-DRβ1*0101 molecule, suggesting that **24166** binding to this Class II molecule was almost identical to that observed in a classical HLA-DRβ1*0101-HA 3D structure.[185]

The Thrβ57Asp difference between HLA-DRβ1*0101 and *Aotus* DRβ* W4301 should be noted, since the absence of the salt bridge established between Aspβ57 and Argα76 in *Aotus* MCHII molecule pocket 9 led to the preferential binding of peptides carrying negatively charged residues, such as D or E in this position, as occurred with **24166**. This situation is commonly found in some HLA-DRβ1* alleles, mouse I-Ag^{7}[186] and human HLA-DQ8 associated with insulin-dependent diabetes.[192]

These results very clearly showed that if some *more* HLA-DRβ1*0101 restricted peptides had to be included in a fully protective antimalarial vaccine, then a larger number of *Aotus* monkeys had to be screened to select monkeys carrying this allele, given that HLA-DRβ1*0101 allele frequency was very low (∼10%) in the wild population,[181] which could partly explain why few modified HABPs have been identified as fitting into HLA-DRβ1*0101 to date and/or being specific for this genetic characteristic.

This data has shown that the residues from immunogenic protection-inducing modified HABPs have to be properly orientated in the MHCII/pTCR complex according to the specific HLA-DRβ1* molecule to which they bind to allow TCRs to contact specific residues in both the peptide and Class II molecules so as to activate an protective immune response.

Such modifications have to be carefully and exquisitely performed, since immunogenic, protection-inducing modified HABPs can display different MHC binding registers that would lead to different immune responses depending on the allele and the way they are bound, as thoroughly shown in this manuscript and elsewhere.[197,220]

7.2. Testing the Minimal Subunit-Based Synthetic Vaccine Concept

7.2.1. Modified HABP 24112 Immunogenicity and Protection-Inducing Activity in Hla-Dr-Like Typed Monkeys.

As *proof of principle*, a recently published study[216] based on previous results obtained with **24112** (4044),[84] which was highly immunogenic and induced protection in ∼20% of the vaccinated monkeys in several monkey trials (Figure 4A5 and in B, several blots), found that protected *Aotus* monkeys immunized with **24112** carried the HLA-DRβ1*04 allele; this modified HABP showed high experimental binding capacity to this class II purified molecule, and it also displayed the binding motifs and binding registers characteristic for HLA-DRβ1*0401 molecules.

In this study, eighteen (18) *Aotus* were selected from a group of 40 recently captured, nonfamily related, nongeographically close, molecularly genotyped *Aotus* monkeys and classified into four immunization groups based on the high similarity existing between *Aotus* monkeys' MHC-DRB exon 2 and HLA-DRβ1* alleles.[181] Group A (HLA-DRβ1*0403-like) contained six MHC-AoDRβ*W45/47 monkeys having 92%−100% of similarity with HLA-DRβ1*0403; group B (HLA-DRβ1*0422-like) included five MHC-AoDRβ*06 genotyped monkeys showing 95% similarity with HLA-DRβ1*0422; group C consisted of two MHC-AoDRβ1*03 (HLA-DRβ1*0301-like) monkeys having 89%−95% similarity with HLA-DRβ1*0301 and one MHC-AoDRβ*W38 (HLA-DRβ1*0701-like) monkey showing 87%−93% similarity with HLA-DRβ1*0701; group D contained four monkeys having diverse MHC-AoDRβ alleles. HLA-DRβ1*04-like[181] was used as immunization control, due to limited monkey typing.

Groups A, B, and C were immunized on days 0, 20, and 40 with **24112** (4044) homogenized in Freund's adjuvant while group D only received saline solution emulsified in the same adjuvant on the same days (negative control). IFA analysis showed that very

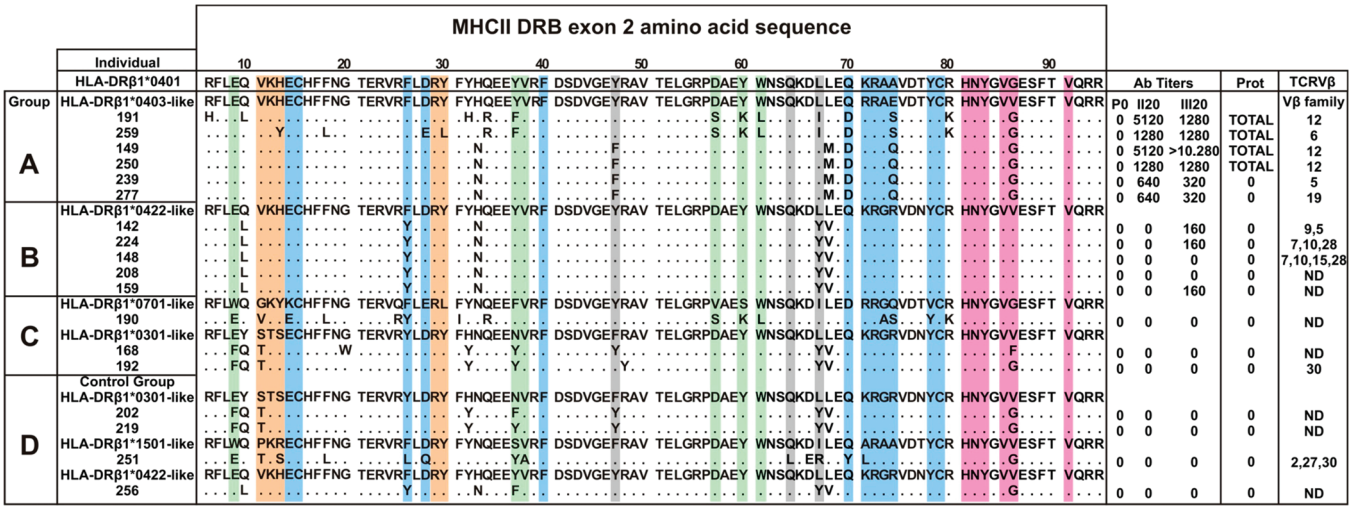

Figure 10. Genotyping, immune response and preferential TCR Vβ usage of immunized *Aotus* monkeys. Amino acid sequence of genotyped monkeys analyzed in this study. At the top, in the first row, the amino acid sequence of the reference HLADRβ1*0401 molecule as reported by Hennecke.[254] Monkeys were classified into different immunization groups (A, B, C, and D) according to the similarity of their MHC class II DRβ exon 2 nucleotide sequences to HLA-DRβ1* alleles, displayed at the top of each group as reference. Each monkey's antibody titers (Ab Titers) determined by IFA before (P0) or 20 days after each immunization (II20, III20), as well as protection results (Prot) against experimental challenge and expanded TCR βV families are shown. Residues forming the HLA-DRβ1*04 pockets are highlighted in different colors according to the previously established code: pocket 1 (P1), fuchsia; pocket 4 (P4), blue; pocket 6 (P6), orange; pocket 7 (P7), gray; and pocket 9 (P9), light green. (Reprinted with permission from ref 216. Copyright 2010 Public Library of Science.)

high antibody titers ($\geq$1:1280) were developed in four out of the six (~67%) HLA-DRβ1*0403-like genotyped monkeys in group A after the second and third immunizations, as indicated by the recognition of a membrane immunofluorescence pattern in late schizonts, which was in complete agreement with MSP-2 surface location from which these 4044 sequences were derived (Figure 4A5). Furthermore, Western blot analysis of *P. falciparum*-schizont lysates using the same hyperimmune sera from group A monkeys showed strong reactivity with 69, 63, and 48 kDa molecules, as well as weaker recognition of 54 and 51 kDa molecules, which were close to MSP-2's molecular weight (~68 kDa) and that of its cleavage fragments (as seen in Figure 4B, far right, showing the Western blot analysis with this new group of anti-**24112** sera). The remaining two HLA-DRβ1*0403-like monkeys in group A developed lower antibody titers (1:320) and showed weaker Western blot recognition of MSP-2 and its cleavage fragments (not shown due to space limitations).

During challenge performed 20 days after the third dose, following the intravenous injection of 100,000 fresh RBC infected with the *Aotus* monkey-adapted *P. falciparum* FVO strain, control as well as nonprotected monkeys developed very high parasitemia by day 5 that reached $\geq$5% by days 8−11 and required immediate treatment, whereas the same four HLA-DRβ1*0403-like monkeys that produced very high antibody titers ($\geq$1:1280) developed sterile immunity and were therefore fully protected against experimental challenge with *P. falciparum*. Sterile immunity was defined as being the complete absence of blood parasites on the whole slide (screening ~1,000,000 RBC per monkey per day by Acridine Orange staining and fluorescence microscopy) during the 15 days that the experiment lasted. According to such criteria, **24112** conferred sterile immunity on two-thirds (66.6%) of the HLA-DRβ1*0403-like genotyped *Aotus* monkeys (Figure 10).

On the contrary, the other two monkeys producing lower antibody titers ($\leq$1:320) developed very high parasitemia levels (>5%) 8−11 days postchallenge, comparable to the levels shown by control monkeys (Figure 10). Some monkeys immunized with **24112** and genotyped as carrying the HLA-DRβ1*0422-like allele developed low antibody titers (1:160) or did not produce any antibodies against the parasite, the same as monkeys carrying the HLA-DRβ1*0301 genetic marker and control monkeys. *None* of the monkeys in groups B, C, and D were protected against experimental challenge.

7.3. Peptide 24112 Docking in Protected Monkeys' Hla-Drβ1*04 Molecule Produced High Antibody Titers While Its Docking with Nonprotected Monkeys' HLA-DRβ1*03 Molecule Produced No Antibody Titers

Previous trials[171,216] found strong association between **HLA-DRβ1*0401** binding characteristics, the *sterile immunity* inducing capacity of **24112** and this modified HABP's 3D structure as determined by us;[84] **24112** docking studies were therefore performed on this MHCII molecule using the HLA-DRβ1*0401 molecule's 3D structure determined by Hennecke as template.[253,254]

^{1}H NMR studies on **24112** have shown that there was a distorted type III′ β-turn spanning residue Y3 to T6 and a classical type III′ β-turn structure between residues A11 and M14 in this immunogenic protection-inducing modified HABP[84] whereas the rest of the molecule was unstructured. This structure was similar to the crystallographic structure of the HA peptide complex formed with the HLA-DRβ1*0401 molecule,[254] where residues fitting inside pocket 1 (Y12 fuchsia) and pocket 9 (M20 green) were downwardly orientated and deeply embedded into these pockets (Figure 11A), whereas residues fitting inside pocket 4 (V15 dark blue) and pocket 6 (R17 brown) were more shallowly embedded.[158,182,185,188]

It was considered that other binding motifs and binding registers could permit **24112** docking inside the HLA-DRβ1*0401 3D structure, but none of them displayed the complete binding motives nor binding registers characteristic

dx.doi.org/10.1021/cr100223m |*Chem. Rev.* 2011, 111, 3459–3507

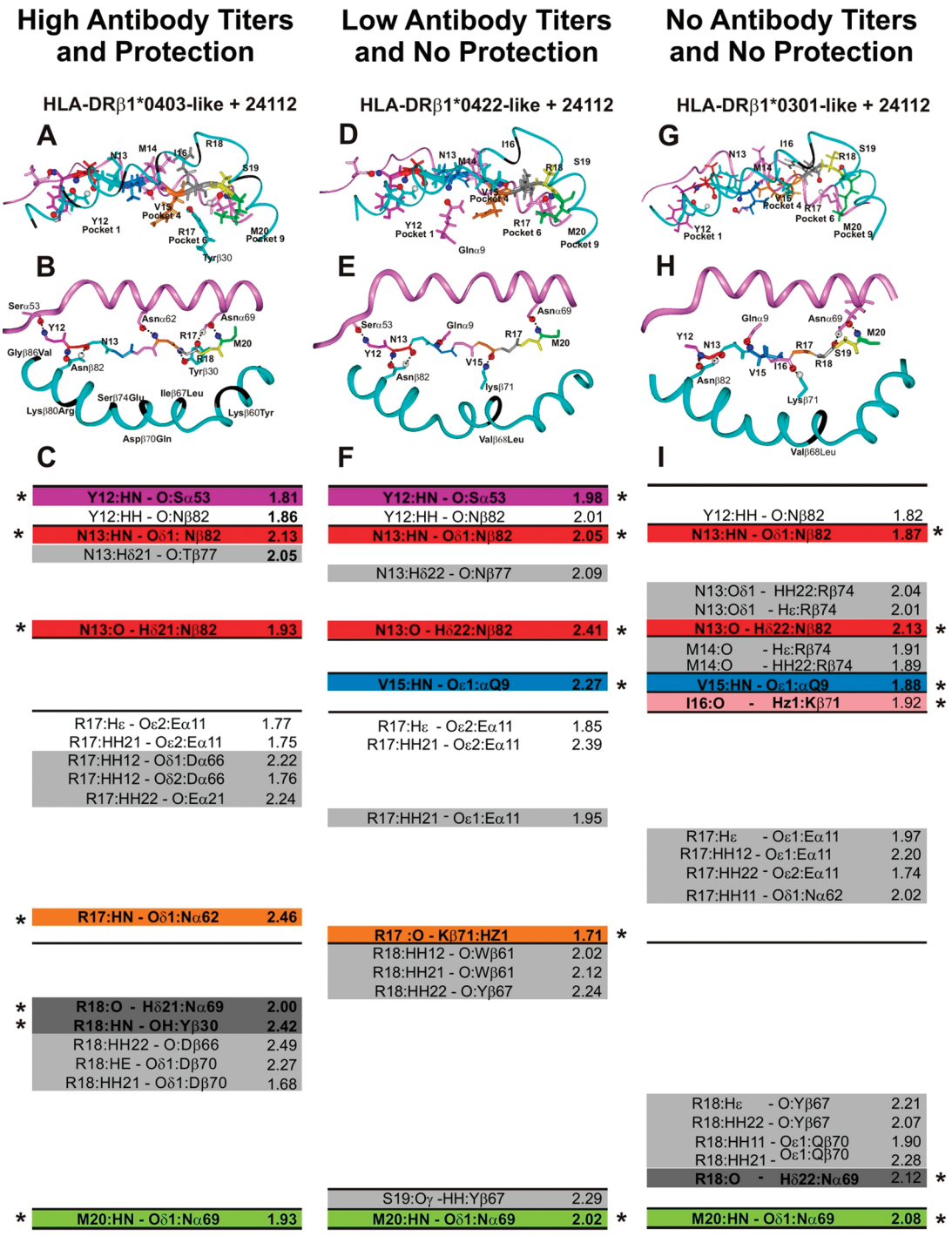

Figure 11. Interatomic interactions of HABP **24112** with HLA-DRβ1*0401 and *Aotus* modified HLA-DRβ1*0301 molecules. **24112** interaction with protected *Aotus* 191 HLA-DRβ1*0403-like: (A) front view; (B) top view. **24112** interaction with nonprotected *Aotus* 148 HLA-DRβ1*0422-like complex: (D) front view; (E) top view. **24112** interaction with the HLA-DRβ1*0301-like molecule from nonprotected *Aotus* 192 which did not produce antibodies: (G) front view; (H) top view. Front view panels A, D, and G show the orientation of **24112** residues' lateral-chains (represented as sticks) and their positions inside MHCII molecules shown according to the previously established color code in Figure 5. The top view panels B, E, and H display the H-bonds (shown as dotted lines) established between **24112** backbone atoms (represented as sticks) and MHCII α- and β-chain residue side-chain atoms (depicted as pink and blue ribbons, respectively) in protected (monkey 191) as well as nonprotected monkeys (148 and 192, respectively). Nitrogen and oxygen atoms are shown as blue and red balls. Black segments in the β-chain correspond to the residues that were modified according to the MHCII sequences of Ao191 (HLA-DRβ1*0403), Ao148 (HLA-DRβ1*0422), and Ao192 (HLA-DRβ1*0301). (C, F, and I) H-bonds and van der Waals interactions, measured in angstroms (Å), between **24112** and HLA-DRβ1*0403 and HLA-DRβ1*0422 and between **24112** and Ao192 (HLA-DRβ1*0301). H-bonds are depicted with an asterisk and interactions involving different atoms are highlighted in pale gray, while interactions involving common residues are not shadowed. The color code for those residues establishing such H-bonds is the same as that used in Figure 5. Note the absence of the critical H bond formation between Y12 and Sα53 in HLA-DRβ1*0301 monkeys (panels G, H, and I). (Adapted with permission from ref 216. Copyright 2010 Public Library of Science.)

dx.doi.org/10.1021/cr100223m |*Chem. Rev.* 2011, 111, 3459–3507

for this allelic molecule, which did not allow a perfect fit inside the PBR of this HLA-DRβ1* molecule, therefore suggesting that the only probable structure was YNMVIRRSM (residues fitting inside pockets 1, 4, 6, and 9 are underlined and in bold, respectively) for a perfect fit into this class II molecule.

HLA-DRβ1*0403 structure was modified according to amino acid sequence differences found in fully protected *Aotus* monkey 191, which had the HLA-DRβ1*0403-like β-chain PBR amino acid sequence (Phe37Tyr, Ser57Asp, Lys60Tyr, Ile67Leu, Asp70Gln, Ser74Glu, Lys80Arg, and Gly86Val). Docking **24112** inside such a modified structure showed that the pMHC structure became stabilized by the spontaneous formation of seven of the ten canonical H-bonds[182,185,188] between **24112** backbone atoms and lateral chain atoms of modified HLA-DRβ1*0403 residues (Figure 11B).

These seven H-bonds, with their corresponding interatomic distances (shown in angstroms inside parentheses throughout this manuscript and indicted by an asterisk in Figure 11C), are depicted according to the color code previously established for **24112**, where Y12 (fuchsia) fit into pocket 1, N13 (red) corresponded to P2, M14 (pale blue) to P3, V15 (dark blue) fit into pocket 4, I16 (pink) corresponded to P5, R17 (brown) to pocket 6, R18 (gray) to P7, S19 (yellow) to pocket P8, and M20 (green) to pocket 9.

By the same token, docking **24112** into the HLA-DRβ1*0422 3D structure modified according to the few differences found in one of the nonprotected, nonantibody producing monkeys (*Aotus* 148) where two amino acid changes were found with the corresponding human allele (Val68Leu, Leu67Tyr) showed the spontaneous formation of six of the 10 canonical H-bonds between atoms from the peptide's backbone and MHCII lateral chain residues, strongly suggesting that **24112** had a greater binding preference for HLA-DRβ1*0403-like molecules than HLA-DRβ1*0422-like molecules (Figure 11D and E).

24112 binding to HLA-DRβ1*0403 in protected monkeys displayed a totally different H-bond pattern in nonprotected HLA-DRβ1*0422 monkeys between V15 with pocket 4 Glnα9 (in dark blue, 2.27 Å) and R17 with pocket 6 Lysβ71 (in brown, 1.71 Å). No H-bonds were found between **24112**'s R18 backbone atoms and HLA-DRβ1*0422 lateral chains (Figure 11F).

Likewise, **24112** docking into the HLA-DRβ1*0301 molecule described by Ghosh et al.,[183] modified in residues Gluβ9Phe, Tyrβ10Gln, Serβ11Thr, Hisβ32Tyr, Asnβ37Tyr, Argβ48Tyr, Leuβ67Tyr, Leuβ68Val, and Valβ86Gly according to the β-chain amino acid sequence of HLA-DRβ1*0301 genotyped monkeys not developing antibodies against this peptide or the parasite or being protected against experimental challenge (*Aotus* 192), showed the establishment of *six* of the 10 canonical H-bonds between atoms from the peptide's backbone and HLA-DRβ1*0301-like *Aotus* modified molecule's lateral chain residues (Figure 11G and H).

The same as in HLA-DRβ1*0422, **24112** binding to nonantibody producing, nonprotected HLA-DRβ1*0301 monkeys displayed a completely different binding pattern compared to HLA-DRβ1*0403 molecules. It was strikingly observed that *no H-bonds* were established between Y12 with Serα53 from pocket 1; this is a critical H-bond formation which is essential for stabilizing the pMHCII complex, since it has been extensively shown that pocket 1 has been the most important pocket for anchoring immunogenic peptides to MHCII molecules (Figure 11I). By the same token, the absence of H-bonds between pocket 6 residues and R17 backbone atoms could account for poor **24112** binding to HLA-DRβ1*03 molecules, as experimentally documented by the absence of **24112**

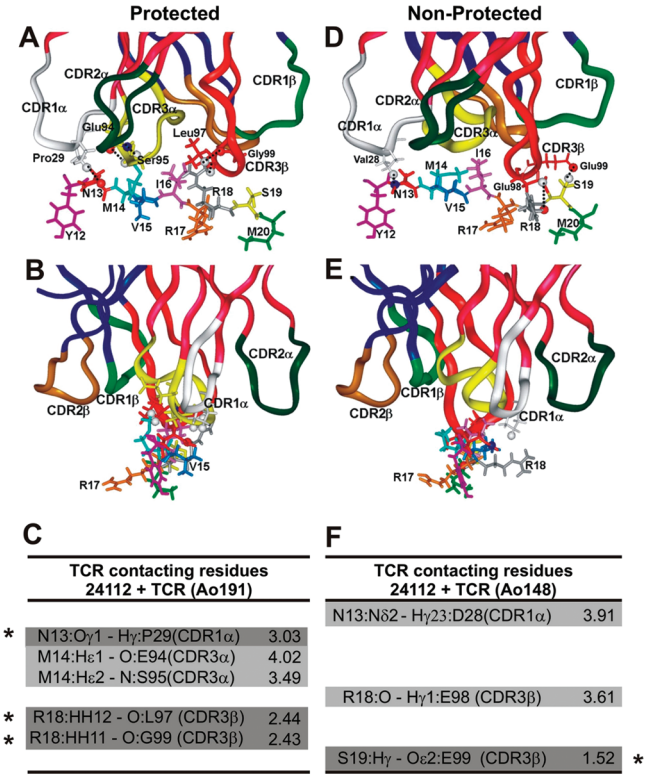

Figure 12. Peptide **24112** interactions with modified HA 1.7 TCR. (A and B) H-bonds and van der Waals interactions established between peptide **24112** and HA 1.7 TCR molecule modified according to the Vβ12 clone 3 sequence from protected *Aotus* 191. (D and E) **24112** H-bonds and van der Waals interactions with the HA 1.7 TCR molecule carrying the Vβ15 clone 5 sequence from the nonantibody producer, nonprotected *Aotus* monkey 148. Small black dots correspond to **24112**'s atoms making contact with modified HA 1.7 TCR molecule atoms. Amino acids conforming each TCR CDR are as follows: in the TCR α-chain (dark pink ribbons shown on top): Tyr24 to Tyr31 for CDR1α (white ribbon), Lys48 to Leu55 for CDR2α (dark green ribbon), and Ser93 to Leu104 for CDR3α (yellow ribbon); in the TCR β-chain CDR (dark blue ribbons on top): Val24 to Asn31 for CDR1β (light green ribbon), Phe48 to Glu56 for the CDR2β (gold ribbon), and Ala93 to Gly109 for CDR3β (red ribbon). (B and E) Front view of the same complex and view rotated 90°. (C and F) H-bonds (dark gray and with an asterisk) and van der Waals interactions established between peptide **24112** and Ao191-Vβ12 TCR (left column) and Ao148-Vβ15 TCR (right column), with their corresponding interatomic distances indicated in angstroms (Å). Interactions involving different atoms are highlighted in pale gray, whereas interactions involving the same residues in both complex are not highlighted. (Reprinted with permission from ref 216. Copyright 2010 Public Library of Science.)

binding capacity to this purified molecule,[171] which could partly explain **24112**'s lack of immunogenicity and protective immunity in individuals carrying this genetic trait. Pocket 6 has been shown to give strong specificity and strong binding capacity to HLA-DRβ1*04 molecules.

Additional differences were observed between these three pMHCII complexes (highlighted in pale gray in Figure 11C, F, and I) regarding van der Waals forces established between other **24112** atoms and HLA-DRβ1*0403, HLA-DRβ1*0422, and HLA-DRβ1*0301 modified molecules.

It was clear from the differences between **24112**'s modes of binding to HLA-DRβ1*0403, HLA-DRβ1*0422, and HLA-DRβ1*0301 modified molecules that the key interactions in

dx.doi.org/10.1021/cr100223m |*Chem. Rev.* 2011, 111, 3459–3507

peptide binding for inducing immunity, either fully protective as in HLA-DRβ1*0403 genotyped *Aotus* monkeys or nonprotective as in HLA-DRβ1*0422 monkeys or completely nonimmunogenic, nonprotection inducing as in HLA-DRβ1*0301 monkeys, involved the canonical formation of H-bonds between specific **24112** backbone atoms and specific atoms in the lateral chains of the residues forming the different pockets.

7.4. Preferential Use of TCR Vβ Families

T-cells from the 18 monkeys involved in a recent study[216] as described in the above section were isolated from blood samples drawn one day prior to the first vaccination and the day before challenging animals with an intravenous inoculation of *P. falciparum* iRBC for deeper analysis of the appropriate MHCII/pTCR complex formation. T-cells were subsequently expanded and cloned for assessing their preferential usage of TCR Vβ families by spectratyping and DNA sequencing of the amplified complementary determining region 3 (CDR3), the most relevant and polymorphic region of the TCR, which establishes direct contact with the antigen presented by MCHII molecules. The results showed that there was preferential usage of T-cell clones for Vβ12 and Vβ6 TCR families in the four (4) fully protected HLA-DRβ1*0403 genotyped monkeys (group A) (Figure 10), while there was *no* predominant usage of any particular TCR family or any preponderant sequence in HLA-DRβ1*0403 monkeys which were not protected and those belonging to the HLA-DRβ1*0422 or another HLA-DR genotype that did not develop any antibody titers or were not protected.[216] This data suggested an exclusion mechanism at the TCR level between protected and nonprotected monkeys in TCR Vβ usage, in spite of some of them showing antibody production (although at a lower level) after being immunized with the same epitope. Therefore, the later groups low antibody titers must have had different specificities, affinities, and/or structural characteristics, a subject which is currently being studied at our institute.

7.4.1. Structural Analysis of the HLA-DRβ1*0403−24112−TCR Complex. Based on the amino acid sequence of the VβCDR3 T-cell clones obtained from fully protected monkeys developing *sterile immunity* and nonprotected ones, the previously reported HLA-DRβ1*0401−HA−HA1.7 TCR crystal structure was modified according to the amino acid sequence of the preferred Vβ TCRs to determine the HLA-DRβ1*0403-like−**24112**−TCR structure of fully protected *Aotus* monkeys versus the HLA-DRβ1*0422-like−**24112**−TCR structure of nonprotected ones. These molecules were analyzed and compared at the atomic level to examine H-bond formation and distance differences.

The TCR Vβ3S1 sequence reported for the HLA-DRβ1*0401−HA−HA1.7 TCR complex was modified in the CDR3β region to study the HLA-DRβ1*0403-like−**24112**−TCR complex according to the variations found in the Vβ12 D region of clone 3 from protected *Aotus* monkey 191. Likewise, the TCR Vβ3S1 sequence was replaced in the HLA-DRβ1*0422-like−**24112**−TCR complex by the Vβ15 family sequence found in clone 5 from nonprotected, nonantibody-producing *Aotus* monkey 148. Superimposing the HLA-DR1*0403−**24112**−TCRVβ12 and HLA-DRβ1*0422−**24112**−TCRVβ15 modified complexes onto the original 3D structure of the HLA-DRβ1*0401−HA−HA1.7 TCR complex gave 1.41 and 1.32 rmsd, respectively.

Based on the information mentioned above and the fact that TCR Vα displayed limited polymorphism (their CDRs were thus not cloned in the referred study), docking analysis using the HLA-DRβ1*0401−HA−HA1.7 TCR complex 3D structure as template showed that such modified HA1.7 TCR binding to both HLA-DRβ1*04−**24112** complexes was mediated by TCR Vα region (Figures 12A and D red ribbon and top) interaction with the peptide's N-terminal portion while the C-terminal fragment established contact with Vβ regions (Figures 12A and D, dark blue ribbon on top), as recently described elsewhere.[216]

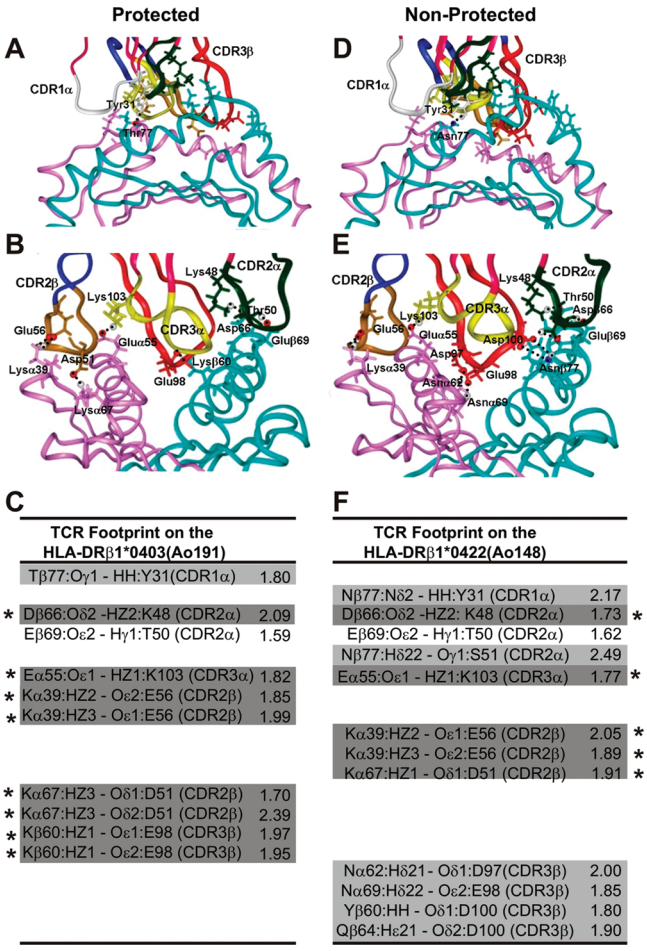

Figure 13. Footprint of modified HA 1.7 TCR on HLA-DRβ1*04 molecules. (A and B) Footprint of the HA 1.7 TCR molecule modified according to the Vβ12 clone 3 sequence of protected *Aotus* 191, in the HLA-DRβ1*0403 molecule. (D and E) Footprint of the HA 1.7 TCR molecule modified according to the Vβ15 clone 5 sequence of the nonantibody producer, nonprotected *Aotus* monkeys 148 on the HLA-DRβ1*0422 molecule. (B and E) Front views of the same complexes and view rotated 90°. (C and F) H-bonds established between HLA-DRβ1*0403 and HA1.7 TCR-like modified molecules and between HLA-DRβ1*0422 and the same TCR with their corresponding interatomic distances indicated in angstroms (Å) highlighted with an asterisk. Salt bridges are highlighted in dark gray and with asterisk while interactions involving different atoms are highlighted in pale gray, and interactions involving the same residues in both complexes are not highlighted. Note that there are *8 salt bridges* between residues established in the footprint of the protected *Aotus* 191 monkey *versus 5* in the footprint of the 148 nonprotected Aotus 148 monkey. (Reprinted with permission from ref 216. Copyright 2010 Public Library of Science.)

7.4.2. Modified Peptide 24112 Atoms Recognized by Modified TCR CDRs. The following *five* residues from highly immunogenic **24112** inducing *sterile immunity* and protection

dx.doi.org/10.1021/cr100223m |*Chem. Rev.* 2011, 111, 3459–3507

were upwardly oriented when **24112** was presented in the context of HLA-DRβ1*0403 (Figure 12A and B): N13 (corresponding to P2 in red), M14 (P3 in pale blue), I16 (P5 in pink), R18 (P7 in gray), S19 (P8 in yellow), but particularly R18 (gray). These five residues were therefore possibly available for TCR inspection. The CDR3β Vβ12 from the protected monkey showed the spontaneous formation of *three* H-bonds (shown as small dots in Figure 12A and B; highlighted in dark gray in Figure 12C where they are indicated by asterisks): one between N13 and Proα29 from CDR1α (white ribbon, at the top) and two between R18 with Leuβ97 (2.44 Å) and R18 with Glyβ99 (2.43 Å) from CDR3β (red ribbon, top). Another TWO van der Waals interactions were observed between M14 with Gluβ94 (4.02 Å) from CDR3α (yellow ribbon) and M14 with Serα95 from CDR3α (yellow ribbon, top) (3.49 Å).

Only *one* H-bond (Figure 12F, dark gray, indicated by an asterisk) was spontaneously formed between S19 and Gluβ99 (1.52 Å) in analysis of the HLA-DRβ1*0422−**24112** TCR contact residues complexed with the CDR3β Vβ15 region from the nonprotected monkey (Figure 12D, E and F) while *two* van der Waals interactions were observed between N13 with Aspα28 (3.91 Å) from CDR1α (white ribbon) and R18 with Gluβ98 (3.61 Å) from CDR3β (red ribbon). This was perhaps due to this peptide's R18 residue's horizontal location. Besides displaying poor or weak interaction between HLA-DRβ1*0422 and **24112**, this complex also displayed fewer and weaker electrostatic interactions with the TCR.

7.4.3. TCR Footprint on the 24112 HLA-DRβ1*04 Molecule Complex. Figure 13A−C shows the H-bonds established between the HLA-DRβ1*0403-modified molecule and the Vβ12-clone-3-modified TCR of protected *Aotus* monkey 191 (whose sera had high antibody titers). The figure also gives their corresponding interatomic distances and 3D structures and interatomic distances between the HLA-DRβ1*0422-modified molecule and the Vβ15-clone-5-derived TCR from nonantibody-producing, nonprotected *Aotus* monkey 148 (Figure 13D−F).

Taking the human influenza TCR−pMHCII complex as a template, the footprint analysis of these TCRs on their corresponding MHCII molecules (Figure 13A and B, white ribbon) shows that eight (8) H-bonds (listed in part C of Figure 13) were specifically established in HLA-DRβ1*0403 with CDR1α residues (Thrβ77 with Tyr1α31), CDR2β residues (Lysα39 with Glu2β56, Lysα67 with Asp2β51, brown ribbon in the same Figure), and CDR3β residues (Lysβ60 with Glu3β98, red ribbon). HLA-DRβ1*0422 preferred specific interactions between CDR1α residues (Asnβ77 with Tyr1α31, white ribbon) and CDR2α residues (Asnβ77 with Ser2α51, green ribbon), CDR2β residues (Lysα39 with Glu2β56 and Asp2β51, brown ribbon), and CDR3β residues (Asnα62 with Asp3β97, Asnα69 with Glu3β98, Tyrβ60 with Asp3β100, and Glnβ64 also with Asp3β100, red ribbon). All the above-mentioned H-bonds induced a twist and slight displacement toward HLA-DRβ1*0422 α-chain residues which have not been quantitatively determined in this study but can be seen most clearly when comparing Figure 13B and E.

Only five (5) salt bridges (Figure 13F, dark gray, with asterisk) were established between the residues forming the nonprotective HLA-DRβ1*0422−Vβ15 TCR complex, whereas eight (8) salt bridges were formed in the protection-associated HLA-DRβ1*0403−Vβ12 TCR complex (Figure 13C, dark gray, with asterisk *). This H-bond formation suggested a stronger and more stable interaction for this pMHCII complex, being a condition needed for stabilizing the complex and properly activating the immune system toward a sterilizing immune response.

Other authors[182] have shown that the strongest interactions were established between MHCII molecules' lateral chain atoms and atoms from the peptide's backbone (Figure 11), whereas the strongest bonds were established with the peptide's lateral chain atoms in the peptide/TCR interaction (Figure 13), with salt bridges being the most important electrostatic forces.

In essence, six extra H-bonds were formed in the HLA-DRβ1*0403−24112-Vβ12 TCR complex (one more between the **24112**-HLA−DRβ1*0403 complex, two more between 24112-Vβ12 TCR, and three more in the Vβ12 TCR footprint on the HLA-DRβ1*0403 molecule) compared to the HLA-DRβ1*0422-**24112**-Vβ15 TCR complex.

It has also been shown[254] that a large array of important differences exist between residues' orientation and electrostatic forces established in these TCR/pMHCII complexes which are associated with two different immunological outcomes induced by the same peptide in slightly different variants of the same HLA-DRβ1*04 allele, this being the essence of this whole section.

7.5. The MHCII/pTCR Synapse

The TCR usually has a diagonal orientation in relation to the MHCII peptide binding groove's long axis. Peptide contacts are made primarily through the CDR3 loops while contacts with MHCII helices are made through CDR1 and CDR2 in the canonical system[247−250,253,254] (Figures 12 and 13).

Variations in orientation with the MHCII−peptide (pMHC) complex have been found to range from 24°−80°, suggesting that their interactions could thus twist, tilt, or shift, where twist refers to the angle between the TCR and pMHC long axes viewed from the TCR projecting it into the pMHCII.[247−250,253−256] Tilts and shifts are better appreciated in the frontal views (Figures 12B and 13B and E) when different MHCII/pTCR complexes are analyzed. In such views, the pivotal point for the twist and tilt seems to be at the Vα domain. All these variations in orientation are contributed by the diversity of Vβ domain contacts with the pMHCII complexes.[255]

The data obtained from superimposing **24112** onto the HLA-DRβ1*0401−HA1.7 TCR complex suggested that this immunogenic protection-inducing peptide fit into this complex in a canonical way, since there were no major deviations in orientation and distances between the different contact residues.

It is also well-known that, as well as variations in crossing angles between the MHCII binding platform helices (or MHCII bound peptides) and an axis drawn between the α- and β-chain TCR CDR loops,[186,187,191,256] the TCR can present different contact sites with the pMHCII complex. Some of these shifts are located toward the peptide's N-terminal region,[251] others have a central canonical diagonal orientation,[247−250,253,254] and some others are located close to the peptide's C-terminus.[252] All of this leads to very different immunological outcomes.[252,257−261]

Consequently, an appropriate selection of highly immunogenic, protection-inducing modified HABPs (Table 1) derived from the ten (10) most studied proteins considered in this paper and forty (40) other previously analyzed merozoite proteins[36] (i.e., the focus of ongoing work in our institute using the experimental *Aotus* monkey model, as it is quite similar to humans) as well as those derived from twenty (20) more sporozoite proteins (also being studied in our institute)[45,115,238,262] may lead to the so desperately needed, fully effective antimalarial vaccine for immediate use in humans.

8. CONCLUSIONS

8.1. General Considerations for Fully Effective, Chemically Synthesized, Minimal Subunit-Based Vaccine Development

This manuscript has described the biological, structural functional, and immunological analysis of almost ninety (90) conserved HABPs and their corresponding modified analogues belonging to 10 of the most relevant *P. falciparum* merozoite proteins involved in the different steps of RBC invasion: recognition and binding (MSP-1, -2, -9), reorientation and tight junction formation (AMA-1), penetration (EBA-175), enzymatic cleavage (SERA), molecular transport (HRP-I, -II, RESA), and cytoadherence (PfEMP-1) at the atomic level.

This work has been designed in the pursuit of our final goal: defining a logical and rational methodology open for developing synthetic vaccines covering a whole range of existing and emergent diseases of concern for public health worldwide. Doing so has allowed us to establish several working *principles or rules* for developing *chemically synthesized, minimal subunit-based, multiantigenic, multistage vaccines*, using malaria as the model disease.

This decalogue of working principles aimed at inducing full protective immunity would thus be as follows:

First, *properly modified, short, chemically synthesized, conserved HABPs (15−20 amino acid long) should be used to induce sterile-immunity*, due to their highly specific and exquisitely adopted 3D structural characteristics. This conclusion is based on the following facts:

When comparing native conserved HABPs' 3D structures (determined by ^{1}H NMR) and the pertinent recombinant proteins' segments (determined by X-ray crystallography) corresponding to such HABPs, we have *demonstrated that their 3D conformation is practically identical*, (by these two different methodologies) irrespective of the molecule from where they have been derived and whether they display α-helical, *β*-turn, or random coil conformations (Figure 2). This clearly implies that such short, conserved HABPs could be partly or totally fulfilling the same biological function which the corresponding amino acid sequence fulfills in the native protein, such as parasite ligands, enzymatic processing, protein−protein interactions, *etc*.

By the same token, the polymers from the HABPs used for immunizing *Aotus* monkeys display the same secondary structure (as determined by CD) to that of their respective monomers, as we have thoroughly shown.[103,111,112] This structural conservation suggests that polymeric modified HABPs could induce a similar immune response directed toward the same structural conformations found in the monomeric forms, thus making polymeric HABPs an excellent multicopy antigen presenting system for synthetic vaccine development. As additional support to the minimal subunit based synthetic vaccine concept, it has been very recently demonstrated that short peptides (16−20 amino acids in length) have the optimal length for achieving the maximal MHCII affinity,[263] which is exactly the same size of the HABPs we have used in all the biological, structural, and immunological studies. Moreover, we have immunologically and structurally shown that elongations beyond this length have resulted in a null or negative effect on affinity and immunogenicity.[112]

This clearly suggests that antibodies induced against these short (15−20-mer long) modified HABPs could block or modify these proteins' biological function or mediate the killing of the parasite, as deduced from the sterile immunity induced in some monkeys, making them fundamental pieces to be included as components in fully effective, chemically synthesized, minimal subunit-based multiepitopic vaccine development.

Second, *HABPs involved in different invasion processes mediated by the same molecule should be clearly identified*, since we have shown that there is *functional compartmentalization* in multifunctional proteins where such HABPs are located in different parts of the same molecule or in different domains.

This occurs in malaria with HABPs involved in RBC as well as hepatocyte invasion, which are located in multifunctional proteins' different regions, which could reduce the number of conserved HABPs required to induce fully protective immunity.

Third, simple physicochemical techniques such as *circular dichroism (CD) can be used for identifying relevant peptides*, since conserved HABPs display a *structural compartmentalization*.

This means that most peptides from the parasite's membrane proteins involved in initial recognition and binding steps of RBC invasion (MSPs 1−10) or being released from the micronemes (EBAs, EBL) and rhoptries (RAPs, RBP, NBP, Rho, *etc*.) during these early processes, fulfilling an enzymatic function (SERA), or being loosely bound to other membrane-anchored molecules have an *α-helical* structure. Meanwhile, conserved HABPs derived from proteins or protein fragments remaining anchored by transmembrane segments (like AMA-1) or by prostetic groups such as GPI-tails (such as MSP-2 and the MSP-1 19 kDa fragment), or carrying PEXEL motifs (RESA, HRP-I, -II), *etc*., all display *random coil or β-turn* structures.

Fourth, conserved *HABPs must be properly modified to fit into pertinent HLA-DR molecules to avoid their immunological silence*, since strong genetic control of these conserved HABPs' immunological silence is exerted by MHCII molecules, particularly by HLA-DR-related molecules. This property is furthermore compartmentalized in such a way that conserved HABPs displaying α-helical structural features bind with high affinity to HLA-DR52 and HLA-DR8 haplotype's allelic molecules, while those showing a random coil or *β*-turn structure bind to HLA-DR53 and HLA-DR1 haplotype's allelic molecules.

This HLA-DR haplotype preferential usage also suggests a *compartmentalization of the immune system* according to conserved HABPs' structural and functional characteristics, thereby facilitating the logical and rational design of subunit-based synthetic vaccines by simple determinations of their secondary structure by CD.

Fifth, *the polarity of some critical binding residues must be shifted in native conserved HABPs to break their immunological code of silence and render them immunogenic and protection inducers*. Therefore, selective substitutions could be made in those critical binding residues as follows: only F could replace R and *vice versa*, W ↔ Y, L ↔ H, I ↔ N, P ↔ D, M ↔ K, C ↔ T or V, Q ↔ E, and A ↔ S; G has special physicochemical properties due to its small size.

Sixth, *the critical binding residues* which should be modified first and *then shifted are those establishing H-bonds* between their backbone atoms and other conserved HABPs, receptor

molecules, or components of enzymatic sites (here named *fundamental* residues).

Seventh, *these site-directed modifications should be made to induce changes in modified HABPs' 3D structure allowing them to fit inside MCHII molecules' peptide binding groove*, as determined by their capacity to bind specific HLA-DRβ1* purified molecules with their corresponding binding motifs and binding registers.

Eight, once these modifications have been performed, *there should be a ~3.0 Å differential distance between the most distant atoms of immunogenic protection-inducing HABP's residues fitting into P1 to P9* when synthesizing modified HABPs for them to fit inside HLA-DR52/DR8 haplotype alleles vs those binding to HLA-DR53/DR1 haplotype molecules (Figure 5).

Ninth, involving *solvent-exposed or putative TCR contact residue modifications should lead to a differential usage of TCR Vβ families for the presentation of modified HABPs to the different haplotypes or alleles*, suggesting a *differential haplotype- or allele-conscious TCR* mode of interaction.

This is a consequence of the foregoing ^{1}H NMR studies [the structures of almost ninety (~90) native and/or modified HABP have been determined], where it has been found that HABP's residues buried inside the pockets of different haplotypes display different conformational orientations and thereby that there is a differential usage of TCR contact residues depending on the HLA-DR allele usage for antigen presentation and appropriate immune response induction (Figure 8).

Tenth, special care should be taken when performing these modifications, since inappropiate *shortening* of peptide *length and varying residue orientation induce a shift in structural and functional characteristics* regarding modified HABPs. Such inappropiate modifications could induce high, *long-lasting, nonprotective* antibody levels, binding to a *different haplotype*, furthermore, when compared to the case of immunogenic, protection-inducing modified HABPs, as the length of the former is 4.6 ± 1.4 Å shorter.

This is better observed in modified HABPs that fit inside HLA-DR53 haplotype molecules (Figure 7A and Tables 2 and 3).

These inappropiate modifications could also lead to variations in modified HABPs' binding characteristics, thereby inducing *short-lived, nonprotection-inducing* antibody levels (Figure 8A and B), binding to a *different allele within the same haplotype* (Table 3) so that the distance between the atoms fitting inside pockets 1−9 of the HLA-DRβ1* molecule is 6.8 ± 0.5 Å shorter in these peptides compared to the case of the corresponding immunogenic protection-inducing modified HABPs.

Reciprocally, this difference is better observed in the modified HABPs that fit inside molecules belonging to the HLA-DR52 haplotype (Figures 7B and Tables 2 and 3).

By the same token, the orientation of the P8 residue is different in modified HABPs inducing nonantibody-associated *high cellular protection* immune responses, as clearly shown in Figures 7C and Tables 2 and 3.

Therefore, structural and functional compartmentalization of immune responses with *long-lasting, nonprotective* antibodies would be more easily induced by modifying peptides binding to HLA-DR53-related molecules, while *short-lived nonprotective-induced antibodies* could be associated with binding to HLA-DR52-associated molecules. This imposes a strict control of molecular design, based on modified HABPs' physicochemical characteristics and the immunogenetic characteristics of the host where they are going to be used to ensure obtaining an appropriate immune response.

Particular structural features could be associated with the compartmentalization of these two major haplotypes and the biased immune responses induced by some modified HABPs inappropriately fitting into the PBR;[252,255−261] however, such analysis is far beyond the scope of this manuscript.

The principles mentioned above must be very seriously taken into account to ensure conserved HABPs' sterile-immunity-inducing modification and to avoid biased immune responses that could be deleterious to an individual.

This decalogue of emerging principles shows that conserved antigens' *code of immunological silence*, the factor exerting such limits on vaccine development, can be broken when these principles are closely observed by the following:

(i) using highly specific and sensitive methodologies such as precise chemical synthesis of peptides thoroughly analyzed by high-performance liquid chromatography (HPLC), mass spectrometry (MS), CD, and the robust receptor−ligand interaction assays for identifying conserved HABPs;

(ii) carefully and systematically replacing each amino acid by glycine analogue scanning to determine which modifications needed to be performed;

(iii) changing critical binding residues' polarity by replacing target amino acids with others having similar mass, volume, and surface but opposite polarity according to previously established rules;

(iv) testing the immunological properties of modified peptides in an appropriate experimental model highly similar to humans, such as the *Aotus* monkey, by means of stringent immunological testing methods such as IFA and Western blot and intravenous inoculation of the microbe for challenge; and

(v) determining the HLA-DR binding preferences and elucidating 3D structures via ^{1}H NMR. All these highly specific and exquisitely sensitive methodologies (and many more, such as mathematical modeling and yet to be discovered technology-related ones) are now being used for developing effective *chemically synthesized, minimal subunit-based, multiantigenic, multistage vaccines*.

Based on the above, from the theoretical point of view, it can be postulated that *P. falciparum* parasites (and pathogens in general) do not accumulate mutations in their pertinent critical amino acid sequences because such sequences are essential for their survival (consequently being conserved HABPs). These critical sequences therefore adopt structurally specific conformations to prevent them from fitting properly into the MHCII/pTCR complex as a way of escaping immune pressure. Conserved HABPs must therefore be modified according to the principles set out herein to be rendered immunogenic and protection-inducing molecules.

However, when microbes (as we have shown here for *P. falciparum*) perform small replacements in these critical binding residues,[264] such replacements may generate slightly modified- or altered-peptide ligands,[265] which in turn form inappropriate MHCII/pTCR complexes inducing biased immune responses and thus preventing dangerous and deleterious immune responses directed against these pathogens.

It is very tempting to suggest that the microbe's awareness of a minimal immune response could thus lead to a small mutation (by changing one or a few critical binding residues in these conserved

HABPs and breaking one or two H-bonds) to induce modified structures associated with a shift in its binding preference for an allele- or haplotype-related MHCII molecule, thereby inducing a biased ineffective protective immune response, such as long-lasting or short-lived, nonprotective antibody production.

Other groups have shown that *immunodominant* epitopes form highly stable pMHCII complexes which remain bound to the MHCII molecules for more than 120 h, thereby slowing down HLA-DM editing[266−268] or inducing proliferation of different T-cell subsets in the presence of a pMHCII complex.[269] Therefore, a shift in some of the properties of the residues fitting inside MHCII molecule pockets could be associated with the antigen's permanence and immunodominance. However, our findings go further beyond immunodominance (which could also be associated with nonprotective modified HABPs inducing long-lasting antibody titers), since our data associates these modifications with *protection* against malaria when analyzing it at a particular atom level.

It can also be suggested that only the proper fit of modified HABPs allowing a stable formation of the appropriate MHCII/pTCR complex can induce suitable, long-lasting protective immune responses, and the principles discovered so far, leading to such protective immunity induction, have been presented in this manuscript.

Therefore, it can be clearly concluded that vaccine development is a far more elaborated and complex process than the simple injection of microbial DNA (either free or integrated into different viral vectors),[159,161−163,165,270−272] recombinant proteins,[160,273−276] synthetic peptides,[277,278] and genetically engineered microbes[279] or minute amounts of them.[280] The approaches mentioned above have always led to very frustrating results[50,164,166] or even deleterious reactions, such as erythema nodosum,[169] anemia,[167] or some other secondary adverse reactions in the vaccinated population.

Furthermore, recent epidemiological data has shown that the clinical immunity observed in individuals living in highly endemic areas and *NOT* developing the disease during the intense malarial transmission season results from *strain-specific* antibodies against most of the molecules studied here. Sometimes different molecules are recognized, perhaps due to the diverse methodological procedures and/or different epidemiological setups or the genetic backgrounds of the populations being studied;[165,281−286] however, as soon as the individuals move away from that area and become exposed to a particular parasite's different set of genetic variants, then they develop the full-blown disease, very clearly suggesting that the acquired immunity was *strain-specific* against parasites from that region. That was one of the reasons we decided long ago to only work with conserved, highly relevant, functional structures, such as conserved HABPs.

Therefore, vaccine development requires all the information already garnered in the storehouses of multiple disciplines, such as protein and carbohydrate chemistry, X-ray crystallography and ^{1}H NMR structural studies, the complex basic immunology, genomics, proteomics, and transcriptome analysis, not only of microbial agents but also of their hosts and interaction between them, as shown here and in previous papers.[171,172]

In essence, we may say that vaccinologists are in our early childhood and that chemistry is committed to playing a key role in vaccine development for human and animal welfare.

9. PERSPECTIVES

A fully effective synthetic vaccine against the asexual blood stages of the *P. falciparum* malaria parasite capable of protecting most of the world's exposed population (taking into account the genetic variability of the parasite as well as that of the human host) must therefore contain a large number of immunogenic protection-inducing modified HABPs (most of them shown in this manuscript) derived from a group of proteins involved in merozoite invasion of RBCs (as elegant proteomic and transcriptomic analysis has shown)[35,287] as well as a similar number of modified peptides derived from sporozoite HABPs, properly fitting inside the most frequent HLA-DRβ1* alleles of the human population at risk so as to activate fully protective or *sterilizing immunity* in most individuals and stop the transmission of this deadly disease.

It is therefore very simplistic to think that such as complex microorganism as the *P. falciparum* malaria parasite could be defeated via vaccination with a single molecule or its fragments, as its genome encodes 5,438 proteins[33] and uses >50 molecules in each of its invasion stages (merozoites, sporozoites)[288] as well as multiple cooperation between different proteins to form macromolecular complexes relevant for invasion[289−291] or mechanisms for switching the different invasion pathways on and off,[292−295] having thousands of genetic variants and countless immune evasion strategies.

These approaches have always lead to "very disappointing results," as clearly concluded by some other groups.

Since immunity to clinical malaria requires high antibody levels to cope with a large number of *P. falciparum* proteins and their extensive number of *genetic variants* (meaning that immunity to this parasite can only be acquired very slowly in natural conditions after covering practically all variants of that particular territory),[289] then a fully effective antimalarial vaccine should tackle the problem in a different way and include properly modified, universally conserved HABPs which can induce an appropriate immune response capable of blocking or permanently destabilizing RBC binding proteins and membrane protein rafts[141] and blocking molecules involved in interaction network formation[290] or killing the parasite, as suggested by the sterile immunity induced by these modified peptides. It should also include therefore modified HABPs corresponding to the classical, alternative, and even savage pathways used by the parasite during invasion, where the most abundant receptors are not present or when sensing a deleterious immune res`ponse.[36,292−295] All these functionally active mechanisms, and probably many more as yet unknown ones, should be considered when developing a fully effective antimalarial vaccine.

It should also be taken into account that a similar number of immunogenic protection-inducing modified HABPs binding to hepatocytes and derived from *P. falciparum* sporozoite molecules[45,115,238,262] have to be identified in these endeavors to develop a *fully effective* antimalarial vaccine against *all stages* of this disease which continues to scourge humanity, an enterprise already undertaken by us almost 30 years ago and for which a large number of highly immunogenic, modified HABPs have already been identified.[58,59,296,297]

As a note of caution, imperfect vaccines, as thoroughly shown in both animal and human vaccination campaigns,[298−302] could lead to the appearance of more virulent strains, thereby exposing individuals to unnecessary risks or even worse and more life-threatening situations. Therefore, only completely effective vaccines may lead to total control of diseases currently scourging humankind. Only deep molecular analysis of the factors involved in this long-lasting interaction can lead to the development of fully effective vaccines.

It has not escaped our attention that this methodology can also be used for developing vaccines against other infectious diseases; ongoing work at our institute is being directed toward this goal. This would open up a promising field for controlling humanity's major transmissible diseases responsible for the deaths of more than 17 million people annually, afflicting 2/3 of the world's population. *P. falciparum* malaria, as has been shown in this manuscript, as well as *P. vivax* malaria,[79,303] tuberculosis,[304−308] the Epstein−Barr virus causing Burkitt's lymphoma,[309,310] and hepatitis[311] are some of them, as well as re-emerging and recently appearing diseases such as Ebola, SARS, avian flu, *etc.*

The structural basis for this approach not only has very deep implications for controlling infectious diseases but also can be used for analyzing and controlling exaggerated immune responses such as allergies, biased immune responses such as autoimmunity (rheumatoid arthritis, systemic lupus erythematosus, myasthenia gravis, *etc.*), and diseases involving nonimmune responsiveness, such as cancer[312] (to bypass their immunological silence and metastasis development) and can even provide explanations for some biological phenomena, such as immune tolerance and pregnancy.

In summary, structural, biological, and immunological analysis of a large panel of modified HABPs used as immunogens in *Aotus* monkeys (which have an immune system highly similar to that of humans) has led us to establish the principles and rules facilitating the logical and rational design of *chemically synthesized, multiantigenic, multistage, minimal subunit-based vaccines*, malaria being one of them.

AUTHOR INFORMATION

Corresponding Author

*Phone number: +57-14815219. Fax number: +57-1-4815269. E-mail: mepatarr@mail.com.

BIOGRAPHIES

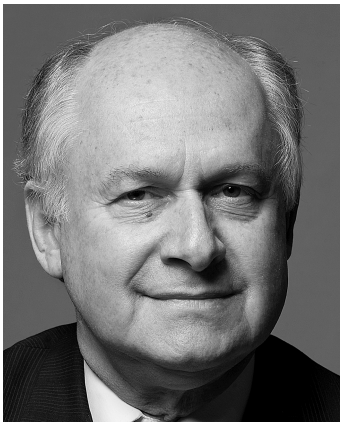

Manuel Elkin Patarroyo (born in 1946) received his M.D. degree from the Universidad Nacional de Colombia (National University of Colombia, School of Medicine) in 1971, where he is Full Professor for Molecular Pathology. He did postdoctoral studies at Rockefeller University in the United States with Professor Henry Kunkel and on Tumor Immunology at Karolinska Institute, Sweden, with Professor George Klein. In 1976, he founded the Instituto de Inmunología at the San Juan de Dios Hospital, fully devoted to the development of chemically synthesized vaccines, with malaria being one of them, with the advice of Professors Bruce Merrifield and David Andreu (Rockefeller University) and Professor Richard Lerner (Scripps Research Institute). The first chemically synthesized vaccine against this scourging disease was published in *Nature* in 1987, followed by a large series of clinical and field trials in different parts of the world that allowed the conclusion of the feasibility of chemically synthesized vaccines. He has received numerous awards, including the Award of the Third World Academy of Science (TWAS) in 1988, the Prince of Asturias Award in Science and Technology (Spain) in 1994, the Robert Koch Award (Germany) in 1994, the Medicin de l'année Award (France) in 1995, the Edinburgh Medal (England) in 1995, the National Science Award (Colombia) in 1986, 1984, 1982, and 1978, and 26 Honoris Causa Doctor degrees from different universities throughout the world. He is founder and current director of the Fundación Instituto de Inmunología de Colombia since 2001.

Adriana Bermúdez received her B.Sc. in Chemistry from the Universidad Nacional de Colombia in 1996. She initiated her research in peptide chemical synthesis in 1997 and joined afterwards the 3D structure group in 2001. She is currently studying for a Ph.D. in Biomedical Sciences at the Universidad del Rosario de Colombia and is a member of the Three-Dimensional Structure Department's Nuclear Magnetic Resonance and Molecular Design section at Fundación Instituto de Inmunología de Colombia. Her research is focused on the structural studies and molecular design of biologically relevant peptides and proteins to determine a correlation with the protective cellular and humoral immune response.

Manuel Alfonso Patarroyo (born in 1972) obtained both his M.D. and Dr.Sc. degrees from the National University of Colombia. He is

currently Full Professor at the Universidad del Rosario School of Medicine in Bogotá, Colombia, and Adjunct Professor at the National University of Colombia School of Medicine. His research interests have been mainly focused on developing vaccines against *Plasmodium vivax* malaria and tuberculosis. He and his group have successfully tested recombinant vaccine candidates against *P. vivax* in *Aotus* monkeys, becoming one of the leading groups in vaccine development against this scourging disease. Besides his work on infectious diseases, Professor Patarroyo has also been working on the molecular characterization of the immune system components of the *Aotus* monkey, an ideal experimental model for testing vaccines for humans. He is currently the head of the Molecular Biology Department at the Fundacion Instituto de Inmunologia de Colombia.

ACKNOWLEDGMENT

We would like to express our gratitude to the many people who have generously added (directly or indirectly) to this research and who have been involved in the background leading up to it. Professors Richard Lerner, Ian Wilson, and Peter Wright from the Scripps Research Institute generously received a large group of our scientists at the beginning of our work to teach them the basis of molecular immunology and 3D structural analysis. Professors Bruce Merrifield (Rockefeller University), David Andreu (Pompeu Fabra University, Barcelona, Spain), and Richard Houghten (Torrey Pines Institute for Molecular Studies, La Jolla, CA, USA) spent weeks in our Institute teaching us all about peptide synthesis 27 years ago, and this has made all the difference. Gladys Cifuentes and the 3D structural analysis group determined the ^{1}H NMR structures, Raul Rodriguez performed most of the endless monkey trials, our peptide chemistry department, lead by Magnolia Vanegas, synthesized and characterized thousands of peptides for the last 27 years, Yolanda Silva performed all the IFA tests, Martha Forero was responsible for the reproducibility of all Western blot analyses, and Armando Moreno Vranich developed the graphics contained within this manuscript. The committed and devoted work of Jose Manuel Lozano, Hernando Curtidor, and Marisol Ocampo in the development of the receptor−ligand ideas has always been appreciated. Professor Fernando Chalem (Universidad Nacional de Colombia), Dr Horst Frank, Dr Jurgen König, Dr Gerhard Goldman, and Miss Karin Rossler from the Germany Leprosy Relief Association (DAHW) have believed in and supported these ideas from a long time ago. Last but not least, we would like to thank our families (Maria Cristina, Tina, and Carlos Gustavo, and the Patarroyo clan) for their encouragement, love, and understanding throughout all these years when these principles were no more than an idea. This research has been supported by the Colombian and Spanish Governments. We would like to thank Jason Garry for patiently helping in translating and extensively reviewing the manuscript and Organizacion Luis Carlos Sarmiento Angulo-Banco de Bogotá and LINDE Colombia S.A. for making their much appreciated, generous donations.

DEDICATION

[†]Dedicated to the memory of Professors Henry G. Kunkel and Bruce Merrifield (Rockefeller University, New York), who introduced us to the fascinating worlds of immunology and protein synthesis, respectively, and to former President of Colombia, Belisario Betancur, who believed and supported these ideas more than 27 years ago.

REFERENCES

(1) Snow, R. W.; Guerra, C. A.; Noor, A. M.; Myint, H. Y.; Hay, S. I. *Nature* **2005**, *434*, 214.
(2) Richie, T. L.; Saul, A. *Nature* **2002**, *415*, 694.
(3) Patarroyo, M. E.; Romero, P.; Torres, M. L.; Clavijo, P.; Moreno, A.; Martinez, A.; Rodriguez, R.; Guzman, F.; Cabezas, E. *Nature* **1987**, *328*, 629.
(4) Patarroyo, M. E.; Amador, R.; Clavijo, P.; Moreno, A.; Guzman, F.; Romero, P.; Tascon, R.; Franco, A.; Murillo, L. A.; Ponton, G.; Trujillo, G. *Nature* **1988**, *332*, 158.
(5) Amador, R.; Moreno, A.; Murillo, L. A.; Sierra, O.; Saavedra, D.; Rojas, M.; Mora, A. L.; Rocha, C. L.; Alvarado, F.; Falla, J. C.; Orozco, M.; Coronell, C; Ortega, N.; Molano, A.; Velásquez, J. F.; Valero, M. V.; Franco, L.; Guzmán, F.; Salazar, L. M.; Espejo, F.; Mora, E.; Farfán, R.; Zapata, N.; Rosas, J.; Calvo, J. C.; Castro, J.; Quiñones, T.; Nuñez, F.; Patarroyo, M. E. *J. Infect. Dis.* **1992**, *166*, 139.
(6) Patarroyo, G.; Franco, L.; Amador, R.; Murillo, L. A.; Rocha, C. L.; Rojas, M.; Patarroyo, M. E. *Vaccine* **1992**, *10*, 175.
(7) Valero, M. V.; Amador, L. R.; Galindo, C.; Figueroa, J.; Bello, M. S.; Murillo, L. A.; Mora, A. L.; Patarroyo, G.; Rocha, C. L.; Rojas, M.; Aponte, J. J.; Sarmiento, L. E.; Lazada, D. M.; Coronell, C. G.; Ortega, N. M.; Rosas, J. E.; Alonso, P. L.; Patarroyo, M. E. *Lancet* **1993**, *341*, 705.
(8) Noya, O.; Gabaldon Berti, Y.; Alarcon de Noya, B.; Borges, R.; Zerpa, N.; Urbaez, J. D.; Madonna, A.; Garrido, E.; Jimenez, M. A.; Borges, R. E.; Garcia, P.; Reyes, I.; Prieto, W.; Colmenares, C.; Pabón, R.; Barraez, T.; de Caceres, L. G.; Godoy, N.; Sifontes, R. *J. Infect. Dis.* **1994**, *170*, 396.
(9) Sempertegui, F.; Estrella, B.; Moscoso, J.; Piedrahita, L.; Hernandez, D.; Gaybor, J.; Naranjo, P.; Mancero, O.; Arias, S.; Bernal, R.; Cordova, M. E.; Suarez, J.; Zickert, F. *Vaccine* **1994**, *12*, 337.
(10) Alonso, P. L.; Smith, T.; Schellenberg, J. R.; Masanja, H.; Mwankusye, S.; Urassa, H.; Bastos de Azevedo, I.; Chongela, J.; Kobero, S.; Menendez, C.; Hurt, N.; Thomas, M. C.; Lyimo, E.; Weiss, N. A.; Hayes, R.; Kitua, A. Y.; Lopez, M. C.; Kilama, W. L.; Teuscher, T.; Tanner, M. *Lancet* **1994**, *344*, 1175.
(11) Valero, M. V.; Amador, R.; Aponte, J. J.; Narvaez, A.; Galindo, C.; Silva, Y.; Rosas, J.; Guzman, F.; Patarroyo, M. E. *Vaccine* **1996**, *14*, 1466.
(12) Alonso, P. L.; Smith, T. A.; Armstrong-Schellenberg, J. R.; Kitua, A. Y.; Masanja, H.; Hayes, R.; Hurt, N.; Font, F.; Menendez, C.; Kilama, W. L.; Tanner, M. *J. Infect. Dis.* **1996**, *174*, 367.
(13) Nosten, F.; Luxemburger, C.; Kyle, D. E.; Ballou, W. R.; Wittes, J.; Wah, E.; Chongsuphajaisiddhi, T.; Gordon, D. M.; White, N. J.; Sadoff, J. C.; Heppner, D. G. *Lancet* **1996**, *348*, 701.
(14) Acosta, C. J.; Galindo, C. M.; Schellenberg, D.; Aponte, J. J.; Kahigwa, E.; Urassa, H.; Schellenberg, J. R.; Masanja, H.; Hayes, R.; Kitua, A. Y.; Lwilla, F.; Mshinda, H.; Menendez, C.; Tanner, M.; Alonso, P. L. *Trop. Med. Int. Health* **1999**, *4*, 368.
(15) Graves, P.; Gelband, H. *Cochrane Database Syst. Rev.* **2006**, CD006199.
(16) Calvo, M.; Guzman, F.; Perez, E.; Segura, C. H.; Molano, A.; Patarroyo, M. E. *Pept. Res.* **1991**, *4*, 324.
(17) Puentes, A.; Garcia, J.; Vera, R.; Lopez, Q. R.; Urquiza, M.; Vanegas, M.; Salazar, L. M.; Patarroyo, M. E. *Parasitol. Int.* **2000**, *49*, 105.
(18) Urquiza, M.; Rodriguez, L. E.; Suarez, J. E.; Guzman, F.; Ocampo, M.; Curtidor, H.; Segura, C.; Trujillo, E.; Patarroyo, M. E. *Parasite Immunol.* **1996**, *18*, 515.
(19) Ocampo, M.; Urquiza, M.; Guzman, F.; Rodriguez, L. E.; Suarez, J.; Curtidor, H.; Rosas, J.; Diaz, M.; Patarroyo, M. E. *J. Pept. Res.* **2000**, *55*, 216.
(20) Rodriguez, L. E.; Urquiza, M.; Ocampo, M.; Suarez, J.; Curtidor, H.; Guzman, F.; Vargas, L. E.; Trivinos, M.; Rosas, M.; Patarroyo, M. E. *Parasitology* **2000**, *120*, 225.
(21) Bermudez, A.; Reyes, C.; Guzman, F.; Vanegas, M.; Rosas, J.; Amador, R.; Rodriguez, R.; Patarroyo, M. A.; Patarroyo, M. E. *Vaccine* **2007**, *25*, 4487.
(22) Merrifield, R. B. *J. Am. Chem. Soc.* **1963**, *85*, 2149.

(23) Pico de Coana, Y.; Rodriguez, J.; Guerrero, E.; Barrero, C.; Rodriguez, R.; Mendoza, M.; Patarroyo, M. A. *Vaccine* **2003**, *21*, 3930.
(24) Rodriguez, R.; Moreno, A.; Guzman, F.; Calvo, M.; Patarroyo, M. E. *Am. J. Trop. Med. Hyg.* **1990**, *43*, 339.
(25) Urquiza, M.; Suarez, J. E.; Cardenas, C.; Lopez, R.; Puentes, A.; Chavez, F.; Calvo, J. C.; Patarroyo, M. E. *Vaccine* **2000**, *19*, 508.
(26) Reyes, C.; Patarroyo, M. E.; Vargas, L. E.; Rodriguez, L. E.; Patarroyo, M. A. *Biochem. Biophys. Res. Commun.* **2007**, *354*, 363.
(27) Trager, W.; Jensen, J. B. *Science* **1976**, *193*, 673.
(28) Gardner, M. J.; Hall, N.; Fung, E.; White, O.; Berriman, M.; Hyman, R. W.; Carlton, J. M.; Pain, A.; Nelson, K. E.; Bowman, S.; Paulsen, I. T.; James, K.; Eisen, J. A.; Rutherford, K.; Salzberg, S. L.; Craig, A.; Kyes, S.; Chan, M. S.; Nene, V.; Shallom, S. J.; Suh, B.; Peterson, J.; Angiuoli, S.; Pertea, M.; Allen, J.; Selengut, J.; Haft, D.; Mather, M. W.; Vaidya, A. B.; Martin, D. M.; Fairlamb, A. H.; Fraunholz, M. J.; Roos, D. S.; Ralph, S. A.; McFadden, G. I.; Cummings, L. M.; Subramanian, G. M.; Mungall, C.; Venter, J. C.; Carucci, D. J.; Hoffman, S. L.; Newbold, C.; Davis, R. W.; Fraser, C. M.; Barrell, B. *Nature* **2002**, *419*, 498.
(29) Pain, A.; Hertz-Fowler, C. *Nat. Rev. Microbiol.* **2009**, *7*, 180.
(30) Lasonder, E.; Janse, C. J.; van Gemert, G. J.; Mair, G. R.; Vermunt, A. M.; Douradinha, B. G.; van Noort, V.; Huynen, M. A.; Luty, A. J.; Kroeze, H.; Khan, S. M.; Sauerwein, R. W.; Waters, A. P.; Mann, M.; Stunnenberg, H. G. *PLoS Pathog.* **2008**, *4*, e1000195.
(31) Florens, L.; Washburn, M. P.; Raine, J. D.; Anthony, R. M.; Grainger, M.; Haynes, J. D.; Moch, J. K.; Muster, N.; Sacci, J. B.; Tabb, D. L.; Witney, A. A.; Wolters, D.; Wu, Y.; Gardner, M. J.; Holder, A. A.; Sinden, R. E.; Yates, J. R.; Carucci, D. J. *Nature* **2002**, *419*, 520.
(32) Smit, S.; Stoychev, S.; Louw, A. I.; Birkholtz, L. M. *J. Proteome Res.* **2010**, *9*, 2170.
(33) Otto, T. D.; Wilinski, D.; Assefa, S.; Keane, T. M.; Sarry, L. R.; Bohme, U.; Lemieux, J.; Barrell, B.; Pain, A.; Berriman, M.; Newbold, C.; Llinas, M. *Mol. Microbiol.* **2010**, *76*, 12.
(34) Tarun, A. S.; Peng, X.; Dumpit, R. F.; Ogata, Y.; Silva-Rivera, H.; Camargo, N.; Daly, T. M.; Bergman, L. W.; Kappe, S. H. *Proc. Natl. Acad. Sci. U. S. A.* **2008**, *105*, 305.
(35) Bozdech, Z.; Llinas, M.; Pulliam, B. L.; Wong, E. D.; Zhu, J.; DeRisi, J. L. *PLoS Biol.* **2003**, *1*, e5.
(36) Rodriguez, L. E.; Curtidor, H.; Urquiza, M.; Cifuentes, G.; Reyes, C.; Patarroyo, M. E. *Chem. Rev.* **2008**, *108*, 3656.
(37) Pinzon, C. G.; Curtidor, H.; Reyes, C.; Mendez, D.; Patarroyo, M. E. *Protein Sci.* **2008**, *17*, 1719.
(38) Garcia, J.; Curtidor, H.; Pinzon, C. G.; Patarroyo, M. A.; Vanegas, M.; Forero, M.; Patarroyo, M. E. *J. Med. Chem.* **2010**, *53*, 811.
(39) Pinzon, C. G.; Curtidor, H.; Bermudez, A.; Forero, M.; Vanegas, M.; Rodriguez, J.; Patarroyo, M. E. *Vaccine* **2008**, *26*, 853.
(40) Garcia, J.; Curtidor, H.; Gil, O. L.; Vanegas, M.; Patarroyo, M. E. *Biochem. Biophys. Res. Commun.* **2009**, *380*, 122.
(41) Garcia, J.; Curtidor, H.; Obando-Martinez, A. Z.; Vizcaino, C.; Pinto, M.; Martinez, N. L.; Patarroyo, M. A.; Patarroyo, M. E. *Vaccine* **2009**, *27*, 6877.
(42) Garcia, J.; Curtidor, H.; Pinzon, C. G.; Vanegas, M.; Moreno, A.; Patarroyo, M. E. *Vaccine* **2009**, *27*, 3953.
(43) Arevalo-Pinzon, G.; Curtidor, H.; Reyes, C.; Pinto, M.; Vizcaino, C.; Patarroyo, M. A.; Patarroyo, M. E. *J. Mol. Med.* **2010**, *88*, 61.
(44) Pinzon, C. G.; Curtidor, H.; Garcia, J.; Vanegas, M.; Vizcaino, C.; Patarroyo, M. A.; Patarroyo, M. E. *Vaccine* **2010**, *28*, 2653.
(45) Garcia, J. E.; Puentes, A.; Patarroyo, M. E. *Clin. Microbiol. Rev.* **2006**, *19*, 686.
(46) Garcia, J. E.; Puentes, A.; Lopez, R.; Vera, R.; Suarez, J.; Rodriguez, L.; Curtidor, H.; Ocampo, M.; Tovar, D.; Forero, M.; Bermudez, A.; Cortes, J.; Urquiza, M.; Patarroyo, M. E. *Peptides* **2003**, *24*, 647.
(47) Puentes, A.; Garcia, J.; Vera, R.; Lopez, R.; Suarez, J.; Rodriguez, L.; Curtidor, H.; Ocampo, M.; Tovar, D.; Forero, M.; Bermudez, A.; Cortes, J.; Urquiza, M.; Patarroyo, M. E. *Vaccine* **2004**, *22*, 1150.
(48) Suarez, J. E.; Urquiza, M.; Puentes, A.; Garcia, J. E.; Curtidor, H.; Ocampo, M.; Lopez, R.; Rodriguez, L. E.; Vera, R.; Cubillos, M.; Torres, M. H.; Patarroyo, M. E. *Vaccine* **2001**, *19*, 4487.
(49) Holder, A. A.; Lockyer, M. J.; Odink, K. G.; Sandhu, J. S.; Riveros-Moreno, V.; Nicholls, S. C.; Hillman, Y.; Davey, L. S.; Tizard, M. L.; Schwarz, R. T.; Freeman, R. R. *Nature* **1985**, *317*, 270.
(50) Holder, A. A. *Parasitology* **2009**, *136*, 1445.
(51) Smythe, J. A.; Coppel, R. L.; Brown, G. V.; Ramasamy, R.; Kemp, D. J.; Anders, R. F. *Proc. Natl. Acad. Sci. U.S.A.* **1988**, *85*, 5195.
(52) Smythe, J. A.; Coppel, R. L.; Day, K. P.; Martin, R. K.; Oduola, A. M.; Kemp, D. J.; Anders, R. F. *Proc. Natl. Acad. Sci. U.S.A.* **1991**, *88*, 1751.
(53) Weber, J. L.; Lyon, J. A.; Wolff, R. H.; Hall, T.; Lowell, G. H.; Chulay, J. D. *J. Biol. Chem.* **1988**, *263*, 11421.
(54) Hodder, A. N.; Crewther, P. E.; Matthew, M. L.; Reid, G. E.; Moritz, R. L.; Simpson, R. J.; Anders, R. F. *J. Biol. Chem.* **1996**, *271*, 29446.
(55) Chesne-Seck, M. L.; Pizarro, J. C.; Vulliez-Le Normand, B.; Collins, C. R.; Blackman, M. J.; Faber, B. W.; Remarque, E. J.; Kocken, C. H.; Thomas, A. W.; Bentley, G. A. *Mol. Biochem. Parasitol.* **2005**, *144*, 55.
(56) Sim, B. K.; Orlandi, P. A.; Haynes, J. D.; Klotz, F. W.; Carter, J. M.; Camus, D.; Zegans, M. E.; Chulay, J. D. *J. Cell Biol.* **1990**, *111*, 1877.
(57) Sim, B. K.; Chitnis, C. E.; Wasniowska, K.; Hadley, T. J.; Miller, L. H. *Science* **1994**, *264*, 1941.
(58) Perlmann, H.; Berzins, K.; Wahlgren, M.; Carlsson, J.; Bjorkman, A.; Patarroyo, M. E.; Perlmann, P. *J. Exp. Med.* **1984**, *159*, 1686.
(59) Berzins, K.; Perlmann, H.; Wahlin, B.; Carlsson, J.; Wahlgren, M.; Udomsangpetch, R.; Bjorkman, A.; Patarroyo, M. E.; Perlmann, P. *Proc. Natl. Acad. Sci. U.S.A.* **1986**, *83*, 1065.
(60) Cowman, A. F.; Coppel, R. L.; Saint, R. B.; Favaloro, J.; Crewther, P. E.; Stahl, H. D.; Bianco, A. E.; Brown, G. V.; Anders, R. F.; Kemp, D. J. *Mol. Biol. Med.* **1984**, *2*, 207.
(61) Triglia, T.; Stahl, H. D.; Crewther, P. E.; Scanlon, D.; Brown, G. V.; Anders, R. F.; Kemp, D. J. *EMBO J.* **1987**, *6*, 1413.
(62) Delplace, P.; Bhatia, A.; Cagnard, M.; Camus, D.; Colombet, G.; Debrabant, A.; Dubremetz, J. F.; Dubreuil, N.; Prensier, G.; Fortier, B.; Haq, A.; Weber, J.; Vernes, A. *Biol. Cell* **1988**, *64*, 215.
(63) Bzik, D. J.; Li, W. B.; Horii, T.; Inselburg, J. *Mol. Biochem. Parasitol.* **1988**, *30*, 279.
(64) Carlson, J.; Wahlgren, M. *J. Exp. Med.* **1992**, *176*, 1311.
(65) Dahlback, M.; Nielsen, M. A.; Salanti, A. *Trends Parasitol.* **2010**, *26*, 230.
(66) Baruch, D. I.; Pasloske, B. L.; Singh, H. B.; Bi, X.; Ma, X. C.; Feldman, M.; Taraschi, T. F.; Howard, R. J. *Cell* **1995**, *82*, 77.
(67) Su, X. Z.; Heatwole, V. M.; Wertheimer, S. P.; Guinet, F.; Herrfeldt, J. A.; Peterson, D. S.; Ravetch, J. A.; Wellems, T. E. *Cell* **1995**, *82*, 89.
(68) Stern, L. J.; Calvo-Calle, J. M. *Curr. Pharm. Des.* **2009**, *15*, 3249.
(69) Schueler-Furman, O.; Altuvia, Y.; Margalit, H. *Proteins* **2001**, *45*, 47.
(70) Pizarro, J. C.; Chitarra, V.; Verger, D.; Holm, I.; Petres, S.; Dartevelle, S.; Nato, F.; Longacre, S.; Bentley, G. A. *J. Mol. Biol.* **2003**, *328*, 1091.
(71) Torres, M. H.; Salazar, L. M.; Vanegas, M.; Guzman, F.; Rodriguez, R.; Silva, Y.; Rosas, J.; Patarroyo, M. E. *Eur. J. Biochem.* **2003**, *270*, 3946.
(72) Feng, Z. P.; Keizer, D. W.; Stevenson, R. A.; Yao, S.; Babon, J. J.; Murphy, V. J.; Anders, R. F.; Norton, R. S. *J. Mol. Biol.* **2005**, *350*, 641.
(73) Bai, T.; Becker, M.; Gupta, A.; Strike, P.; Murphy, V. J.; Anders, R. F.; Batchelor, A. H. *Proc. Natl. Acad. Sci. U.S.A* **2005**, *102*, 12736.
(74) Cubillos, M.; Salazar, L. M.; Torres, L.; Patarroyo, M. E. *Biochimie* **2002**, *84*, 1181.

(75) Purmova, J.; Salazar, L. M.; Espejo, F.; Torres, M. H.; Cubillos, M.; Torres, E.; Lopez, Y.; Rodriguez, R.; Patarroyo, M. E. *Biochim. Biophys. Acta* **2002**, *1571*, 27.
(76) Tolia, N. H.; Enemark, E. J.; Sim, B. K.; Joshua-Tor, L. *Cell* **2005**, *122*, 183.
(77) Cifuentes, G.; Guzman, F.; Alba, M. P.; Salazar, L. M.; Patarroyo, M. E. *J. Struct. Biol.* **2003**, *141*, 115.
(78) Singh, S. K.; Hora, R.; Belrhali, H.; Chitnis, C. E.; Sharma, A. *Nature* **2006**, *439*, 741.
(79) Ocampo, M.; Vera, R.; Eduardo Rodriguez, L.; Curtidor, H.; Urquiza, M.; Suarez, J.; Garcia, J.; Puentes, A.; Lopez, R.; Trujillo, M.; Torres, E.; Patarroyo, M. E. *Peptides* **2002**, *23*, 13.
(80) Hadley, T. J.; Peiper, S. C. *Blood* **1997**, *89*, 3077.
(81) Hans, D.; Pattnaik, P.; Bhattacharyya, A.; Shakri, A. R.; Yazdani, S. S.; Sharma, M.; Choe, H.; Farzan, M.; Chitnis, C. E. *Mol. Microbiol.* **2005**, *55*, 1423.
(82) VanBuskirk, K. M.; Sevova, E.; Adams, J. H. *Proc. Natl. Acad. Sci. U.S.A.* **2004**, *101*, 15754.
(83) Low, A.; Chandrashekaran, I. R.; Adda, C. G.; Yao, S.; Sabo, J. K.; Zhang, X.; Soetopo, A.; Anders, R. F.; Norton, R. S. *Biopolymers* **2007**, *87*, 12.
(84) Cifuentes, G.; Patarroyo, M. E.; Urquiza, M.; Ramirez, L. E.; Reyes, C.; Rodriguez, R. *J. Med. Chem.* **2003**, *46*, 2250.
(85) Zhang, X.; Perugini, M. A.; Yao, S.; Adda, C. G.; Murphy, V. J.; Low, A.; Anders, R. F.; Norton, R. S. *J. Mol. Biol.* **2008**, *379*, 105.
(86) Hodder, A. N.; Malby, R. L.; Clarke, O. B.; Fairlie, W. D.; Colman, P. M.; Crabb, B. S.; Smith, B. J. *J. Mol. Biol.* **2009**, *392*, 154.
(87) Alba, M. P.; Salazar, L. M.; Puentes, A.; Pinto, M.; Torres, E.; Patarroyo, M. E. *Peptides* **2003**, *24*, 999.
(88) Patarroyo, M. E.; Cifuentes, G.; Pirajan, C.; Moreno-Vranich, A.; Vanegas, M. *Biochem. Biophys. Res. Commun.* **2010**, *394*, 529.
(89) Higgins, M. K. *J. Biol. Chem.* **2008**, *283*, 21842.
(90) Singh, K.; Gittis, A. G.; Nguyen, P.; Gowda, D. C.; Miller, L. H.; Garboczi, D. N. *Nat. Struct. Mol. Biol.* **2008**, *15*, 932.
(91) Singh, K.; Gitti, R. K.; Diouf, A.; Zhou, H.; Gowda, D. C.; Miura, K.; Ostazeski, S. A.; Fairhurst, R. M.; Garboczi, D. N.; Long, C. A. *J. Biol. Chem.* **2010**, *285*, 38700.
(92) Khunrae, P.; Philip, J. M.; Bull, D. R.; Higgins, M. K. *J. Mol. Biol.* **2009**, *393*, 202.
(93) Patarroyo, M. E.; Cifuentes, G.; Martinez, N. L.; Patarroyo, M. A. *Prog. Biophys. Mol. Biol.* **2010**, *102*, 38.
(94) Blackman, M. J.; Heidrich, H. G.; Donachie, S.; McBride, J. S.; Holder, A. A. *J. Exp. Med.* **1990**, *172*, 379.
(95) Dluzewski, A. R.; Ling, I. T.; Hopkins, J. M.; Grainger, M.; Margos, G.; Mitchell, G. H.; Holder, A. A.; Bannister, L. H. *PLoS One* **2008**, *3*, e3085.
(96) Miller, L. H.; Roberts, T.; Shahabuddin, M.; McCutchan, T. F. *Mol. Biochem. Parasitol.* **1993**, *59*, 1.
(97) Remarque, E. J.; Faber, B. W.; Kocken, C. H.; Thomas, A. W. *Trends Parasitol.* **2008**, *24*, 74.
(98) Pizarro, J. C.; Vulliez-Le Normand, B.; Chesne-Seck, M. L.; Collins, C. R.; Withers-Martinez, C.; Hackett, F.; Blackman, M. J.; Faber, B. W.; Remarque, E. J.; Kocken, C. H.; Thomas, A. W.; Bentley, G. A. *Science* **2005**, *308*, 408.
(99) Camus, D.; Hadley, T. J. *Science* **1985**, *230*, 553.
(100) Orlandi, P. A.; Sim, B. K.; Chulay, J. D.; Haynes, J. D. *Mol. Biochem. Parasitol.* **1990**, *40*, 285.
(101) Sim, B. K. *Mol. Biochem. Parasitol.* **1990**, *41*, 293.
(102) Orlandi, P. A.; Klotz, F. W.; Haynes, J. D. *J. Cell Biol.* **1992**, *116*, 901.
(103) Bermudez, A.; Cifuentes, G.; Guzman, F.; Salazar, L. M.; Patarroyo, M. E. *Biol. Chem.* **2003**, *384*, 1443.
(104) Adda, C. G.; Murphy, V. J.; Sunde, M.; Waddington, L. J.; Schloegel, J.; Talbo, G. H.; Vingas, K.; Kienzle, V.; Masciantonio, R.; Howlett, G. J.; Hodder, A. N.; Foley, M.; Anders, R. F. *Mol. Biochem. Parasitol.* **2009**, *166*, 159.
(105) Chen, Q.; Barragan, A.; Fernandez, V.; Sundstrom, A.; Schlichtherle, M.; Sahlen, A.; Carlson, J.; Datta, S.; Wahlgren, M. *J. Exp. Med.* **1998**, *187*, 15.
(106) Chen, Q.; Heddini, A.; Barragan, A.; Fernandez, V.; Pearce, S. F.; Wahlgren, M. *J. Exp. Med.* **2000**, *192*, 1.
(107) Smith, J. D.; Craig, A. G.; Kriek, N.; Hudson-Taylor, D.; Kyes, S.; Fagan, T.; Pinches, R.; Baruch, D. I.; Newbold, C. I.; Miller, L. H. *Proc. Natl. Acad. Sci. U.S.A.* **2000**, *97*, 1766.
(108) MacPherson, G. G.; Warrell, M. J.; White, N. J.; Looareesuwan, S.; Warrell, D. A. *Am. J. Pathol.* **1985**, *119*, 385.
(109) Aguiar, J. C.; Albrecht, G. R.; Cegielski, P.; Greenwood, B. M.; Jensen, J. B.; Lallinger, G.; Martinez, A.; McGregor, I. A.; Minjas, J. N.; Neequaye, J.; Patarroyo, M. E.; Sherwood, J. A.; Howard, R. J. *Am. J. Trop. Med. Hyg.* **1992**, *47*, 621.
(110) van Schravendijk, M. R.; Rock, E. P.; Marsh, K.; Ito, Y.; Aikawa, M.; Neequaye, J.; Ofori-Adjei, D.; Rodriguez, R.; Patarroyo, M. E.; Howard, R. J. *Blood* **1991**, *78*, 226.
(111) Cifuentes, G.; Espejo, F.; Vargas, L. E.; Parra, C.; Vanegas, M.; Patarroyo, M. E. *Biochemistry* **2004**, *43*, 6545.
(112) Espejo, F.; Bermudez, A.; Vanegas, M.; Rivera, Z.; Torres, E.; Salazar, L. M.; Patarroyo, M. E. *J. Struct. Biol.* **2005**, *150*, 245.
(113) Silvie, O.; Franetich, J. F.; Charrin, S.; Mueller, M. S.; Siau, A.; Bodescot, M.; Rubinstein, E.; Hannoun, L.; Charoenvit, Y.; Kocken, C. H.; Thomas, A. W.; Van Gemert, G. J.; Sauerwein, R. W.; Blackman, M. J.; Anders, R. F.; Pluschke, G.; Mazier, D. *J. Biol. Chem.* **2004**, *279*, 9490.
(114) Guzman, F.; Jaramillo, K.; Salazar, L. M.; Torres, A.; Rivera, A.; Patarroyo, M. E. *Life Sci.* **2002**, *71*, 2773.
(115) Bermudez, A.; Vanegas, M.; Patarroyo, M. E. *Vaccine* **2008**, *26*, 6908.
(116) Gruner, A. C.; Brahimi, K.; Letourneur, F.; Renia, L.; Eling, W.; Snounou, G.; Druilhe, P. *J. Infect. Dis.* **2001**, *184*, 892.
(117) Bodescot, M.; Silvie, O.; Siau, A.; Refour, P.; Pino, P.; Franetich, J. F.; Hannoun, L.; Sauerwein, R.; Mazier, D. *Parasitol. Res.* **2004**, *92*, 449.
(118) Valbuena, J.; Rodriguez, L.; Vera, R.; Puentes, A.; Curtidor, H.; Cortes, J.; Rosas, J.; Patarroyo, M. E. *Biochimie* **2006**, *88*, 1447.
(119) Garcia, Y.; Puentes, A.; Curtidor, H.; Cifuentes, G.; Reyes, C.; Barreto, J.; Moreno, A.; Patarroyo, M. E. *J. Med. Chem.* **2007**, *50*, 5665.
(120) Puentes, A.; Garcia, J.; Ocampo, M.; Rodriguez, L.; Vera, R.; Curtidor, H.; Lopez, R.; Suarez, J.; Valbuena, J.; Vanegas, M.; Guzman, F.; Tovar, D.; Patarroyo, M. E. *Peptides* **2003**, *24*, 1015.
(121) Puentes, A.; Ocampo, M.; Rodriguez, L. E.; Vera, R.; Valbuena, J.; Curtidor, H.; Garcia, J.; Lopez, R.; Tovar, D.; Cortes, J.; Rivera, Z.; Patarroyo, M. E. *Biochimie* **2005**, *87*, 461.
(122) Salazar, L. M.; Alba, M. P.; Torres, M. H.; Pinto, M.; Cortes, X.; Torres, L.; Patarroyo, M. E. *FEBS Lett.* **2002**, *527*, 95.
(123) Hiller, N. L.; Bhattacharjee, S.; van Ooij, C.; Liolios, K.; Harrison, T.; Lopez-Estrano, C.; Haldar, K. *Science* **2004**, *306*, 1934.
(124) Marti, M.; Good, R. T.; Rug, M.; Knuepfer, E.; Cowman, A. F. *Science* **2004**, *306*, 1930.
(125) Sam-Yellowe, T. Y. *Trends Parasitol.* **2009**, *25*, 277.
(126) Maier, A. G.; Cooke, B. M.; Cowman, A. F.; Tilley, L. *Nat. Rev. Microbiol.* **2009**, *7*, 341.
(127) Crabb, B. S.; de Koning-Ward, T. F.; Gilson, P. R. *Int. J. Parasitol.* **2010**, *40*, 509.
(128) de Koning-Ward, T. F.; Gilson, P. R.; Boddey, J. A.; Rug, M.; Smith, B. J.; Papenfuss, A. T.; Sanders, P. R.; Lundie, R. J.; Maier, A. G.; Cowman, A. F.; Crabb, B. S. *Nature* **2009**, *459*, 945.
(129) Alba, M. P.; Salazar, L. M.; Vargas, L. E.; Trujillo, M.; Lopez, Y.; Patarroyo, M. E. *Biochem. Biophys. Res. Commun.* **2004**, *315*, 1154.
(130) Bermudez, A.; Alba, P.; Espejo, F.; Vargas, L. E.; Parra, C.; Rodriguez, R.; Reyes, C.; Patarroyo, M. E. *Int. J. Biochem. Cell Biol.* **2005**, *37*, 336.
(131) Cifuentes, G.; Patarroyo, M. E.; Reyes, C.; Cortes, J.; Patarroyo, M. A. *Biochem. Biophys. Res. Commun.* **2007**, *360*, 149.
(132) Feng, Z. P.; Zhang, X.; Han, P.; Arora, N.; Anders, R. F.; Norton, R. S. *Mol. Biochem. Parasitol.* **2006**, *150*, 256.
(133) Espejo, F.; Bermudez, A.; Torres, E.; Urquiza, M.; Rodriguez, R.; Lopez, Y.; Patarroyo, M. E. *Biochem. Biophys. Res. Commun.* **2004**, *315*, 418.

(134) Espejo, F.; Cubillos, M.; Salazar, L. M.; Guzman, F.; Urquiza, M.; Ocampo, M.; Silva, Y.; Rodriguez, R.; Lioy, E.; Patarroyo, M. E. *Angew. Chem., Int. Ed. Engl.* **2001**, *40*, 4654.
(135) Rodriguez, L. E.; Curtidor, H.; Ocampo, M.; Garcia, J.; Puentes, A.; Valbuena, J.; Vera, R.; Lopez, R.; Patarroyo, M. E. *Protein Sci.* **2005**, *14*, 1778.
(136) Lopez, R.; Valbuena, J.; Rodriguez, L. E.; Ocampo, M.; Vera, R.; Curtidor, H.; Puentes, A.; Garcia, J.; Ramirez, L. E.; Patarroyo, M. E. *Peptides* **2006**, *27*, 1685.
(137) Curtidor, H.; Urquiza, M.; Suarez, J. E.; Rodriguez, L. E.; Ocampo, M.; Puentes, A.; Garcia, J. E.; Vera, R.; Lopez, R.; Ramirez, L. E.; Pinzon, M.; Patarroyo, M. E. *Vaccine* **2001**, *19*, 4496.
(138) Li, X.; Chen, H.; Oo, T. H.; Daly, T. M.; Bergman, L. W.; Liu, S. C.; Chishti, A. H.; Oh, S. S. *J. Biol. Chem.* **2004**, *279*, 5765.
(139) Kauth, C. W.; Woehlbier, U.; Kern, M.; Mekonnen, Z.; Lutz, R.; Mucke, N.; Langowski, J.; Bujard, H. *J. Biol. Chem.* **2006**, *281*, 31517.
(140) Kadekoppala, M.; Holder, A. A. *Int. J. Parasitol.* **2010**, *40*, 1155.
(141) Sanders, P. R.; Gilson, P. R.; Cantin, G. T.; Greenbaum, D. C.; Nebl, T.; Carucci, D. J.; McConville, M. J.; Schofield, L.; Hodder, A. N.; Yates, J. R., 3rd; Crabb, B. S. *J. Biol. Chem.* **2005**, *280*, 40169.
(142) Alba, M. P.; Salazar, L. M.; Purmova, J.; Vanegas, M.; Rodriguez, R.; Patarroyo, M. E. *Vaccine* **2004**, *22*, 1281.
(143) Cubillos, M.; Alba, M. P.; Bermudez, A.; Trujillo, M.; Patarroyo, M. E. *Biochimie* **2003**, *85*, 651.
(144) Salazar, L. M.; Bermudez, A.; Patarroyo, M. E. *Biochem. Biophys. Res. Commun.* **2008**, *372*, 114.
(145) Iyer, J.; Gruner, A. C.; Renia, L.; Snounou, G.; Preiser, P. R. *Mol. Microbiol.* **2007**, *65*, 231.
(146) Dowse, T. J.; Soldati, D. *Trends Parasitol.* **2005**, *21*, 254.
(147) Maier, A. G.; Rug, M.; O'Neill, M. T.; Brown, M.; Chakravorty, S.; Szestak, T.; Chesson, J.; Wu, Y.; Hughes, K.; Coppel, R. L.; Newbold, C.; Beeson, J. G.; Craig, A.; Crabb, B. S.; Cowman, A. F. *Cell* **2008**, *134*, 48.
(148) Amador, R.; Moreno, A.; Valero, V.; Murillo, L.; Mora, A. L.; Rojas, M.; Rocha, C.; Salcedo, M.; Guzman, F.; Espejo, F.; Núñez, F.; Patarroyo, M. E. *Vaccine* **1992**, *10*, 179.
(149) Salcedo, M.; Barreto, L.; Rojas, M.; Moya, R.; Cote, J.; Patarroyo, M. E. *Clin. Exp. Immunol.* **1991**, *84*, 122.
(150) Murillo, L. A.; Rocha, C. L.; Mora, A. L.; Kalil, J.; Goldenberg, A. K.; Patarroyo, M. E. *Parasite Immunol.* **1991**, *13*, 201.
(151) Murillo, L. A.; Tenjo, F. A.; Clavijo, O. P.; Orozco, M. A.; Sampaio, S.; Kalil, J.; Patarroyo, M. E. *Parasite Immunol.* **1992**, *14*, 87.
(152) Calvo-Calle, J. M.; Oliveira, G. A.; Nardin, E. H. *J. Immunol.* **2005**, *175*, 7575.
(153) Nardin, E. H.; Calvo-Calle, J. M.; Oliveira, G. A.; Nussenzweig, R. S.; Schneider, M.; Tiercy, J. M.; Loutan, L.; Hochstrasser, D.; Rose, K. *J. Immunol.* **2001**, *166*, 481.
(154) Nardin, E. H.; Oliveira, G. A.; Calvo-Calle, J. M.; Castro, Z. R.; Nussenzweig, R. S.; Schmeckpeper, B.; Hall, B. F.; Diggs, C.; Bodison, S.; Edelman, R. *J. Infect. Dis.* **2000**, *182*, 1486.
(155) Marsh, S. G. E.; Parham, P.; Barber, L. D. *The HLA factsbook*; Academic Press: San Diego, 2000.
(156) Andersson, G.; Andersson, L.; Larhammar, D.; Rask, L.; Sigurdardottir, S. *Immunol. Today* **1994**, *15*, 58.
(157) Sinigaglia, F.; Romagnoli, P.; Guttinger, M.; Takacs, B.; Pink, J. R. *Methods Enzymol.* **1991**, *203*, 370.
(158) Rammensee, H. G.; Friede, T.; Stevanoviic, S. *Immunogenetics* **1995**, *41*, 178.
(159) Bejon, P.; Mwacharo, J.; Kai, O.; Mwangi, T.; Milligan, P.; Todryk, S.; Keating, S.; Lang, T.; Lowe, B.; Gikonyo, C.; Molyneux, C.; Fegan, G.; Gilbert, S. C.; Peshu, N.; Marsh, K.; Hill, A. V. *PLoS Clin. Trials* **2006**, *1*, e29.
(160) Genton, B.; Al-Yaman, F.; Betuela, I.; Anders, R. F.; Saul, A.; Baea, K.; Mellombo, M.; Taraika, J.; Brown, G. V.; Pye, D.; Irving, D. O.; Felger, I.; Beck, H. P.; Smith, T. A.; Alpers, M. P. *Vaccine* **2003**, *22*, 30.
(161) Le, T. P.; Coonan, K. M.; Hedstrom, R. C.; Charoenvit, Y.; Sedegah, M.; Epstein, J. E.; Kumar, S.; Wang, R.; Doolan, D. L.; Maguire, J. D.; Parker, S. E.; Hobart, P.; Norman, J.; Hoffman, S. L. *Vaccine* **2000**, *18*, 1893.
(162) Moorthy, V. S.; Imoukhuede, E. B.; Milligan, P.; Bojang, K.; Keating, S.; Kaye, P.; Pinder, M.; Gilbert, S. C.; Walraven, G.; Greenwood, B. M.; Hill, A. S. *PLoS Med.* **2004**, *1*, e33.
(163) Ockenhouse, C. F.; Sun, P. F.; Lanar, D. E.; Wellde, B. T.; Hall, B. T.; Kester, K.; Stoute, J. A.; Magill, A.; Krzych, U.; Farley, L.; Wirtz, R. A.; Sadoff, J. C.; Kaslow, D. C.; Kumar, S.; Church, L. W.; Crutcher, J. M.; Wizel, B.; Hoffman, S.; Lalvani, A.; Hill, A. V.; Tine, J. A.; Guito, K. P.; de Taisne, C.; Anders, R.; Horii, T.; Paoletti, E.; Ballou, W. R. *J. Infect. Dis.* **1998**, *177*, 1664.
(164) Richards, J. S.; Beeson, J. G. *Immunol. Cell Biol.* **2009**, *87*, 377.
(165) Ogutu, B. R.; Apollo, O. J.; McKinney, D.; Okoth, W.; Siangla, J.; Dubovsky, F.; Tucker, K.; Waitumbi, J. N.; Diggs, C.; Wittes, J.; Malkin, E.; Leach, A.; Soisson, L. A.; Milman, J. B.; Otieno, L.; Holland, C. A.; Polhemus, M.; Remich, S. A.; Ockenhouse, C. F.; Cohen, J.; Ballou, W. R.; Martin, S. K.; Angov, E.; Stewart, V. A.; Lyon, J. A.; Heppner, D. G.; Withers, M. R. *PLoS One* **2009**, *4*, e4708.
(166) Coppel, R. L. *Trends Parasitol.* **2009**, *25*, 205.
(167) Sagara, I.; Dicko, A.; Ellis, R. D.; Fay, M. P.; Diawara, S. I.; Assadou, M. H.; Sissoko, M. S.; Kone, M.; Diallo, A. I.; Saye, R.; Guindo, M. A.; Kante, O.; Niambele, M. B.; Miura, K.; Mullen, G. E.; Pierce, M.; Martin, L. B.; Dolo, A.; Diallo, D. A.; Doumbo, O. K.; Miller, L. H.; Saul, A. *Vaccine* **2009**, *27*, 3090.
(168) Cummings, J. F.; Spring, M. D.; Schwenk, R. J.; Ockenhouse, C. F.; Kester, K. E.; Polhemus, M. E.; Walsh, D. S.; Yoon, I. K.; Prosperi, C.; Juompan, L. Y.; Lanar, D. E.; Krzych, U.; Hall, B. T.; Ware, L. A.; Stewart, V. A.; Williams, J.; Dowler, M.; Nielsen, R. K.; Hillier, C. J.; Giersing, B. K.; Dubovsky, F.; Malkin, E.; Tucker, K.; Dubois, M. C.; Cohen, J. D.; Ballou, W. R.; Heppner, D. G. *Vaccine* **2009**, *28*, 5135.
(169) Wu, Y.; Ellis, R. D.; Shaffer, D.; Fontes, E.; Malkin, E. M.; Mahanty, S.; Fay, M. P.; Narum, D.; Rausch, K.; Miles, A. P.; Aebig, J.; Orcutt, A.; Muratova, O.; Song, G.; Lambert, L.; Zhu, D.; Miura, K.; Long, C.; Saul, A.; Miller, L. H.; Durbin, A. P. *PLoS One* **2008**, *3*, e2636.
(170) Day, M. *Br. Med. J.* **2006**, *333*, 1235.
(171) Patarroyo, M. E.; Cifuentes, G.; Bermudez, A.; Patarroyo, M. A. *J. Cell Mol. Med.* **2008**, *12*, 1915.
(172) Patarroyo, M. E.; Patarroyo, M. A. *Acc. Chem. Res.* **2008**, *41*, 377.
(173) Diaz, D.; Daubenberger, C. A.; Zalac, T.; Rodriguez, R.; Patarroyo, M. E. *Immunogenetics* **2002**, *54*, 251.
(174) Castillo, F.; Guerrero, C.; Trujillo, E.; Delgado, G.; Martinez, P.; Salazar, L. M.; Barato, P.; Patarroyo, M. E.; Parra-Lopez, C. *Immunogenetics* **2004**, *56*, 480.
(175) Diaz, D.; Naegeli, M.; Rodriguez, R.; Nino-Vasquez, J. J.; Moreno, A.; Patarroyo, M. E.; Pluschke, G.; Daubenberger, C. A. *Immunogenetics* **2000**, *51*, 528.
(176) Guerrero, J. E.; Pacheco, D. P.; Suarez, C. F.; Martinez, P.; Aristizabal, F.; Moncada, C. A.; Patarroyo, M. E.; Patarroyo, M. A. *Tissue Antigens* **2003**, *62*, 472.
(177) Hernandez, E. C.; Suarez, C. F.; Mendez, J. A.; Echeverry, S. J.; Murillo, L. A.; Patarroyo, M. E. *Immunogenetics* **2002**, *54*, 645.
(178) Hernandez, E. C.; Suarez, C. F.; Parra, C. A.; Patarroyo, M. A.; Patarroyo, M. E. *Tissue Antigens* **2005**, *66*, 640.
(179) Moncada, C. A.; Guerrero, E.; Cardenas, P.; Suarez, C. F.; Patarroyo, M. E.; Patarroyo, M. A. *Immunogenetics* **2005**, *57*, 42.
(180) Suarez, C. F.; Cardenas, P. P.; Llanos-Ballestas, E. J.; Martinez, P.; Obregon, M.; Patarroyo, M. E.; Patarroyo, M. A. *Tissue Antigens* **2003**, *61*, 362.
(181) Suarez, C. F.; Patarroyo, M. E.; Trujillo, E.; Estupinan, M.; Baquero, J. E.; Parra, C.; Rodriguez, R. *Immunogenetics* **2006**, *58*, 542.
(182) Dessen, A.; Lawrence, C. M.; Cupo, S.; Zaller, D. M.; Wiley, D. C. *Immunity* **1997**, *7*, 473.
(183) Ghosh, P.; Amaya, M.; Mellins, E.; Wiley, D. C. *Nature* **1995**, *378*, 457.
(184) Smith, K. J.; Pyrdol, J.; Gauthier, L.; Wiley, D. C.; Wucherpfennig, K. W. *J. Exp. Med.* **1998**, *188*, 1511.
(185) Stern, L. J.; Brown, J. H.; Jardetzky, T. S.; Gorga, J. C.; Urban, R. G.; Strominger, J. L.; Wiley, D. C. *Nature* **1994**, *368*, 215.

(186) Corper, A. L.; Stratmann, T.; Apostolopoulos, V.; Scott, C. A.; Garcia, K. C.; Kang, A. S.; Wilson, I. A.; Teyton, L. *Science* **2000**, *288*, 505.
(187) Zhu, Y.; Rudensky, A. Y.; Corper, A. L.; Teyton, L.; Wilson, I. A. *J. Mol. Biol.* **2003**, *326*, 1157.
(188) Fremont, D. H.; Hendrickson, W. A.; Marrack, P.; Kappler, J. *Science* **1996**, *272*, 1001.
(189) Marrack, P.; Bender, J.; Jordan, M.; Rees, W.; Robertson, J.; Schaefer, B. C.; Kappler, J. *J. Immunol.* **2001**, *167*, 617.
(190) Li, Y.; Li, H.; Martin, R.; Mariuzza, R. A. *J. Mol. Biol.* **2000**, *304*, 177.
(191) Reinherz, E. L.; Tan, K.; Tang, L.; Kern, P.; Liu, J.; Xiong, Y.; Hussey, R. E.; Smolyar, A.; Hare, B.; Zhang, R.; Joachimiak, A.; Chang, H. C.; Wagner, G.; Wang, J. *Science* **1999**, *286*, 1913.
(192) Lee, K. H.; Wucherpfennig, K. W.; Wiley, D. C. *Nat. Immunol.* **2001**, *2*, 501.
(193) Patarroyo, M. E.; Cifuentes, G.; Vargas, L. E.; Rosas, J. *ChemBioChem* **2004**, *5*, 1588.
(194) Salazar, L. M.; Alba, M. P.; Curtidor, H.; Bermudez, A.; Luis, E. V.; Rivera, Z. J.; Patarroyo, M. E. *Biochem. Biophys. Res. Commun.* **2004**, *322*, 119.
(195) Patarroyo, M. E.; Bermudez, A.; Salazar, L. M.; Espejo, F. *Biochimie* **2006**, *88*, 775.
(196) Patarroyo, M. E.; Alba, M. P.; Vargas, L. E.; Silva, Y.; Rosas, J.; Rodriguez, R. *Biochemistry* **2005**, *44*, 6745.
(197) Patarroyo, M. E.; Salazar, L. M.; Cifuentes, G.; Lozano, J. M.; Delgado, G.; Rivera, Z.; Rosas, J.; Vargas, L. E. *Biochimie* **2006**, *88*, 219.
(198) Cohen, S.; McGregor, I.; Carrington, S. *Nature* **1961**, *192*, 733.
(199) Cohen, S.; Butcher, G. A. *Trans. R. Soc. Trop. Med. Hyg.* **1971**, *65*, 125.
(200) Mitchell, G. H.; Butcher, G. A.; Voller, A.; Cohen, S. *Parasitology* **1976**, *72*, 149.
(201) Lyon, J. A.; Haynes, J. D.; Diggs, C. L.; Chulay, J. D.; Haidaris, C. G.; Pratt-Rossiter, J. *J. Immunol.* **1987**, *138*, 895.
(202) Chulay, J. D.; Lyon, J. A.; Haynes, J. D.; Meierovics, A. I.; Atkinson, C. T.; Aikawa, M. *J. Immunol.* **1987**, *139*, 2768.
(203) Bergmann-Leitner, E. S.; Duncan, E. H.; Angov, E. *Malar. J.* **2009**, *8*, 183.
(204) Woehlbier, U.; Epp, C.; Hackett, F.; Blackman, M. J.; Bujard, H. *Malar. J.* **2010**, *9*, 77.
(205) Peterson, M. G.; Marshall, V. M.; Smythe, J. A.; Crewther, P. E.; Lew, A.; Silva, A.; Anders, R. F.; Kemp, D. J. *Mol. Cell. Biol.* **1989**, *9*, 3151.
(206) Healer, J.; Crawford, S.; Ralph, S.; McFadden, G.; Cowman, A. F. *Infect. Immun.* **2002**, *70*, 5751.
(207) Triglia, T.; Healer, J.; Caruana, S. R.; Hodder, A. N.; Anders, R. F.; Crabb, B. S.; Cowman, A. F. *Mol. Microbiol.* **2000**, *38*, 706.
(208) Mitchell, G. H.; Thomas, A. W.; Margos, G.; Dluzewski, A. R.; Bannister, L. H. *Infect. Immun.* **2004**, *72*, 154.
(209) Narum, D. L.; Thomas, A. W. *Mol. Biochem. Parasitol.* **1994**, *67*, 59.
(210) Yeoh, S.; O'Donnell, R. A.; Koussis, K.; Dluzewski, A. R.; Ansell, K. H.; Osborne, S. A.; Hackett, F.; Withers-Martinez, C.; Mitchell, G. H.; Bannister, L. H.; Bryans, J. S.; Kettleborough, C. A.; Blackman, M. J. *Cell* **2007**, *131*, 1072.
(211) Harris, P. K.; Yeoh, S.; Dluzewski, A. R.; O'Donnell, R. A.; Withers-Martinez, C.; Hackett, F.; Bannister, L. H.; Mitchell, G. H.; Blackman, M. J. *PLoS Pathog.* **2005**, *1*, 241.
(212) Arastu-Kapur, S.; Ponder, E. L.; Fonovic, U. P.; Yeoh, S.; Yuan, F.; Fonovic, M.; Grainger, M.; Phillips, C. I.; Powers, J. C.; Bogyo, M. *Nat. Chem. Biol.* **2008**, *4*, 203.
(213) Koussis, K.; Withers-Martinez, C.; Yeoh, S.; Child, M.; Hackett, F.; Knuepfer, E.; Juliano, L.; Woehlbier, U.; Bujard, H.; Blackman, M. J. *EMBO J.* **2009**, *28*, 725.
(214) Sim, B. K.; Toyoshima, T.; Haynes, J. D.; Aikawa, M. *Mol. Biochem. Parasitol.* **1992**, *51*, 157.
(215) Struck, N. S.; Herrmann, S.; Schmuck-Barkmann, I.; de Souza Dias, S.; Haase, S.; Cabrera, A. L.; Treeck, M.; Bruns, C.; Langer, C.; Cowman, A. F.; Marti, M.; Spielmann, T.; Gilberger, T. W. *Mol. Microbiol.* **2008**, *67*, 1320.
(216) Patarroyo, M. A.; Bermudez, A.; Lopez, C.; Yepes, G.; Patarroyo, M. E. *PLoS One* **2010**, *5*, e9771.
(217) Staalsoe, T.; Giha, H. A.; Dodoo, D.; Theander, T. G.; Hviid, L. *Cytometry* **1999**, *35*, 329.
(218) Freeman, R. R.; Holder, A. A. *J. Exp. Med.* **1983**, *158*, 1647.
(219) Heidrich, H. G.; Matzner, M.; Miettinen-Baumann, A.; Strych, W. *Z. Parasitenkd.* **1986**, *72*, 681.
(220) Cifuentes, G.; Salazar, L. M.; Vargas, L. E.; Parra, C. A.; Vanegas, M.; Cortes, J.; Patarroyo, M. E. *Vaccine* **2005**, *23*, 1579.
(221) Cubillos, M.; Espejo, F.; Purmova, J.; Martinez, J. C.; Patarroyo, M. E. *Proteins* **2003**, *50*, 400.
(222) Klein, J.; Klein, D. . *Molecular evolution of the major histocompatibility complex*; Springer-Verlag: Berlin, New York, 1991.
(223) Geysen, H. M.; Meloen, R. H.; Barteling, S. J. *Proc. Natl. Acad. Sci. U.S.A.* **1984**, *81*, 3998.
(224) Ampudia, E.; Patarroyo, M. A.; Patarroyo, M. E.; Murillo, L. A. *Mol. Biochem. Parasitol.* **1996**, *78*, 269.
(225) Xainli, J.; Adams, J. H.; King, C. L. *Mol. Biochem. Parasitol.* **2000**, *111*, 253.
(226) Liang, H.; Sim, B. K. *Mol. Biochem. Parasitol.* **1997**, *84*, 241.
(227) Crewther, P. E.; Matthew, M. L.; Flegg, R. H.; Anders, R. F. *Infect. Immun.* **1996**, *64*, 3310.
(228) Cortes, A.; Mellombo, M.; Masciantonio, R.; Murphy, V. J.; Reeder, J. C.; Anders, R. F. *Infect. Immun.* **2005**, *73*, 422.
(229) Healer, J.; Murphy, V.; Hodder, A. N.; Masciantonio, R.; Gemmill, A. W.; Anders, R. F.; Cowman, A. F.; Batchelor, A. *Mol. Microbiol.* **2004**, *52*, 159.
(230) Dutta, S.; Dlugosz, L. S.; Clayton, J. W.; Pool, C. D.; Haynes, J. D.; Gasser, R. A., 3rd; Batchelor, A. H. *Infect. Immun.* **2010**, *78*, 661.
(231) Dutta, S.; Lee, S. Y.; Batchelor, A. H.; Lanar, D. E. *Proc. Natl. Acad. Sci. U.S.A.* **2007**, *104*, 12488.
(232) Hammer, J.; Bono, E.; Gallazzi, F.; Belunis, C.; Nagy, Z.; Sinigaglia, F. *J. Exp. Med.* **1994**, *180*, 2353.
(233) Wang, P.; Sidney, J.; Dow, C.; Mothe, B.; Sette, A.; Peters, B. *PLoS Comput. Biol.* **2008**, *4*, e1000048.
(234) Nielsen, M.; Lundegaard, C.; Blicher, T.; Peters, B.; Sette, A.; Justesen, S.; Buus, S.; Lund, O. *PLoS Comput. Biol.* **2008**, *4*, e1000107.
(235) Andersen, C. A.; Palmer, A. G.; Brunak, S.; Rost, B. *Structure* **2002**, *10*, 175.
(236) Greenfield, N. J. *Anal. Biochem.* **1996**, *235*, 1.
(237) Curtidor, H.; Torres, M. H.; Alba, M. P.; Patarroyo, M. E. *Biol. Chem.* **2007**, *388*, 25.
(238) Cifuentes, G.; Bermudez, A.; Rodriguez, R.; Patarroyo, M. A.; Patarroyo, M. E. *Med. Chem.* **2008**, *4*, 278.
(239) Lopez, R.; Urquiza, M.; Curtidor, H.; Eduardo Caminos, J.; Mora, H.; Puentes, A.; Patarroyo, M. E. *Acta Trop.* **2000**, *75*, 349.
(240) Jones, E. Y.; Fugger, L.; Strominger, J. L.; Siebold, C. *Nat. Rev. Immunol.* **2006**, *6*, 271.
(241) James, E. A.; Moustakas, A. K.; Bui, J.; Nouv, R.; Papadopoulos, G. K.; Kwok, W. W. *J. Immunol.* **2009**, *183*, 3249.
(242) Vidal, K.; Daniel, C.; Vidavsky, I.; Nelson, C. A.; Allen, P. M. *Mol. Immunol.* **2000**, *37*, 203.
(243) McFarland, B. J.; Sant, A. J.; Lybrand, T. P.; Beeson, C. *Biochemistry* **1999**, *38*, 16663.
(244) Kersh, G. J.; Miley, M. J.; Nelson, C. A.; Grakoui, A.; Horvath, S.; Donermeyer, D. L.; Kappler, J.; Allen, P. M.; Fremont, D. H. *J. Immunol.* **2001**, *166*, 3345.
(245) Wilson, I. A. *Science* **1999**, *286*, 1867.
(246) Wilson, I. A.; Stanfield, R. L. *Nat. Immunol.* **2005**, *6*, 434.
(247) Garcia, K. C.; Degano, M.; Stanfield, R. L.; Brunmark, A.; Jackson, M. R.; Peterson, P. A.; Teyton, L.; Wilson, I. A. *Science* **1996**, *274*, 209.

(248) Garcia, K. C.; Degano, M.; Pease, L. R.; Huang, M.; Peterson, P. A.; Teyton, L.; Wilson, I. A. *Science* **1998**, *279*, 1166.
(249) Garcia, K. C.; Degano, M.; Speir, J. A.; Wilson, I. A. *Rev. Immunogenet.* **1999**, *1*, 75.
(250) Manning, T. C.; Schlueter, C. J.; Brodnicki, T. C.; Parke, E. A.; Speir, J. A.; Garcia, K. C.; Teyton, L.; Wilson, I. A.; Kranz, D. M. *Immunity* **1998**, *8*, 413.
(251) Bankovich, A. J.; Girvin, A. T.; Moesta, A. K.; Garcia, K. C. *Mol. Immunol.* **2004**, *40*, 1033.
(252) Hahn, M.; Nicholson, M. J.; Pyrdol, J.; Wucherpfennig, K. W. *Nat. Immunol.* **2005**, *6*, 490.
(253) Hennecke, J.; Carfi, A.; Wiley, D. C. *EMBO J.* **2000**, *19*, 5611.
(254) Hennecke, J.; Wiley, D. C. *J. Exp. Med.* **2002**, *195*, 571.
(255) Maynard, J.; Petersson, K.; Wilson, D. H.; Adams, E. J.; Blondelle, S. E.; Boulanger, M. J.; Wilson, D. B.; Garcia, K. C. *Immunity* **2005**, *22*, 81.
(256) Rudolph, M. G.; Stanfield, R. L.; Wilson, I. A. *Annu. Rev. Immunol.* **2006**, *24*, 419.
(257) He, X. L.; Radu, C.; Sidney, J.; Sette, A.; Ward, E. S.; Garcia, K. C. *Immunity* **2002**, *17*, 83.
(258) Huseby, E. S.; White, J.; Crawford, F.; Vass, T.; Becker, D.; Pinilla, C.; Marrack, P.; Kappler, J. W. *Cell* **2005**, *122*, 247.
(259) Rudolph, M. G.; Wilson, I. A. *Curr. Opin. Immunol.* **2002**, *14*, 52.
(260) Sant'Angelo, D. B.; Waterbury, G.; Preston-Hurlburt, P.; Yoon, S. T.; Medzhitov, R.; Hong, S. C.; Janeway, C. A. *Immunity* **1996**, *4*, 367.
(261) Zavala-Ruiz, Z.; Strug, I.; Walker, B. D.; Norris, P. J.; Stern, L. J. *Proc. Natl. Acad. Sci. U.S.A.* **2004**, *101*, 13279.
(262) Patarroyo, M. E.; Cifuentes, G.; Rodriguez, R. *Int. J. Biochem. Cell Biol.* **2008**, *40*, 543.
(263) O'Brien, C.; Flower, D. R.; Feighery, C. *Immunome Res.* **2008**, *4*, 6.
(264) Belmares, M. P.; Busch, R.; Mellins, E. D.; McConnell, H. M. *Biochemistry* **2003**, *42*, 838.
(265) Evavold, B. D.; Sloan-Lancaster, J.; Allen, P. M. *Immunol. Today* **1993**, *14*, 602.
(266) Lazarski, C. A.; Chaves, F. A.; Sant, A. J. *J. Exp. Med.* **2006**, *203*, 1319.
(267) Lovitch, S. B.; Petzold, S. J.; Unanue, E. R. *J. Immunol.* **2003**, *171*, 2183.
(268) Sant, A. J.; Chaves, F. A.; Jenks, S. A.; Richards, K. A.; Menges, P.; Weaver, J. M.; Lazarski, C. A. *Immunol. Rev.* **2005**, *207*, 261.
(269) Pu, Z.; Carrero, J. A.; Unanue, E. R. *Proc. Natl. Acad. Sci. U.S.A.* **2002**, *99*, 8844.
(270) Hill, A. V.; Reece, W.; Gothard, P.; Moorthy, V.; Roberts, M.; Flanagan, K.; Plebanski, M.; Hannan, C.; Hu, J. T.; Anderson, R.; Degano, P.; Schneider, J.; Prieur, E.; Sheu, E.; Gilbert, S. C. *Dev. Biol. (Basel)* **2000**, *104*, 171.
(271) Jones, T. R.; Narum, D. L.; Gozalo, A. S.; Aguiar, J.; Fuhrmann, S. R.; Liang, H.; Haynes, J. D.; Moch, J. K.; Lucas, C.; Luu, T.; Magill, A. J.; Hoffman, S. L.; Sim, B. K. *J. Infect. Dis.* **2001**, *183*, 303.
(272) Moore, A. C.; Hill, A. V. *Immunol. Rev.* **2004**, *199*, 126.
(273) Fluck, C.; Smith, T.; Beck, H. P.; Irion, A.; Betuela, I.; Alpers, M. P.; Anders, R.; Saul, A.; Genton, B.; Felger, I. *Infect. Immun.* **2004**, *72*, 6300.
(274) Saul, A.; Lawrence, G.; Allworth, A.; Elliott, S.; Anderson, K.; Rzepczyk, C.; Martin, L. B.; Taylor, D.; Eisen, D. P.; Irving, D. O.; Pye, D.; Crewther, P. E.; Hodder, A. N.; Murphy, V. J.; Anders, R. F. *Vaccine* **2005**, *23*, 3076.
(275) Stoute, J. A.; Gombe, J.; Withers, M. R.; Siangla, J.; McKinney, D.; Onyango, M.; Cummings, J. F.; Milman, J.; Tucker, K.; Soisson, L.; Stewart, V. A.; Lyon, J. A.; Angov, E.; Leach, A.; Cohen, J.; Kester, K. E.; Ockenhouse, C. F.; Holland, C. A.; Diggs, C. L.; Wittes, J.; Heppner, D. G. *Vaccine* **2007**, *25*, 176.
(276) Walther, M.; Dunachie, S.; Keating, S.; Vuola, J. M.; Berthoud, T.; Schmidt, A.; Maier, C.; Andrews, L.; Andersen, R. F.; Gilbert, S.; Poulton, I.; Webster, D.; Dubovsky, F.; Tierney, E.; Sarpotdar, P.; Correa, S.; Huntcooke, A.; Butcher, G.; Williams, J.; Sinden, R. E.; Thornton, G. B.; Hill, A. V. *Vaccine* **2005**, *23*, 857.
(277) Prato, S.; Maxwell, T.; Pinzon-Charry, A.; Schmidt, C. W.; Corradin, G.; Lopez, J. A. *Eur. J. Immunol.* **2005**, *35*, 681.
(278) Theisen, M.; Dodoo, D.; Toure-Balde, A.; Soe, S.; Corradin, G.; Koram, K. K.; Kurtzhals, J. A.; Hviid, L.; Theander, T.; Akanmori, B.; Ndiaye, M.; Druilhe, P. *Infect. Immun.* **2001**, *69*, 5223.
(279) Mueller, A. K.; Labaied, M.; Kappe, S. H.; Matuschewski, K. *Nature* **2005**, *433*, 164.
(280) Pombo, D. J.; Lawrence, G.; Hirunpetcharat, C.; Rzepczyk, C.; Bryden, M.; Cloonan, N.; Anderson, K.; Mahakunkijcharoen, Y.; Martin, L. B.; Wilson, D.; Elliott, S.; Elliott, S.; Eisen, D. P.; Weinberg, J. B.; Saul, A.; Good, M. F. *Lancet* **2002**, *360*, 610.
(281) Langhorne, J.; Ndungu, F. M.; Sponaas, A. M.; Marsh, K. *Nat. Immunol.* **2008**, *9*, 725.
(282) Doolan, D. L.; Mu, Y.; Unal, B.; Sundaresh, S.; Hirst, S.; Valdez, C.; Randall, A.; Molina, D.; Liang, X.; Freilich, D. A.; Oloo, J. A.; Blair, P. L.; Aguiar, J. C.; Baldi, P.; Davies, D. H.; Felgner, P. L. *Proteomics* **2008**, *8*, 4680.
(283) Osier, F. H.; Fegan, G.; Polley, S. D.; Murungi, L.; Verra, F.; Tetteh, K. K.; Lowe, B.; Mwangi, T.; Bull, P. C.; Thomas, A. W.; Cavanagh, D. R.; McBride, J. S.; Lanar, D. E.; Mackinnon, M. J.; Conway, D. J.; Marsh, K. *Infect. Immun.* **2008**, *76*, 2240.
(284) Iriemenam, N. C.; Khirelsied, A. H.; Nasr, A.; ElGhazali, G.; Giha, H. A.; Elhassan, A. E. T. M.; Agab-Aldour, A. A.; Montgomery, S. M.; Anders, R. F.; Theisen, M.; Troye-Blomberg, M.; Elbashir, M. I.; Berzins, K. *Vaccine* **2009**, *27*, 62.
(285) Gray, J. C.; Corran, P. H.; Mangia, E.; Gaunt, M. W.; Li, Q.; Tetteh, K. K.; Polley, S. D.; Conway, D. J.; Holder, A. A.; Bacarese-Hamilton, T.; Riley, E. M.; Crisanti, A. *Clin. Chem.* **2007**, *53*, 1244.
(286) Crompton, P. D.; Kayala, M. A.; Traore, B.; Kayentao, K.; Ongoiba, A.; Weiss, G. E.; Molina, D. M.; Burk, C. R.; Waisberg, M.; Jasinskas, A.; Tan, X.; Doumbo, S.; Doumtabe, D.; Kone, Y.; Narum, D. L.; Liang, X.; Doumbo, O. K.; Miller, L. H.; Doolan, D. L.; Baldi, P.; Felgner, P. L.; Pierce, S. K. *Proc. Natl. Acad. Sci. U.S.A.* **2010**, *107*, 6958.
(287) Le Roch, K. G.; Zhou, Y.; Blair, P. L.; Grainger, M.; Moch, J. K.; Haynes, J. D.; De La Vega, P.; Holder, A. A.; Batalov, S.; Carucci, D. J.; Winzeler, E. A. *Science* **2003**, *301*, 1503.
(288) Persson, K. E.; McCallum, F. J.; Reiling, L.; Lister, N. A.; Stubbs, J.; Cowman, A. F.; Marsh, K.; Beeson, J. G. *J. Clin. Invest.* **2008**, *118*, 342.
(289) Takala, S. L.; Plowe, C. V. *Parasite Immunol.* **2009**, *31*, 560.
(290) LaCount, D. J.; Vignali, M.; Chettier, R.; Phansalkar, A.; Bell, R.; Hesselberth, J. R.; Schoenfeld, L. W.; Ota, I.; Sahasrabudhe, S.; Kurschner, C.; Fields, S.; Hughes, R. E. *Nature* **2005**, *438*, 103.
(291) Kadekoppala, M.; Ogun, S. A.; Howell, S.; Gunaratne, R. S.; Holder, A. A. *Eukaryot Cell* **2010**, *9*, 1064.
(292) Baum, J.; Maier, A. G.; Good, R. T.; Simpson, K. M.; Cowman, A. F. *PLoS Pathog.* **2005**, *1*, e37.
(293) Cortes, A.; Carret, C.; Kaneko, O.; Yim Lim, B. Y.; Ivens, A.; Holder, A. A. *PLoS Pathog.* **2007**, *3*, e107.
(294) Nery, S.; Deans, A. M.; Mosobo, M.; Marsh, K.; Rowe, J. A.; Conway, D. J. *Mol. Biochem. Parasitol.* **2006**, *149*, 208.
(295) Verra, F.; Chokejindachai, W.; Weedall, G. D.; Polley, S. D.; Mwangi, T. W.; Marsh, K.; Conway, D. J. *Mol. Biochem. Parasitol.* **2006**, *149*, 182.
(296) Troye-Blomberg, M.; Romero, P.; Patarroyo, M. E.; Bjorkman, A.; Perlmann, P. *Clin. Exp. Immunol.* **1984**, *58*, 380.
(297) Troye-Blomberg, M.; Sjoholm, P. E.; Perlmann, H.; Patarroyo, M. E.; Perlmann, P. *Clin. Exp. Immunol.* **1983**, *53*, 335.
(298) Anderson, R. M.; May, R. M. *J. Hyg.* **1983**, *90*, 259.
(299) Best, S. M.; Kerr, P. J. *Virology* **2000**, *267*, 36.
(300) Witter, R. L. *Avian Dis.* **1997**, *41*, 149.
(301) Gandon, S.; Mackinnon, M. J.; Nee, S.; Read, A. F. *Nature* **2001**, *414*, 751.

(302) Mackinnon, M. J.; Read, A. F. *PLoS Biol.* **2004**, *2*, e230.
(303) Urquiza, M.; Patarroyo, M. A.; Mari, V.; Ocampo, M.; Suarez, J.; Lopez, R.; Puentes, A.; Curtidor, H.; Garcia, J.; Rodriuez, L. E.; Vera, R.; Torres, A.; Laverde, M.; Robles, A. P.; Patarroyo, M. E. *Peptides* **2002**, *23*, 2265.
(304) Chapeton-Montes, J. A.; Plaza, D. F.; Curtidor, H.; Forero, M.; Vanegas, M.; Patarroyo, M. E.; Patarroyo, M. A. *Protein Sci.* **2008**, *17*, 342.
(305) Forero, M.; Puentes, A.; Cortes, J.; Castillo, F.; Vera, R.; Rodriguez, L. E.; Valbuena, J.; Ocampo, M.; Curtidor, H.; Rosas, J.; Garcia, J.; Barrera, G.; Alfonso, R.; Patarroyo, M. A.; Patarroyo, M. E. *Protein Sci.* **2005**, *14*, 2767.
(306) Garcia, J.; Puentes, A.; Rodriguez, L.; Ocampo, M.; Curtidor, H.; Vera, R.; Lopez, R.; Valbuena, J.; Cortes, J.; Vanegas, M.; Barrero, C.; Patarroyo, M. A.; Urquiza, M.; Patarroyo, M. E. *Protein Sci.* **2005**, *14*, 2236.
(307) Plaza, D. F.; Curtidor, H.; Patarroyo, M. A.; Chapeton-Montes, J. A.; Reyes, C.; Barreto, J.; Patarroyo, M. E. *FEBS J.* **2007**, *274*, 6352.
(308) Vera-Bravo, R.; Torres, E.; Valbuena, J. J.; Ocampo, M.; Rodriguez, L. E.; Puentes, A.; Garcia, J. E.; Curtidor, H.; Cortes, J.; Vanegas, M.; Rivera, Z. J.; Diaz, A.; Calderon, M. N.; Patarroyo, M. A.; Patarroyo, M. E. *Biochem. Biophys. Res. Commun.* **2005**, *332*, 771.
(309) Urquiza, M.; Lopez, R.; Patino, H.; Rosas, J. E.; Patarroyo, M. E. *J. Biol. Chem.* **2005**, *280*, 35598.
(310) Urquiza, M.; Suarez, J.; Lopez, R.; Vega, E.; Patino, H.; Garcia, J.; Patarroyo, M. A.; Guzman, F.; Patarroyo, M. E. *Biochem. Biophys. Res. Commun.* **2004**, *319*, 221.
(311) Garcia, J. E.; Puentes, A.; Suarez, J.; Lopez, R.; Vera, R.; Rodriguez, L. E.; Ocampo, M.; Curtidor, H.; Guzman, F.; Urquiza, M.; Patarroyo, M. E. *J. Hepatol.* **2002**, *36*, 254.
(312) Vera-Bravo, R.; Ocampo, M.; Urquiza, M.; Garcia, J. E.; Rodriguez, L. E.; Puentes, A.; Lopez, R.; Curtidor, H.; Suarez, J. E.; Torres, E.; Guzman, F.; Diaz, D.; Cortes, J.; Bravo, M. M.; Combita, A. L.; Orozco, O.; Patarroyo, M. E. *Int. J. Cancer* **2003**, *107*, 416.